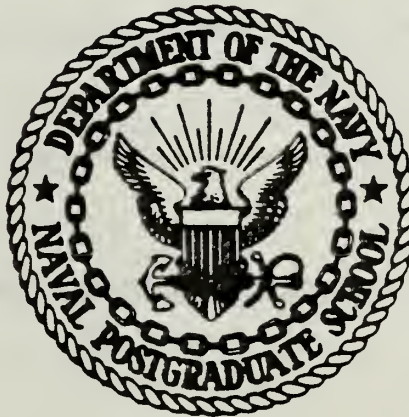


WILEY KNOX LIBRARY
MAY 1951
GRADUATE SCHOOL
1951

NAVAL POSTGRADUATE SCHOOL

Monterey, California



THESIS

OPTIMIZATION OF A LOW ΔT RANKINE
POWER SYSTEM

by

Raymond C. Schaubel

December 1980

Thesis Advisor:

R. H. Nunn

Approved for public release; distribution unlimited.

T197815

REPORT DOCUMENTATION PAGE		READ INSTRUCTIONS BEFORE COMPLETING FORM
1. REPORT NUMBER	2. GOVT ACCESSION NO.	3. RECIPIENT'S CATALOG NUMBER
4. TITLE (and Subtitle) Optimization of a Low ΔT Rankine Power System		5. TYPE OF REPORT & PERIOD COVERED Master's Thesis; December 1980
		6. PERFORMING ORG. REPORT NUMBER
7. AUTHOR(s) Raymond C. Schaubel		8. CONTRACT OR GRANT NUMBER(s)
9. PERFORMING ORGANIZATION NAME AND ADDRESS Naval Postgraduate School Monterey, California 93940		10. PROGRAM ELEMENT, PROJECT, TASK AREA & WORK UNIT NUMBERS
11. CONTROLLING OFFICE NAME AND ADDRESS Naval Postgraduate School Monterey, California 93940		12. REPORT DATE December 1980
		13. NUMBER OF PAGES 235
14. MONITORING AGENCY NAME & ADDRESS (if different from Controlling Office) Naval Postgraduate School Monterey, California 93940		15. SECURITY CLASS. (of this report) Unclassified
		15a. DECLASSIFICATION/DOWNGRADING SCHEDULE
16. DISTRIBUTION STATEMENT (of this Report) Approved for public release; distribution unlimited.		
17. DISTRIBUTION STATEMENT (of the abstract entered in Block 20, if different from Report)		
18. SUPPLEMENTARY NOTES		
19. KEY WORDS (Continue on reverse side if necessary and identify by block number) OTEC Rankine COPES/CONMIN		
20. ABSTRACT (Continue on reverse side if necessary and identify by block number) The Ocean Thermal Energy Conversion (OTEC) uses the low thermal energy potential available from ocean temperature gradients. A method is presented to analyze such systems and, for this purpose, a comprehensive simulation is developed. The simulation includes parasitic power requirements, losses due to interconnecting lines, and heat exchanger pressure drops. Cost functions are included and numerical optimization is employed to obtain optimal designs based upon minimum cost.		

BLOCK 20. ABSTRACT (Continued)

The analysis is converted to a computer code and coupled to the COPES/CONMIN optimization code to facilitate a fully-automated design where the computer makes the design decisions and performance trade-off studies. The final product is an optimum power system module design for the designated net electrical output required and the specified system and design constraints.

Preliminary results are presented for a range of system power levels. Optimum designs are obtained and compared for systems in which either titanium or aluminum tubes are used in the heat exchangers.

Approved for public release; distribution unlimited.

Optimization of a Low ΔT Rankine
Power System

by

Raymond C. Schaubel
Lieutenant Commander, United States Navy
B.S., United States Naval Academy

Submitted in partial fulfillment of the
requirements for the degree of

MASTER OF SCIENCE IN MECHANICAL ENGINEERING

from the

NAVAL POSTGRADUATE SCHOOL
December 1980

Thesis
8273
c. 1

ABSTRACT

The Ocean Thermal Energy Conversion (OTEC) uses the low thermal energy potential available from ocean temperature gradients. A method is presented to analyze such systems and, for this purpose, a comprehensive simulation is developed. The simulation includes parasitic power requirements, losses due to interconnecting lines, and heat exchanger pressure drops. Cost functions are included and numerical optimization is employed to obtain optimal designs based upon minimum cost. The analysis is converted to a computer code and coupled to the COPES/CONMIN optimization code to facilitate a fully-automated design where the computer makes the design decisions and performance trade-off studies. The final product is an optimum power system module design for the designated net electrical output required and the specified system and design constraints.

Preliminary results are presented for a range of system power levels. Optimum designs are obtained and compared for systems in which either titanium or aluminum tubes are used in the heat exchangers.

TABLE OF CONTENTS

I.	INTRODUCTION-	11
A.	BACKGROUND-	11
B.	OBJECTIVES-	13
C.	OVERVIEW OF THE OTEC POWER SYSTEM ANALYSIS-	14
II.	POWER CYCLE DESCRIPTIONS-	17
A.	INTRODUCTION-	17
B.	IDEAL OTEC RANKINE CYCLE-	17
C.	ACTUAL OTEC RANKINE CYCLE	19
III.	EVAPORATOR AND MOISTURE SEPARATOR	22
A.	INTRODUCTION-	22
B.	ANALYSIS OF THE EVAPORATOR AND MOISTURE SEPARATOR-	24
IV.	PARASITIC LOSSES-	62
A.	INTRODUCTION-	62
B.	ANALYSIS OF PARASITIC LOSSES-	65
V.	TURBINE AND ELECTRICAL POWER-	87
A.	INTRODUCTION-	87
B.	ANALYSIS OF THE TURBINE AND ELECTRICAL POWER REQUIREMENTS-	89
VI.	CONDENSER	93
A.	INTRODUCTION-	93
B.	ANALYSIS OF THE CONDENSER	94
VII.	NUMERICAL OPTIMIZATION-	117
A.	INTRODUCTION-	117

B.	COPEs/CONMIN-	- - - - -	-118
C.	DESIGNATED DESIGN VARIABLES, CONSTRAINTS AND OBJECTIVE FUNCTION-	- - - - -	-122
VIII.	CONCLUSIONS AND RECOMMENDATIONS	- - - - -	-124
A.	CONCLUSIONS	- - - - -	-124
B.	RECOMMENDATIONS	- - - - -	-126
TABLES	- - - - -	- - - - -	-128
APPENDIX A:	SAMPLE INPUT DATA FOR OTEC ANALYSIS	- - -	-150
APPENDIX B:	SAMPLE OTEC ANALYSIS OPTIMIZATION OUTPUT DATA	- - - - -	-152
APPENDIX C:	SAMPLE COPEs OPTIMIZATION AND SENSITIVITY ANALYSIS DATA	- - - - -	-157
NOMENCLATURE AND OTEC ANALYSIS CODE-	- - - - -	- - - - -	-160
LIST OF REFERENCES	- - - - -	- - - - -	-231
INITIAL DISTRIBUTION LIST-	- - - - -	- - - - -	-233

LIST OF FIGURES

1.	Power System Sequential Analysis - - - - -	16
2.	Idealized OTEC Rankine Cycle - - - - -	18
3.	Actual OTEC Rankine Cycle- - - - -	20

LIST OF TABLES

1. OTEC Power System Comparison (Titanium Tubed Heat Exchangers)- - - - -128
2. OTEC Power System Comparison (Aluminum Tubed Heat Exchangers)- - - - -134
3. OTEC Heat Exchanger Comparisons (Titanium Tubed)- -140
4. OTEC Heat Exchanger Comparisons (Aluminum Tubed)- -145

PARTIAL LIST OF SYMBOLS

A	heat transfer surface area
A_f	tube bundle frontal area
A_{ff}	free-flow area
C_p	constant pressure specific heat
d	diameter
\dot{E}	power
f	friction factor
F	correction to LMTD
G	mass velocity
g	acceleration of gravity
g_c	conversion factor ($32.2 \text{ lb}_m \cdot \text{ft} / \text{lb}_f \cdot \text{sec}^2$)
h	specific state point enthalpy
\bar{h}	average heat transfer coefficient
k	thermal conductivity
K_m	mean salt water compressibility
L	tube or pipe length
\dot{m}	mass flow rate number
N_t	number of heat exchange tubes
Re	Reynolds number
P	static pressure
\dot{Q}	heat transfer rate
S	specific state point entropy
T	temperature
LMTD	log mean temperature difference

U	overall heat transfer coefficient
v	specific volume
V	velocity
X	quality of working fluid
Z	elevation
ϵ	heat exchange effectiveness
η	efficiency
ρ	density
μ	absolute or dynamic viscosity

I. INTRODUCTION

A. BACKGROUND

Ocean Thermal Energy Conversion (OTEC) is a concept using the low thermal energy potential available from the ocean temperature gradient that exists between warm surface ocean water and cold water in deep ocean regions.

The idea of converting the stored ocean energy to useful power originated with French physicist Jacques d'Arsonval in 1881 [Ref. 1]. It was nearly a half-century later that the technical feasibility of ocean thermal energy conversion could be demonstrated. In 1926, George Claude used an open cycle power system to extract heat from surface water for indirect conversion of the thermal energy of a working fluid. Operating at a low pressure the working fluid was used to drive a turbine providing electrical power generation.

Though Claude's limited power system produced only 22 kilowatts of electricity while requiring approximately 80 kilowatts of power to drive its equipment, it stirred the scientific and research community to consider the attractiveness of ocean thermal energy conversion [Ref. 2].

Claude called for immediate action on his ocean thermal power system, because of the Federal Oil Conservation Board's dire predictions that the United States had only six years of oil production remaining. Obviously the dire predictions ascribed to by the Federal Oil Conservation Board did not

come true, but the oil crisis of that period heightened scientific interest in extracting energy from the ocean.

Now, 55 years later, the United States is faced with an energy crisis because of increasing industrial and social dependence on foreign petroleum. Dwindling supplies and erratic price hikes have rekindled interest in ocean thermal energy conversion, since it utilizes an inexhaustible supply of fuel.

Currently, the United States Department of Energy is attempting to develop the necessary technology and demonstrate the feasibility of large-scale OTEC power systems. However, there are major engineering development problems which must be solved before OTEC can be standardized and become a viable source of electrical power generation.

The single controlling factor which creates troublesome technical encounters is low thermal power system efficiency (one to four percent depending upon parasitic power requirements). Because the heat energy used by OTEC must be extracted from a small ocean temperature difference, extremely large volumes of surface water must pass through a proportionately sized evaporator to provide sufficient indirect heat energy to convert the working fluid into vapor to drive a turbine-generator for electrical power generation. Concurrently, to convert the turbine exhaust to a saturated liquid, completing the closed cycle, a condenser having compatible heat absorption capacity must be employed.

Economic handling of the volume of fluids required for the heat absorption, expansion, and heat rejection phases of the cycle requires close scrutiny of evaporator, turbine, condenser, and pump design to minimize the parasitic losses with respect to the generated electrical output. Because of the low thermal efficiency, relative to nuclear or fossil fuel-fired power plants, the margins for design and operating error in OTEC plants will be narrow.

With the advent of high-speed computers, numerical methods for solving these complex engineering problems with multiple design variables and constraints are now possible. The case for utilizing an optimizing scheme for not just one system component, but rather the complete power generation cycle, can easily be made. In effect, it would serve as a systems analysis tool, to optimize component design and cost, relative to a specific electrical output or to enable comparison and evaluation of competing OTEC designs.

B. OBJECTIVES

The objectives of this work are to develop a computer code for the Ocean Thermal Energy Conversion (OTEC) power system and to couple the analysis to a numerical optimization code to provide an optimum system design capability, considering both performance and economics.

This would create an optimum modular design relative to a specified objective function for a desired net electrical output, such as a 25 MW (net) power system. Such a design

would permit construction of higher capacity power systems using the optimized modules as substations of the total power plant. Cost savings, improved plant performance, redundancy, and reliability could be the immediate beneficiaries of such a venture.

C. OVERVIEW OF THE OTEC POWER SYSTEM ANALYSIS

To analyze the closed-cycle OTEC power system, the fundamental relationships of heat transfer, fluid mechanics and thermodynamics are used to simulate a variety of system component designs, which form the basis of the power system algorithm. The scope of this analysis will be limited to the OTEC power system and sea water systems only. Mooring systems, power delivery, hull, and cold pipe design will not be addressed.

The performance analysis will be divided into four sequential sections as shown in Figure 1, and discussed in detail in subsequent chapters of this thesis.

Input parameters (design constants) for the power cycle analysis will include:

- . Required net electrical output.
- . Salt water inlet temperature to the evaporator and condenser.
- . Length of hot and cold salt water pipes.
- . Heat exchanger tubing material (aluminum or titanium).
- . Heat exchanger tube orientation and profile.
- . Pump mechanical and motor efficiencies.

- . Turbine mechanical efficiency.
- . Generator mechanical and electrical efficiency.
- . Biofouling control factor.
- . Piping absolute roughness.
- . Projected annual inflation rate for aluminum heat exchanger retubing.

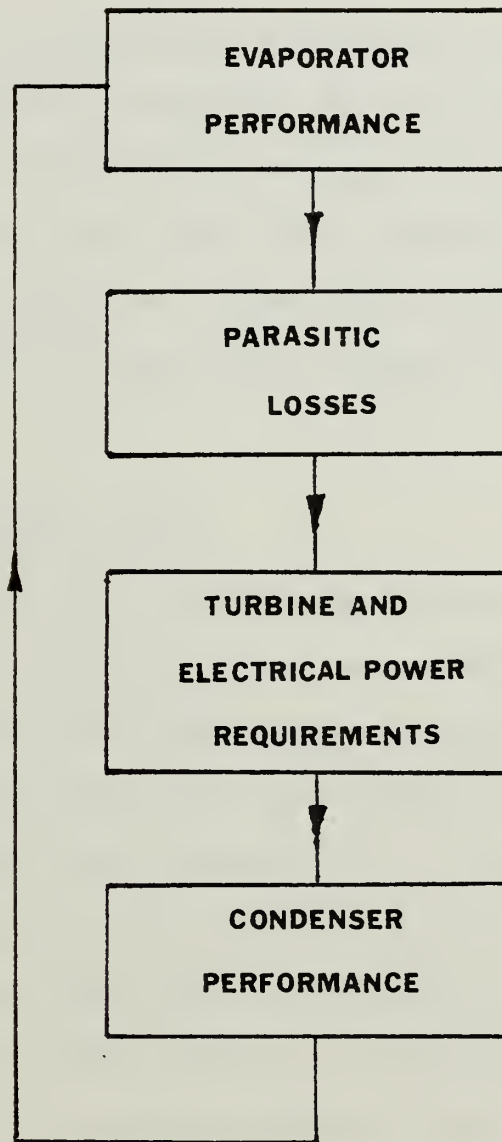


Figure 1. Power System Sequential Analysis

II. POWER CYCLE DESCRIPTIONS

A. INTRODUCTION

This chapter will provide a brief description of the OTEC power system. First, looking at the ideal Rankine cycle, the fundamental thermodynamic concepts will be enumerated. Then the deviations from the ideal cycle will be presented, creating the configuration assumed for the present cycle analysis which will be amplified in detail by follow-on chapters.

B. IDEAL OTEC RANKINE CYCLE

The closed-cycle OTEC concept is based upon a Rankine power cycle that is driven by the low thermal energy potential available from the ocean temperature gradient that exists between warm surface water and cold deep water in ocean regions. The power cycle consists of a working fluid circulation pump, evaporator (heat absorption), turbine (expansion), and condenser (heat rejection), as shown in Figure 2. The majority of current OTEC designs are based upon ammonia as the working fluid -- a design decision that is adopted for this analysis.

Figure 2 also illustrates an ideal OTEC Rankine cycle, plotted on temperature-entropy coordinates. In the ideal cycle, the low pressure working fluid (state point 1) is isentropically pumped to the evaporator operating pressure (state point 2). The working fluid (ammonia) is then

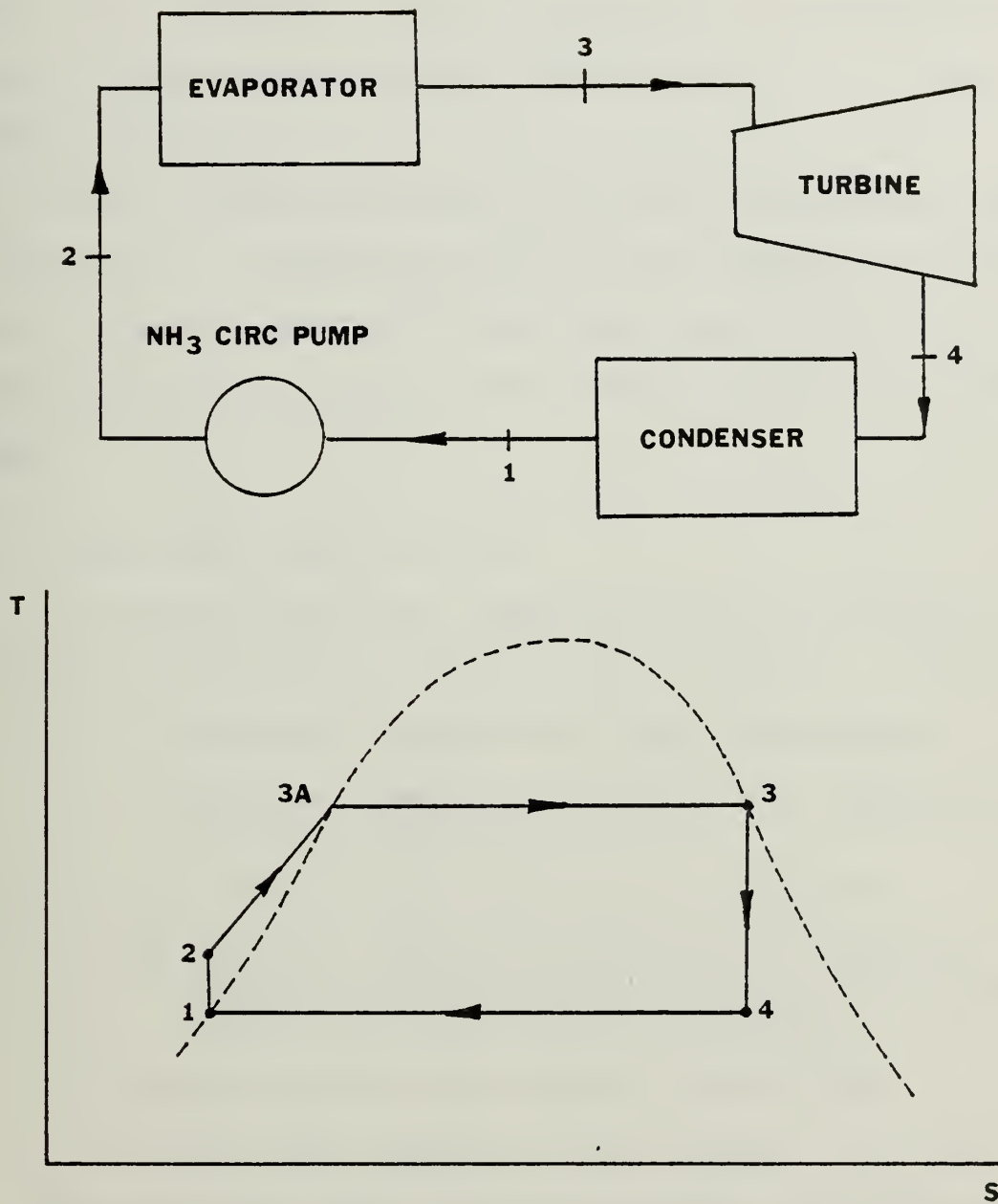


Figure 2. Idealized OTEC Rankine Cycle

converted to a saturated vapor in the evaporator by indirect heat energy exchange from warm surface ocean water (state point 3). Mechanical power is generated by isentropic expansion of the saturated ammonia vapor through the turbine (state point 4).

After exiting the turbine, the wet, low-pressure vapor is converted to a saturated liquid in the condenser by indirect heat absorption from cold ocean water (state point 1), returning the cycle back to the working fluid circulation pump.

C. ACTUAL OTEC RANKINE CYCLE

In actuality there are numerous deviations from the ideal cycle which must be considered in this analysis. These are:

- (1) Turbine, generator and pump efficiencies.
- (2) Pressure drops in evaporator and condenser (tube-side and shellside).
- (3) Pressure drop across moisture separator.
- (4) Elevation change and frictional losses in piping: (a) re-flux pump piping, (b) piping from circulation pump to evaporator.
- (5) Evaporator outlet quality (85 to 95%).
- (6) Moisture separator outlet quality (99 to 99.5%).

The deviations from the ideal Rankine cycle described above are depicted in the flow diagram and temperature-entropy plot of Figure 3. In the actual OTEC Rankine cycle, the low pressure working fluid (state point 1) is pumped up to the evaporator operating pressure by the ammonia circulation pump with an adiabatic efficiency (state point 2). The working

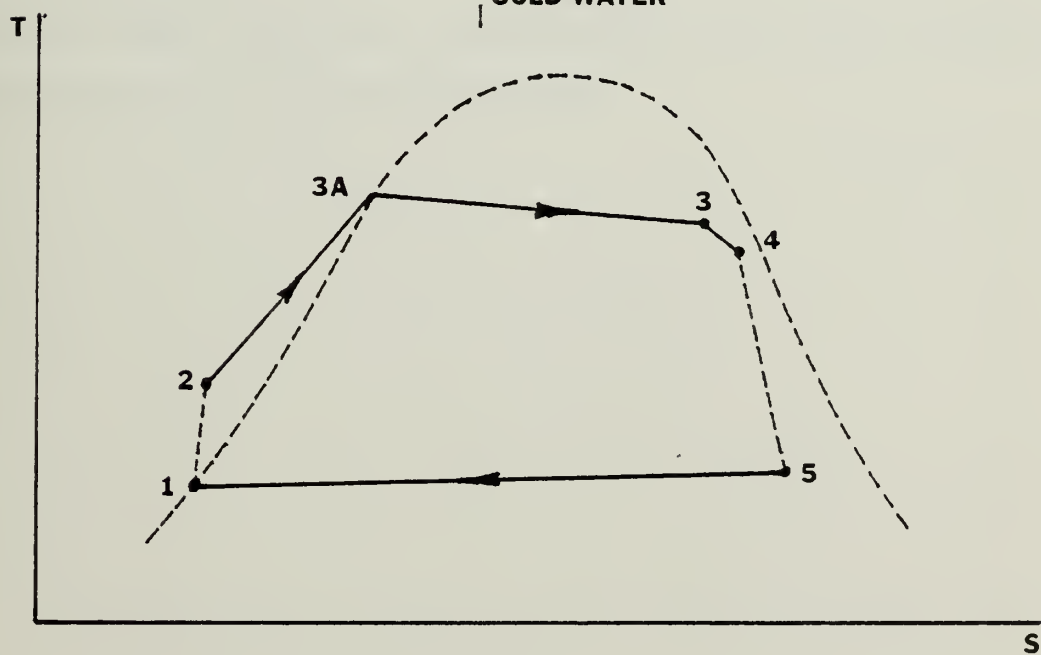
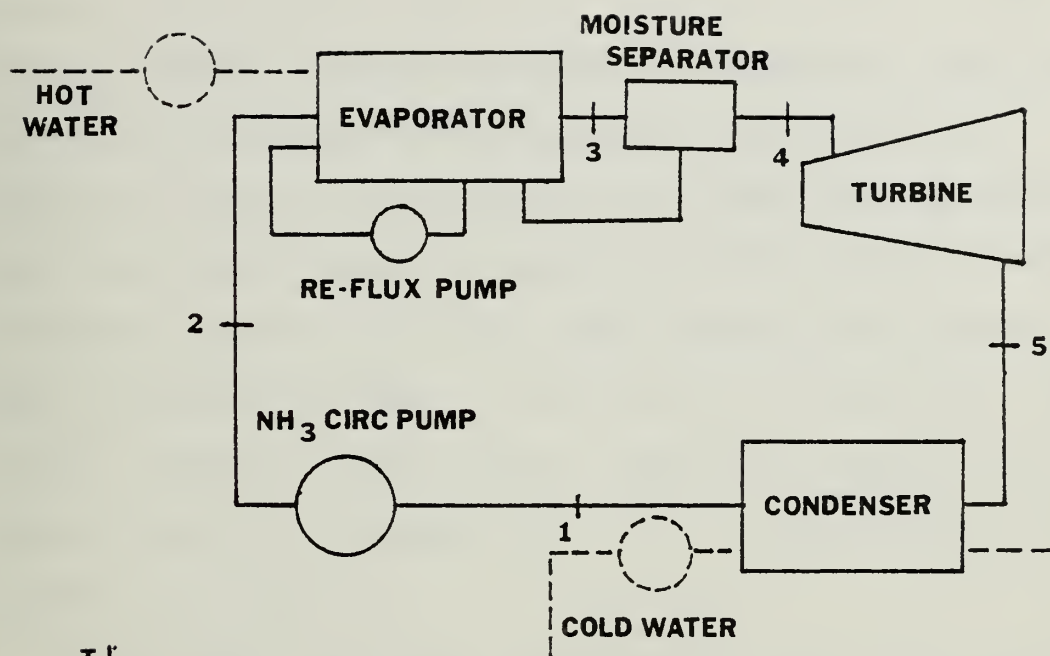


Figure 3. Actual OTEC Rankine Cycle

fluid (ammonia) is then converted to a wet vapor with an evaporator outlet quality (85-95%) acting under a shellside pressure drop (state point 3). Evaporator outlet vapor then passes through a moisture separator to improve vapor quality (99-99.5%) creating a pressure drop (state point 4). Mechanical power is generated by the expansion of the moisture separator outlet vapor through the turbine with an adiabatic efficiency (state point 5). After exiting the turbine, the wet, low pressure vapor is converted to a saturated liquid in the condenser acting under a shellside pressure drop (state point 1), returning the cycle to the working fluid circulation pump.

This figure forms the thermodynamic basis for the OTEC power system analysis which follows.

III. EVAPORATOR AND MOISTURE SEPARATOR

A. INTRODUCTION

Several heat exchanger concepts have been proposed for closed-cycle OTEC systems. Among these designs are:

- . Conventional shell and tube heat exchanger.
- . Plate type heat exchanger.

Within these basic concepts, variations in design have been proposed, including:

- . Orientation of tubes (horizontal or vertical).
- . Heat exchanger tube material (i.e., titanium, aluminum).
- . Method of tube enhancement (i.e., fluted, porous coatings).
- . Location of tube enhancement (i.e., internal and/or external).
- . Location of the vapor separator (i.e., internal or external).
- . Location of the heat exchangers relative to the sea surface.
- . Method of biofouling control.

The analysis to be presented for the evaporative heat exchanger will be based on the following design characteristics:

- . Single-pass shell and tube heat exchanger.
- . Internal vapor separator with a gravity drain to evaporator inlet.
- . Horizontal orientation of tubes with an equilateral triangle or square tube profile.
- . Smooth plain-tube configuration (no enhancements).

- . Tube material (titanium or aluminum based on a 30-year life-cycle criterion).
- . Biofouling control based upon an achievable fouling factor.
- . Heat exchanger centerline located on sea surface.

As an overview of the evaporator-moisture separator analysis, the following major steps in the algorithm are listed in order of their execution (numbers in parentheses refer to equations developed in the subsequent analysis):

- . Specification of system constants (see I.C.).
- . Initialization of design variables (D.V.).
 - .. Tube length.
 - .. SW velocity through hot pipe.
 - .. Inner diameter of hot pipe.
 - .. Tube outer diameter.
 - .. SW velocity through evaporator tubes.
 - .. Inner diameter of NH₃ piping.
 - .. Inner diameter of NH₃ re-flux piping.
 - .. Tube profile pitch ratio.
- . Salt water mass flow rate (1).
- . Total number of tubes (2).
- . Total heat transfer surface area (3).
- . Assume an initial salt water bulk temperature (6), and ammonia heat transfer coefficient (9).
- . Overall heat transfer coefficient (4).
- . Number of transfer units (11).
- . Heat exchanger effectiveness (13).
- . Salt water outlet temperature (15).

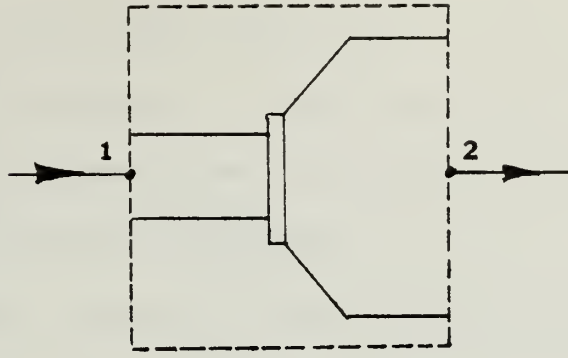
- . Revised bulk temperature (16); iterate with (6).
- . Amount of heat absorption (17).
- . Log mean temperature difference (18).
- . Film temperature (19).
- . Initial ammonia mass flow rate (21) without the effects of moisture separator.
- . Initially assume state point 1 thermodynamic properties are ideal (21).
- . Thermodynamic pump work (23).
- . Tube profile, flow parameters across the tube bank (24, etc.).
- . Tube sheet diameter (30).
- . Evaporator shellside pressure drop for two phase flow (33).
- . Moisture separator pressure drop (38).
- . Properties at state points 3 and 4 (39-41).
- . Revised ammonia mass flow rate and velocity (50) includes the effects of the moisture separator; iterate with (31).
- . Revised ammonia heat transfer coefficient (51, etc.); iterate with (9).
- . Heat exchanger cost analysis.

In the following section, the basic steps summarized above will be described in detail.

B. ANALYSIS OF THE EVAPORATOR AND MOISTURE SEPARATOR

1. Salt Water Mass Flow rate, \dot{m}_{sw}

The salt water mass flow rate through the hot pipe must be equivalent to the flow rate through the evaporator (assuming no leakage)



$$\dot{m}_1 (\text{HOT PIPE}) = \dot{m}_2 (\text{EVAPORATOR})$$

and

$$\dot{m} = \rho_{sw} A V \quad (1)$$

where A = cross-sectional area of the hot pipe.
 V = salt water velocity through hot pipe.
 ρ_{sw} = density of salt water evaluated for an average hot pipe salt water temperature.

As previously stated, the diameter of the hot pipe and salt water velocity are among the initializing conditions of the optimization and will be treated as design variables.

2. Total Number of Evaporator Tubes, N_t

Using equation (1), it follows that

$$\dot{m}_1 = \rho_{sw} \frac{\pi d_i^2}{4} V_t N_t \quad (2)$$

where ρ_{sw} = salt water density evaluated at the average bulk temperature initially assumed as the hot pipe salt water temperature.

d_i = tube inner diameter.

N_t = the number of tubes required to maintain the mass flow rate for an average salt water velocity per tube.

The total number of tubes can be determined by solving Eq. (2) for N_t .

The diameter of the tube and average salt water velocity per tube are initialized for the analysis and will be treated as design variables by the optimization code.

3. Total Evaporator Heat Transfer Surface Area (Outer), A_t

Having determined the number of evaporator tubes, the total heat transfer surface area can be determined using initializing values of outer tube diameter and tube length.

For tubes without extended surfaces

$$A_t = \pi d_o L_t N_t \quad (3)$$

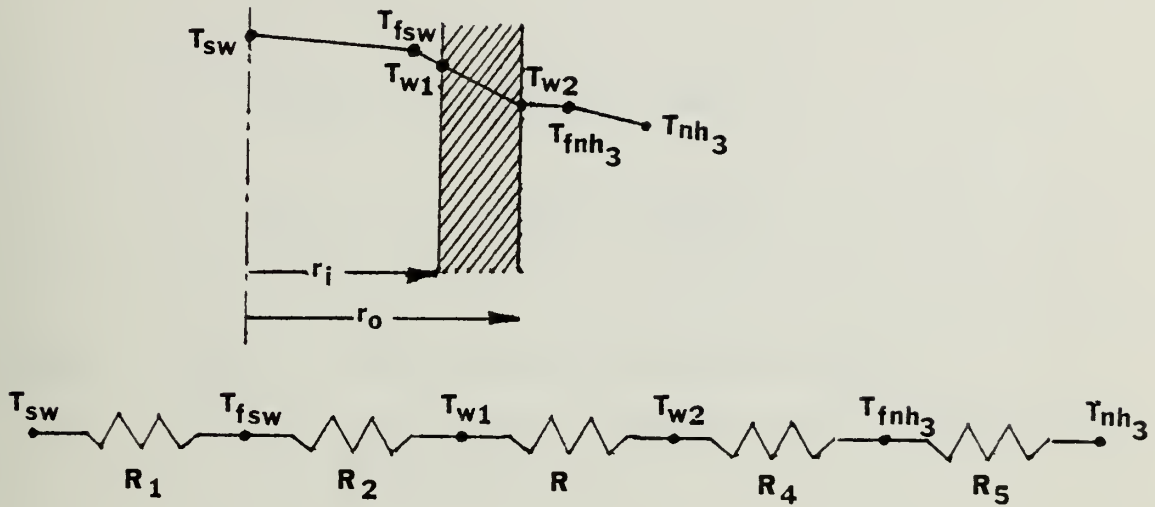
As previously, the outer tube diameter and tube length are initializing conditions and will be treated as design variables.

4. Overall Heat Transfer Coefficient, U

The quantity "U" provides a measure of the total thermal resistance in the flow path, based on either inside or outside surface area.

This analysis will be based on the value of U for the outside surface area derived from Eq. (3).

Using a resistance analysis, assuming one dimensional (radial) heat flow,



the overall heat transfer coefficient may be expressed as

$$U_o = \frac{1}{\frac{A_o}{\eta_i h_{sw} A_i} + \frac{A_o}{A_i} R_{fsw} + \frac{d_o \ln d_o / d_i}{2K} + R_{fNH_3} + \frac{1}{\eta_o h_{NH_3}}} \quad (4)$$

where h_{sw} = tubeside heat transfer coefficient.
 R_{fsw} = salt water fouling heat transfer resistance.
 K = thermal conductivity of the tube material.
 d_o, d_i = outer and inner tube diameter.
 R_{fNH_3} = ammonia fouling heat transfer resistance
 (assumed to be negligible).
 η_o, η_i = outer and inner total fin efficiency (for plain tube analysis, total fin efficiency equals 1).
 A_o = total outer surface area (including fin and bare tube).

A_i = total inner surface area (including fin and bare tube).¹

$$\eta_i = 1 - \frac{A_{fni}}{A_i} (1 - \eta_{fi})$$

$$\eta_o = 1 - \frac{A_{fno}}{A_o} (1 - \eta_{fo})$$

where A_{fni} = total inner fin surface area.
 A_i = total inner surface area (including fin and bare tube).
 A_{fno} = total outer fin surface area.
 A_o = total outer surface area (including fin and bare tube).
 η_{fi} = fin efficiency of single internal fin.
 η_{fo} = fin efficiency of single external fin.

a. Tubeside Reynolds Number, Re_d

Since the heat transfer coefficient correlations for the evaporator and condenser are dependent on tubeside flow, Reynolds number must be calculated.

The tube Reynolds number is defined as

$$Re_d = \frac{\rho_{sw} V_{sw} d_i}{\mu_{sw}} \quad (5)$$

¹Note that this analysis will hereafter consider smooth plain tube configurations only.

where μ_{sw} = dynamic viscosity of salt water.

ρ_{sw} = density of salt water.

Initially, properties are evaluated for

$$T_{BULK} = T_{SW} (INLET) \quad (6)$$

Reynolds numbers greater than 2300 will be indicative of turbulent flow [Ref. 3]. Transition flow was considered laminar for numerical evaluation.

b. Salt Water Heat Transfer Coefficient, h_{sw}

The simple empirical relation proposed by Sieder and Tate [Ref. 3], expressed as

$$Nu_d = 1.86 (Re_d Pr)^{1/3} \left(\frac{d_i}{L_t} \right)^{1/3} \left(\frac{\mu}{\mu_w} \right)^{0.14} \quad (7)$$

was used for laminar heat transfer in tubes as defined by Eq. (5).

Nusselt and Prandtl numbers, Nu_d and Pr , are defined as

$$Nu_d = \frac{h_{sw} d_i}{k_{sw}}$$

$$Pr = \frac{c_{p_{sw}} \mu_{sw}}{k_{sw}}$$

where μ_{sw} , $c_{p_{sw}}$ and k_{sw} (dynamic viscosity, specific heat, and thermal conductivity) of salt water are evaluated at salt water bulk temperature.

The effect of the viscosity ratio term in

Eq. (7)

$$\left(\frac{\mu}{\mu_w} \right)^{0.14}$$

where μ_w is salt water viscosity evaluated at tube wall temperature, is considered negligible and will hereafter be dropped from the expression of Eq. (7).

Relation (7) is based upon the following assumptions:

- . fully developed flow in smooth tubes.
- . fluid properties are evaluated at the bulk fluid temperature.

and is valid for the following condition

$$Re_d Pr \frac{d}{L} > 10$$

For fully developed turbulent flow in a tube as defined by Eq. (5), the Dittus-Boelter correlation [Ref. 3] expressed as

$$Nu_d = 0.023 Re_d^{0.8} Pr^{0.4} \quad (8)$$

was used. Nusselt and Prandtl numbers, Nu_d and Pr , are previously defined by Eq. (9).

Relation (8) is based upon the following assumptions:

- . fully developed flow in smooth tubes.
- . fluid properties are evaluated at the bulk fluid temperature

and is valid for the following conditions:

- . Prandtl numbers ranging from 0.6 to 100.
- . moderate temperature differences between the wall and fluid conditions.

c. Salt Water Fouling Heat Transfer Resistance

In this document, it will be assumed that the fouling resistance coefficient for tubeside salt water can be maintained at $.00025 \text{ (hr.ft}^2\text{.F}^\circ\text{/BTU)}$ using one of the following techniques:

- . Chlorination.
- . MAN Brush System.
- . Amertap.
- . Chemical cleaning

Pressure drops associated with cleaning techniques will not be considered in this analysis. Piping losses will be a function of tube length, inner diameter, salt water velocity and the absolute roughness of the tubing design material only.

- d. Ammonia Shellside Heat Transfer Coefficient, h_{NH_3}
Initially, h_{NH_3} will be assumed

$$h_{NH_3} = 1000 \text{ (BTU/hr.ft}^2\text{.F}^\circ\text{)} \quad (9)$$

since its value cannot be directly calculated during this phase of the analysis.

Using the thermal resistance expressed as

$$R_1 = \frac{d_o}{\eta_i h_{sw} d_i}$$

$$R_2 = \frac{d_o}{\eta_i h_{tsw} d_i}$$

$$R_3 = \frac{d_o \ln d_o / d_i}{2k}$$

$$R_5 = \frac{1}{\eta_o h_{NH_3}}$$

an initial value for the overall heat transfer coefficient may be calculated.

$$U_o = \frac{1}{R_1 + R_2 + R_3 + R_5} \quad (10)$$

5. NTU-effectiveness Relations

The NTU-effectiveness relationships will be used to determine the evaporator outlet salt water temperature. Currently, all salt water properties have been based upon the initial assumption that

$$T_{BULK} = T_{Hi} \text{ (SW INLET TO EVAP)}$$

The expression for the number of transfer units (NTU) which is a measure of the size of the heat exchanger is given by

$$NTU = U_o A_t / C_{min}$$

where C_{min} is defined as capacity rate of the single phase flow in an evaporative or condensing two phase flow regime.

$$C_{min} = \dot{m}_{sw} C_{p_{sw}} \quad (11)$$

Evaporator effectiveness can then be expressed as

$$\epsilon = 1 - e^{(-NTU)} \quad (12)$$

for two phase flow regardless of the flow geometry.

Using the definition of effectiveness

$$\text{Effectiveness} = \frac{\text{actual heat transfer}}{\text{maximum possible heat transfer}} \quad (13)$$

$$\epsilon = \frac{\dot{Q}}{\dot{Q}_{max}} = \frac{\Delta T_{min}}{\Delta T_{max}} = \frac{T_{Hi} - T_{Ho}}{T_{Hi} - T_{Ci}} \quad (14)$$

The expression for ΔT_{min} represents the single phase (salt water) flow and T_{Ci} represents ammonia inlet temperature to evaporator taken at state point 3A.

6. Evaporator Salt Water Outlet Temperature and Bulk Temperature

Using the relationships of Eqs. (12) and (14), the following expression may be formulated for salt water outlet temperature

$$T_{Ho} = T_{Hi} - (T_{Hi} - T_{Ci})(1 - e^{(-NTU)}) \quad (15)$$

Concurrently, a revised evaporator average salt water temperature can be expressed as

$$T_{BULK} = (T_{Hi} + T_{Ho})/2 \quad (16)$$

Using the revised value for average salt water temperature, iterate with equation (1) until the revised and current values of bulk temperature satisfy a specified convergence criterion.

7. Amount of Heat Absorption, \dot{Q}

Using the results of Eq. (16) and (12), the amount of heat absorption by the evaporator may be expressed as

$$\dot{Q} = C_{min} (T_{Hi} - T_{Ho}) \quad (17)$$

8. Log Mean Temperature Difference, $LMTD$

The NTU-effectiveness method can be used to determine the mean effective temperature difference ($LMTD$) across the evaporator (heat exchanger).

Using Eq. (17) and the definition of

$$\dot{Q} = U_o A_t F LMTD$$

with $\dot{Q}_{max} = C_{min} \Delta T_{max}$

the log mean temperature difference across the evaporator may be expressed as

$$LMTD = \frac{C_{min}(1 - e^{(-NTU)})}{U_o A_t F} (T_{Hi} - T_{Ci}) \quad (18)$$

where $T_{Ci} = T_{NH_3}$ evaluated at state point 3.

F = correction factor on $LMTD$, equal to 1 for two phase flow.

9. Film Temperature for Property Evaluation, T_f

In order to evaluate the shellside ammonia heat transfer coefficient, working fluid properties (i.e., viscosity, specific heat, etc.) must be evaluated at the film temperature to validate critical heat transfer expressions.

By modifying the expression in Eq. (10) multiplying by a single tube outer area, a value for single tube conductance can be expressed as

$$U_o A = \frac{A}{R_1 + R_2 + R_3 + R_5}$$

Subsequently, the average amount of heat transferred per tube would equate to

$$\dot{Q} = U_o \dot{A} (T_{BULK} - T_3)$$

where $T_3 = T_{NH_3}$ evaluated at state point 3.

Again using the resistance analysis in Section 3, shellside wall temperature may be derived from

$$T_{W2} = T_{BULK} - \dot{Q} \left(\frac{R_1 + R_2 + R_3}{A} \right)$$

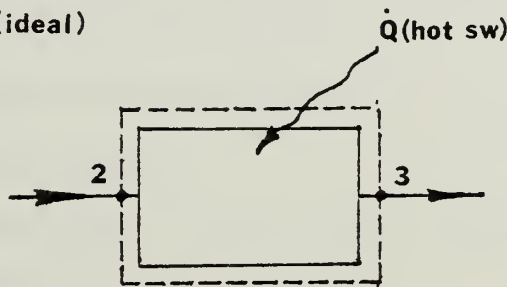
Knowing shellside wall temperature and the free-stream temperature, film temperature can be derived from their arithmetic mean.

$$T_f = \frac{T_{w2} + T_3}{2} \quad (19)$$

10. Ammonia Mass Flow Rate, \dot{m}_{NH_3}

According to first law of thermodynamics for steady state, steady-flow conditions in the evaporator:

EVAPORATOR (ideal)



$$\dot{m}_{NH_3} h_2 + \dot{Q} = \dot{m}_{NH_3} h_3 \quad (20)$$

from which the ammonia mass flow rate, \dot{m}_{NH_3} , may be determined if the enthalpies at state points 2 and 3 are known.

If we initialize the lower and upper bounds of the analysis in terms of pressure P_1 and P_3 , respectively, and initially assume that a saturated vapor leaves the evaporator, the following relations may be expressed

$$\begin{aligned}
 h_1 = h_f \big|_{P_1} \quad T_1 = T_{SAT} \big|_{P_1} \\
 h_3 = h_g \big|_{P_3} \quad T_3 = T_{SAT} \big|_{P_3}
 \end{aligned}
 \tag{21}$$

where h_1 = represents enthalpy at state point 1 at the suction inlet to the working fluid circulation pump.

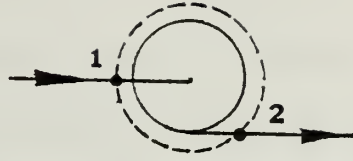
h_3 = represents enthalpy at (ideal)/state point 3 as a saturated vapor.

T_1, T_3 = represent the respective saturation temperatures.

v_1 = represents the specific volume at state point 1.

To summarize, the upper and lower pressure bounds of the system (P_1 and P_3) will be initialized in the analysis and treated as design variables by the optimization code. Temperature at state point 3 is initially assumed to be a saturated vapor (ideal T_3); however, the working fluid is subject to a shellside pressure drop as it passes across the evaporator with an outlet quality of 90-95%. Properties at state point 3 (actual) will be assessed in follow-on sections.

AMMONIA CIRC PUMP



$$\dot{m}_{\text{NH}_3} h_1 + \dot{W}_{CP} = \dot{m}_{\text{NH}_3} h_2 \quad (22)$$

Assuming steady state, steady-incompressible flow, the change in kinetic and potential energies, and heat losses are negligible for isentropic conditions, and the isentropic pump work can be expressed as

$$\dot{W}_{CPs} = v_1 (P_2 - P_1) \quad \text{where } P_2 = P_{2s}$$

After the isentropic pump work is calculated, the actual (adiabatic) pump work may be determined using pump efficiency, η_p .

$$\dot{W}_{CP} = \frac{\dot{W}_{CPs}}{\eta_p} \quad (23)$$

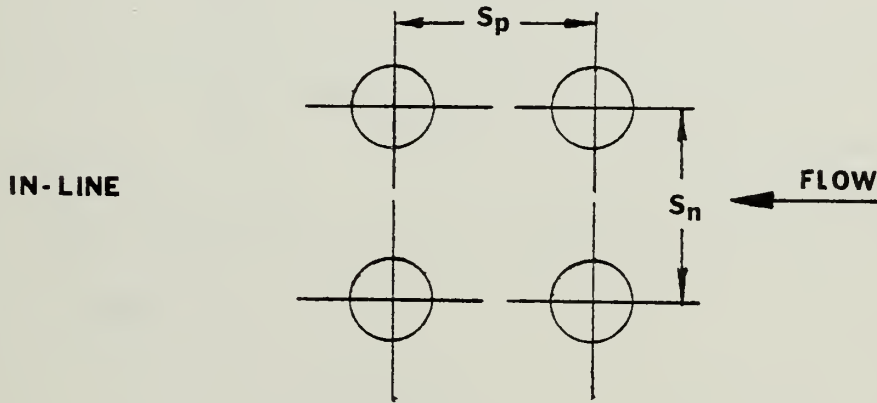
Actual outlet enthalpy at state point 2 may be determined using the results of Eq. (23) with Eq. (22) knowing the enthalpy at state point 1 from Eq. (21).

Using the results of Eqs. (21) and (22), the mass flow rate in Eq. (20) may be calculated as the average shell-side mass flow rate for the working fluid (ammonia).

11. Tube Profile, Flow across Tube Bank, and Tube Sheet Diameter

Since the heat-exchanger arrangements (evaporator and condenser) involve multiple rows of tubes, the geometric arrangement of the tube profiles is important in the determination of the heat transfer coefficient, the tube sheet diameter and the shell side pressure drop associated with two-phase flow (homogeneous model) [Ref. 4].

The following geometric arrangements are used:



where S_n = pitch ratio x outer tube diameter, equal to S_p .

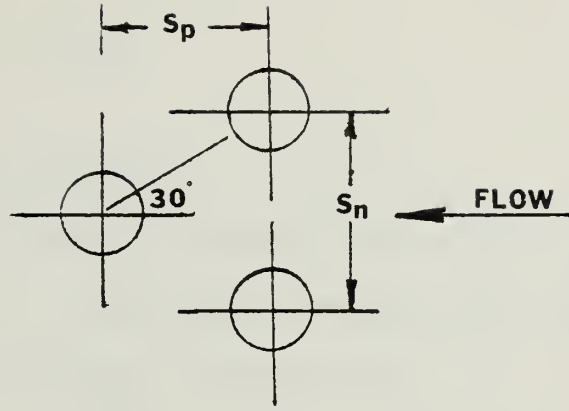
P_R = pitch ratio; the distance between tube centers with respect to outer tube diameter.

A_p = tube profile area (centerline to centerline) per tube.

$$S_n = P_R d_o \quad (24)$$

$$A_p = S_n^2 \quad (25)$$

STAGGERED



$$S_n = 2 P_R d_o \sin 30^\circ \quad (26)$$

$$S_p = P_R d_o \cos 30^\circ \quad (27)$$

Therefore, the tube profile area (centerline to centerline) per tube is equal to

$$A_p = S_n S_p \quad (28)$$

The ratio of minimum flow area to the frontal area can be expressed as

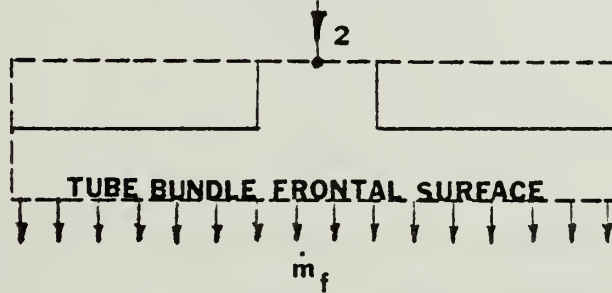
$$\frac{A_{ff}}{A_f} = \frac{S_n - d_o}{S_n} \quad (29)$$

Using the selected tube profile geometry, either in-line or staggered, and knowing the required number of tubes by equation (2), the tube sheet diameter for heat exchanger design can be assessed as follows:

$$N_t A_p = \frac{\pi T_{SD}^2}{4} \quad (30)$$

where T_{SD} = tube sheet diameter.

To estimate the shellside ammonia flow velocity the following control volume is introduced (ammonia circulation piping and the top portion of the evaporator).



If the mass flow rate remains unchanged across any boundary (continuity),

$$\dot{m}_2 = \dot{m}_f$$

Furthermore, if we assume the evaporator has the means to evenly distribute liquid droplets across the top of the tube bundle (spray nozzles and baffling), the following expressions can be applied to estimate the mean droplet velocity approaching the bundle:

Let $(A_f)_{LIQ} = A_f \eta$

where η = percent of tube frontal area which is occupied by droplets.

The mass flow rates are

$$\dot{m}_2 = \rho A_p V_p$$

$$\dot{m}_f = \rho (A_f)_{L,f} V_f$$

where A_p = ammonia pipe cross-sectional area.

V_p = average ammonia velocity in the pipe.

Therefore

$$V_f = \frac{A_p}{(A_f)\eta} V_p$$

and since

$$\eta \approx \frac{A_p}{A_f}$$

it follows that the average velocity of ammonia through the circulation pipe is equivalent to the average velocity of ammonia at the tube frontal area boundary.

$$V_p = V_f \quad (31)$$

Thus the assumption that $\eta = A_p/A_f$ is equivalent to the assumption of constant liquid kinetic energy in the transition from the pipe exit to the bundle entrance. Considering the minimum free-flow area for shellside flow passage, A_{ff} can be derived from Eqs. (29) and (30):

$$A_f = T_{SD} L_t$$

$$A_{ff} = A_f \left(\frac{S_{r1} - c_{l0}}{S_{r1}} \right) \quad (32)$$

where A_f = represents the flow frontal area.

L_t = tube length.

Using the calculated values of Eqs. (32) and (20), the mass velocity for the minimum free-flow area can be expressed

$$G = \dot{m}_{NH_3} / A_{ff}$$

where \dot{m}_{NH_3} represents the average ammonia mass flow rate.

12. Pressure Drop of Two-Phase Flow across a Bank of Tubes, ΔP

This portion of the analysis will use an analytical model for two-phase pressure drops applicable for a fog or spray flow pattern occurring at high void fractions -- the homogeneous model [Ref. 4].

The model asserts that if the pressure drop in the two-phase flow for a liquid-vapor mixture is relatively small compared to the absolute pressure, the flow is considered incompressible. Subsequently, the density of each phase is practically constant. During the process of phase change, the phase and velocity distributions are changed, and so is the momentum of the flow. Therefore, the pressure drop of a vertical two-phase flow consists of three components: friction loss, momentum change, and elevation pressure drop arising from the effects of the gravitational force field.

The local pressure gradient for a two-phase flow may be expressed as

$$\Delta P_{TOT} = \Delta P_{FRICTION} + \Delta P_{MOMENTUM} + \Delta P_{ELEVATION} \quad (33)$$

For a given channel length, L_c , the pressure drop components can be represented by

$$\Delta P_{\text{FRICTION}} = \frac{f G^2 \bar{v}}{D_e 2 g_c} L_c \quad (34)$$

$$\Delta P_{\text{MOMENTUM}} = \frac{G^2 \bar{v}}{g_c}$$

$$\Delta P_{\text{ELEVATION}} = \frac{g}{\bar{v} g_c} L_c$$

and the total pressure drop, ΔP_{EVAP} , is given by the sum of these expressions

where f = single-phase friction factor by Jakob expressed in Eqs. (35) and (36).

L_c = channel flow length, defined for horizontal tubed evaporators as $L_c = T_{SD}$ (tube sheet diameter).

D_e = equivalent diameter of flow channel, defined by $D_e = P_R d_o - d_o$.

\bar{v} = mean specific volume defined by

$$\bar{v} = v_f \left[1 + \frac{x}{v_f} (v_g - v_f) \right]$$

where x = quality of mixture (state point 3).

v_f = specific volume of liquid (state point 1).

v_g = specific volume of vapor (state point 3).

The basic assumptions of the homogeneous model (fog flow model) [Ref. 4] are:

- (1) equal linear velocities of vapor and liquid,
- (2) thermodynamic equilibrium between the two phases, and
- (3) a suitably defined single-phase friction factor is applicable to the two-phase flow.

Using assumption (3) and the correlations by Jakob [Ref. 3], a suitable single-phase friction factor can be calculated from previously defined tube profile relationships: for staggered tube arrangements:

$$f = \left\{ 0.25 + \frac{0.118}{[(S_n - d_o)/d_o]^{1.08}} \right\} Re_{max}^{-0.16} \quad (35)$$

and for in-line tube arrangements:

$$f = \left\{ 0.044 + \frac{0.08 S_n/d_o}{[(S_n - d_o)/d_o]^{0.43 + 1.13 d_o/S_n}} \right\} Re_{max}^{-0.15} \quad (36)$$

where Reynolds number (max) is determined from the shellside ammonia flow and the nozzling effect of the tube geometry as expressed by

$$V_{max} = V_f \left(\frac{S_n}{S_n - d_o} \right)$$

where V_f = the ammonia velocity at the tube frontal area boundary determined by equation (31).

Reynolds number for maximum shellside flow can be calculated using the following expression

$$Re_{max} = \frac{\rho_f V_{max} d_o}{\mu_f} \quad (37)$$

Eq. (37) and tube profile data can then be used to evaluate the single-phase friction factor, required for Eq. (34). All other components of the total pressure drop Eq. (33) can be determined from previously calculated data.

13. Pressure Drop Across the Moisture Separator. $\Delta P_{m.sep}$

This portion of the analysis will simulate the use of a cyclone separator to improve the evaporator outlet vapor quality. The flow pattern in a cyclone separator is complex and simplifying assumptions are inadequate to allow the calculation of the corresponding pressure drop, which can vary from 1 to 20 inlet velocity heads [Ref. 5]. Therefore, the worst case condition will be applied with an approximation for the fluid flow inlet area to the separator banks.

By approximating the inlet area as a fraction of the evaporator frontal area

$$A_{INLET} = 0.1 T_{SD} L_t$$

the inlet fluid velocity can then be determined using the working fluid mass flow rate, Eq. (20).

$$\dot{m}_{NH_3} = \rho A_{INLET} V$$

where ρ = density of ammonia at state point 3.

Therefore, if the pressure drop across the moisture separator is equal to 20 times the inlet velocity head,

$$\Delta P_{in.sep} = 20 \rho \frac{V^2}{2gc} \quad (38)$$

14. Enthalpy at State Points 3 and 4

Since Eq. (33) represents the pressure drop across the evaporator shellside, the actual pressure at state point 3 or evaporator outlet may be determined from

$$P_{3(NEW)} = P_3 - \Delta P_{EVAP} \quad (39)$$

where P_3 was previously described as the pressure for a saturated vapor.

Similarly the actual pressure at state point 4, the moisture separator outlet, may be expressed as

$$P_4 = P_{3(NEW)} - \Delta P_{in.sep} \quad (40)$$

Operating under the dome of the Temperature-Entropy diagram, the following properties are defined

$$\begin{aligned} h_{3f(NEW)} &= h_f \big|_{P_{3(NEW)}} & h_{4f} &= h_f \big|_{P_4} \\ h_{3g(NEW)} &= h_g \big|_{P_{3(NEW)}} & h_{4g} &= h_g \big|_{P_4} \end{aligned} \quad (41)$$

The subscript (NEW) representing a revised property will hereafter be dropped from the expressions in Eq. (41).

Assuming an evaporator outlet quality of 90-95%, and a moisture separator outlet quality of 99-99.5%, enthalpies at state points 3 and 4 may be determined using the relationships of Eqs. (41)

$$\begin{aligned}h_3 &= h_{3f} + x_3 (h_{3g} - h_{3f}) \\h_4 &= h_{4f} + x_4 (h_{4g} - h_{4f})\end{aligned}\tag{42}$$

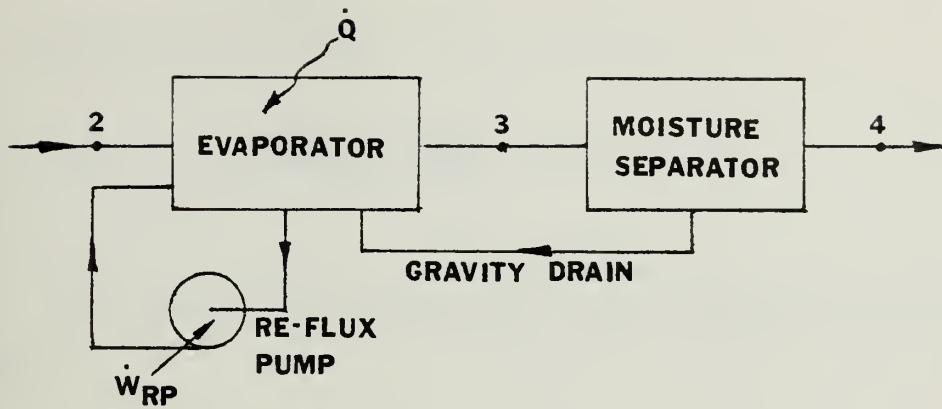
15. Revised Ammonia Mass Flow Rate and Velocity

Till now, we assumed that the shellside mass flow rate was given in accordance with the ideal system defined by Eq. (20); however, in actuality this is not the case.

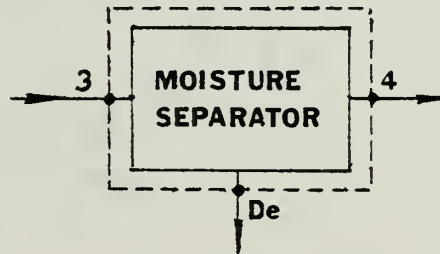
The diagramatic representation that follows better illustrates the heat absorption phase of the OTEC power system and will provide the basis for the analysis and optimization.

Note, as in the previous control volume analysis, the following conditions are assumed.

- . Steady state.
- . Steady-incompressible flow.
- . Change in potential and kinetic energies is negligible.



Analyzing the moisture separator as a separate control volume,



If we assume that there is no carry-over of vapor in the separator drain, then

$$x_3 \dot{m}_3 = x_4 \dot{m}_4$$

and

$$\dot{m}_3 = \frac{x_4}{x_3} \dot{m}_4 \quad (43)$$

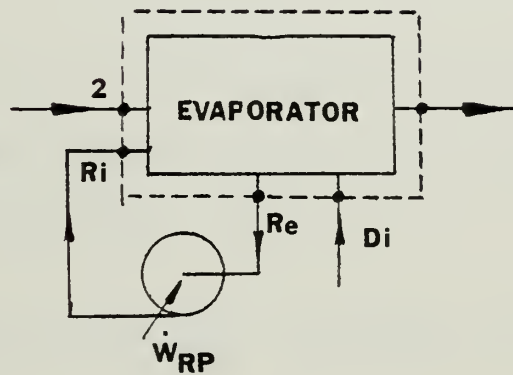
However, for reasons of flow continuity, the mass flow rate through the separator drain must be included in the control volume analysis; therefore

$$\dot{m}_3 = \dot{m}_4 + \dot{m}_{De} \quad (44)$$

Substituting Eq. (43) into (44) and solving for \dot{m}_{De} , the following expression can be derived

$$\dot{m}_{De} = \left(\frac{x_4}{x_3} - 1 \right) \dot{m}_4 \quad (45)$$

Looking at the evaporator as a separate control volume,



the energy balance is

$$\dot{Q} + \dot{m}_2 h_2 + \dot{m}_{Ri} h_{Ri} + \dot{m}_{Di} h_{Di} = \dot{m}_3 h_3 + \dot{m}_{Re} h_{Re}$$

Assuming the change in enthalpy across the re-flux pump and the difference between the separator drain outlet and evaporator inlet are negligible, the energy balance becomes

$$\dot{Q} + \dot{m}_2 h_2 + \dot{m}_{De} h_{De} = \dot{m}_3 h_3 \quad (46)$$

where $h_{oe} = h_f \left(\frac{P_3 + P_4}{2} \right)$ fluid drained from the separator is assumed to be a saturated liquid.

Furthermore, a mass balance of the evaporator control volume can be expressed as

$$\dot{m}_2 + \dot{m}_{Ri} + \dot{m}_{Di} = \dot{m}_3 + \dot{m}_{Re} \quad (47)$$

where $\dot{m}_{Re} = \dot{m}_{Ri}$.

Solving Eq. (47) for the mass flow rate at state point 3 and substituting into Eq. (46) with Eq. (45) yields the following expression

$$\dot{Q} + \dot{m}_2 h_2 + \left(\frac{x_4}{x_3} - 1 \right) \dot{m}_4 h_{oe} = \dot{m}_2 \frac{x_4}{x_3} h_3 \quad (48)$$

In addition, a mass balance for steady-state, steady-flow indicates that the mass flow rates at state points 2 and 4 are equal and therefore

$$\dot{m}_4 = \dot{m}_2 \quad (49)$$

Using Eqs. (48) and (49), the revised mass flow rate at state point 2 may be determined. Concurrently, the revised average ammonia velocity acting on the tube profile geometry may be determined from this revised mass flow rate.

Using the revised ammonia velocity acting on the tube profile geometry and iterating from Eq. (31) until

an acceptable convergence criterion is achieved provides the pressure drops across the evaporator and moisture separator, and the properties at state points 3 and 4 for a given film temperature. The result is more representative of the heat absorption phase in the OTEC power cycle than is the commonly used ideal analysis.

In addition, solving for the revised temperature at state point 3,

$$T_3 = T_{SAT} \Big|_{P_3} \quad (50)$$

and iterating through Eq. (18) revises the film temperature and subsequent working fluid properties.

16. Revised Shellside Ammonia Heat Transfer Coefficient

In the search for acceptable correlations to predict the average evaporative heat transfer coefficient, two analytical treatments were found that lent themselves to OTEC power system conditions.

The first of these correlations seeks to predict thin film evaporation heat transfer coefficient for horizontal tubes [Ref. 6]. Owens [Ref. 6] uses (1) the similarity between evaporation and condensation, (2) the correlation forms of local evaporation heat transfer coefficients for water on a vertical tube developed by Chun and Seban, and (3) the dependence of heat transfer on the vertical spacing of the tubes as was experimentally demonstrated by Liu, to arrive at the following correlations for non-boiling thin film evaporation:

for laminar flow

$$\bar{h} = 2.2 \left(\frac{H}{d_o} \right)^{0.1} \left(\frac{\mu_f}{g \rho_f^2 K_f^3} \right)^{-1/3} \left(\frac{4\Gamma}{\mu_f} \right)^{-1/3} \quad (51)$$

for turbulent flow

$$\bar{h} = 0.185 \left(\frac{H}{d_o} \right)^{0.1} \left(\frac{\mu_f}{g \rho_f^2 K_f^3} \right)^{-1/3} \left(\frac{C_p \mu_f}{K_f} \right)^{0.5} \quad (52)$$

where $\frac{H}{d_o}$ = vertical spacing with respect to tube outer diameter.

Γ = tube flow rate per unit length.

The laminar-turbulent transition point is defined by the intersection of Eqs. (51) and (52)

$$Re_{TR} = 1680 \left(\frac{C_p \mu_f}{K_f} \right)^{-1.5}$$

The pseudo-Reynolds number for horizontal vertical falling film evaporation is defined by Ref. 7.

$$Re = \frac{4\Gamma}{\mu_f}$$

The second correlation combines boiling and evaporation of liquid films on horizontal tubes, applicable for vertical banks of plain and enhanced tubes [Ref. 8].

The overall model for a single tube is expressed as

$$\bar{h} = h_b + h_d \frac{L_d}{L} + h_c \left(1 - \frac{L_d}{L}\right) \quad (53)$$

where h_b = Rohsenow pool boiling correlation over the entire tube length given by

$$h_b = \frac{\mu_f h_{fg}}{C_{sf} \sqrt[3]{\frac{g_c \sigma}{g \rho_f}}} \left(\frac{C_{pf}}{h_{fg} Pr} \right) \Delta T^2 \quad (54)$$

with C_{sf} = function of the fluid-surface combination.

ΔT = wall temperature minus free stream saturation temperature.

σ_f = surface tension

h_d = heat transfer coefficient in the developing region.

$$h_d = \frac{3}{8} C_p \frac{\Gamma}{L_d}$$

$$L_d = \frac{\Gamma^{4/3}}{4\pi \rho \alpha} \left(\frac{3\mu_f}{g \rho_f^2} \right)^{1/3}$$

and h_c = fully developed heat transfer coefficient given for laminar flow by

$$h_c = 0.821 \left(\frac{2}{K^3 g} \right)^{-1/3} \left(\frac{4\Gamma}{\mu_f} \right)^{-0.22} \quad (55)$$

and, for turbulent flow,

$$h_c = 3.8 \times 10^{-3} \left(\frac{\gamma^2}{k^3 g} \right)^{-1/3} \left(\frac{4\Gamma}{\mu_f} \right)^{0.4} \left(\frac{\gamma}{\alpha} \right)^{0.65} \quad (56)$$

where L = circumferential length of heated surface.

α = thermal diffusivity.

L_d = developing length around tube circumference.

Γ = flow rate per unit axial length of tube.

To apply Eq. (51) for a vertical bank of tubes, L is expressed as

$$L = N_t \pi d_o / 2$$

The laminar-turbulent transition point is defined by the intersection of Eqs. (55) and (56)

$$Re_{TR} = 5800 \left(\frac{\gamma}{\alpha} \right)^{-1.06}$$

As before, the pseudo-Reynolds number is defined by Ref. 7

$$Re = \frac{4\Gamma}{\mu_f} \quad (57)$$

After using Eq. (57) to establish which flow regime the system is operating in, the revised heat transfer coefficient for non-boiling thin film evaporation or nucleate

boiling may be calculated and then iterated with the initial assumption for the shellside heat transfer coefficient, Eq. (9). This will have a convergence effect on variables which are a function of the shellside heat transfer coefficient, moving them closer to actual OTEC system performance characteristics.

The user should be aware that the predictions for the OTEC power system using ammonia have been for the case where no boiling occurs in the film. This condition is dictated by industrial preference for plain tube heat exchangers to minimize fouling and the characteristic of ammonia to wet surfaces well, flooding out nucleation sites. A number of enhancement techniques have been developed to create nucleate boiling, including a variety of tube configurations and surface preparations; however, a preference for them has not materialized. The nucleate boiling development in Eq. (51) which would be indicative of tube enhancement is provided for information only and will not be included in the optimization or summary of conclusions.

Having described the methods used to predict the shellside heat transfer coefficient, we can complete this chapter of the OTEC power system analysis by constructing the heat exchanger cost analysis.

17. Evaporator Cost Analysis

At the request of TRW, Wyatt Industries, a large exchanger fabricator, prepared cost estimates for three different sizes of vertically configured evaporators and condensers, based upon initial design specifications prepared

by TRW. Based upon these estimates, TRW developed sets of equations that represent the costs of various heat exchanger component parts for shell diameters ranging from 10-35 ft and 35-50 ft [Ref. 9].

The following are the TRW evaporator cost (\$) equations as a function of outer tube diameter (inch), total number of tubes and tube-sheet diameter (ft) for tube-sheet diameters of 10-35 ft.

. Drilling time/tube sheet thickness

$$t_d = 0.66 (d_o - 0.5) \quad (58)$$

. Thickness of the tube sheet

$$t_{Ts} = 0.56 T_{SD}^{0.68} \quad (59)$$

. Tube sheet labor cost

$$C_{TSL} = 156695 (N_t / 9630) (t_d / 0.66) (t_{Ts} / 4) \quad (60)$$

. Tube sheet material cost

$$C_{TSM} = 189.486 T_{SD}^{2.3} \quad (61)$$

. Tube installation cost

$$C_{TI} = 34 N_t d_o^{0.7} \quad (62)$$

. Heat exchanger shell cost

$$C_{HXS} = 177265 \left(\frac{L_t + 6}{31} \right) (T_{SD} / 18)^2 \quad (63)$$

. Ammonia distribution plate and battles cost

$$C_{DPB} = 93865.75 (N_t/9630) (t_d/0.66) (T_{SD}/18)^2 \quad (64)$$

. Bustle, flanges channels and flow plates cost

$$C_{BFCF} = 308550 (T_{SD}/18)^2 \quad (65)$$

. Tube material cost

$$C_{TM} = (E1 L_t + E2) N_t \frac{d_o}{1.5} \quad (66)$$

where $E1$ = curve fit of tube cost per foot.

$E2$ = tube machining cost if required

. Heat exchanger head costs

$$C_{HXX} = 53240 (T_{SD}/18)^3 \quad (67)$$

. Water inlet, nozzles and supports cost

$$C_{WNS} = 220310.75 (T_{SD}/18)^2 \quad (68)$$

. Tube welding costs (Titanium tubes)

for $N_t \leq 36000$

$$C_{TW} = 14.73 N_t^{1.03} (d_o/1.5)^{0.7} \quad (69)$$

for $N_t > 36000$

$$C_{TW} = 0.8797 N_t^{1.3} (d_o/1.5)^{0.7}$$

The sum of cost Eqs. (60) through (69) would equal the cost to fabricate one OTEC evaporator with a tube sheet diameter of 10-35 feet (all the preceding component costs have been adjusted for current pricing at a 10% annual rate of inflation).

If our analysis is based on a 30-year life-cycle criterion, no adjustments are necessary to any component cost equation if titanium tubing is used due to its anti-corrosive qualities; however, using aluminum tubing (i.e., Al-5052), the expense of retubing must be considered to meet the criterion of a 10-year life cycle for aluminum tubing. This implies Eq. (61) and (66) must be modified to reflect the costs of retubing at the 10 and 20-year point in the cycle.

. Aluminum tube installation cost

$$C_{ATI} = C_{TI} [1 + (1+i)^{10} + (1+i)^{20}] \quad (70)$$

where i = projected inflationary rate (input by customer)

. Aluminum tube material cost

$$C_{ATM} = C_{TM} [1 + (1+i)^{10} + (1+i)^{20}] \quad (71)$$

For tube sheet diameters of 35-50 ft the following cost relationships apply [Ref. 9]:

. Equations for drilling time/tube sheet thickness (58), thickness of tube sheet (59), and tube material costs remain unchanged.

. Tube sheet labor and material cost (titanium)

$$C_{TSL} = 55.189 N_t^{0.791} T_{SD}^{0.68} t_d \quad (72)$$

$$C_{TSM} = 29.566 T_{SD}^{2.014} t_d \quad (73)$$

. Tube sheet labor and material cost (aluminum)

$$C_{TSL} = 73.181 N_t^{0.741} T_{SD}^{0.68} t_d \quad (74)$$

$$C_{TSM} = 354.3 T_{SD}^{1.61} t_{TS} \quad (75)$$

. Tube installation costs

$$C_{TI} = 36.542 N_t d_o^{0.7} \quad (76)$$

. Heat exchanger shell cost

$$C_{HXS} = 12.544 (L_t + 6) T_{SD}^{2.06} \quad (77)$$

. Ammonia distribution plate and baffle costs

$$C_{DPB} = 158.099 T_{SD}^{1.82} + 72.419 N_t^{0.873} t_d \quad (78)$$

. Bustle, flanges, channels, and flow plate costs

$$C_{BFCF} = 472.977 T_{SD}^{2.12} \quad (79)$$

. Heat exchanger head cost

$$C_{HXH} = 1725.31 T_{SD}^{1.45} \quad (80)$$

. Water inlet, nozzles and support cost

$$C_{WINS} = 7445.297 T_{SD}^{1.1} \quad (81)$$

. Tube welding costs (titanium tubes)

for $N_t \leq 36000$

$$C_{TW} = 14.73 N_t^{1.03} (d_o/1.5)^{0.7} \quad (82)$$

for $N_t > 36000$

$$C_{TW} = 0.8797 N_t^{1.03} (d_o/1.5)^{0.7}$$

As indicated previously, the cost to fabricate one OTEC evaporator with a tube sheet diameter 35 to 50 ft is equal to the sum of component costs Eqs. (72) through (83) (all the preceding component costs have been adjusted for current pricing at a 10% annual rate of inflation).

For an analysis based on a 30-year system life-cycle criterion, the additional costs for aluminum retubing must be considered and Eqs. (70) and (71) apply.

IV. PARASITIC LOSSES

A. INTRODUCTION

This chapter describes in detail the programming analysis for parasitic losses which include: (1) pumping and pipe requirements for both cold and hot salt water systems, (2) pumping and pipe requirements for the working fluid (ammonia) circulation and re-flux systems, and (3) turbine generator losses due to inefficiencies. Hotel requirements have not been incorporated into the analysis, but could be included for the final design analysis.

Pumping power requirements will be determined through the use of the general energy equation between the inlet and outlet of the system control volume [Ref. 3].

$$\int_0^i \frac{dP}{\rho} + \frac{V_i^2}{2} + g Z_i = \frac{V_o^2}{2} + g Z_o + \dot{W}_s + (Losses)_{i \rightarrow o}$$

To determine the pumping power \dot{W}_s the following effects will be evaluated:

1. Density head.
2. Friction losses.
 - . Intake piping.
 - . Heat exchanger tubing.
 - . Exit piping (if employed).
3. Thermodynamic pressure head.
4. Elevation head.

5. Minor losses.

- . Intake piping inlet configuration (contraction).
- . Intake piping screen (obstruction).
- . Flow through valves, elbows, etc.
- . Outlet piping (expansion).
- . Inlet to heat exchanger tubing (contraction).
- . Outlet from heat exchanger tubing (expansion).
- . Outlet of exit piping (if employed).

In the above pump head evaluations, the following inputs are specified:

- . Pipe lengths (hot, cold, ammonia circulation and re-flux piping).
- . Inner pipe diameters (initialized and treated as a design variable by the optimization code).
- . Absolute roughness corresponding to piping/tubing material (designer specified).
- . Fluid velocity (initialized and treated as a design variable by the optimization code).
- . Pump mechanical and electrical efficiencies.

As an overview of the parasitic pump loss analysis, the following major steps in the algorithm are listed in order of their execution:

- . Hot pipe salt water pump.
 - .. Inlet piping friction losses (86).
 - .. Minor piping losses due to inlet screen (87) and plenum design to evaporator core (88).
 - .. Evaporator core minor losses (89, 90) and tubeside friction losses.
 - .. Total pressure losses (92) and pumping head (93).
 - .. Pumping power requirements (95).

- .. Pump cost analysis (96).
- . Cold pipe salt water pump.
 - .. Initialize cold pipe inner diameter and SW velocity (design variables).
 - .. Minor losses due to inlet ducting (97) and plenum design to condenser core (98).
 - .. Inlet piping friction losses (99).
 - .. Condenser core minor losses (100, 101) and tubeside friction losses (103).
 - .. Density head (104).
 - .. Total pressure losses (105).
 - .. Pumping power requirement (107).
 - .. Pump cost analysis (108).
- . Ammonia circulation pump.
 - .. Piping friction (109) and minor losses due to valving/elbows (110).
 - .. Pressure drop across evaporator shellside (112).
 - .. Thermodynamic head (113).
 - .. Elevation head (114).
 - .. Total pressure losses (115).
 - .. Pumping power requirement (116).
 - .. Pump cost analysis (118).
- . Ammonia re-flux pump.
 - .. Piping friction (119) and minor losses due to valving/elbows (120).
 - .. Thermodynamic head due to pressure drop of saturated liquid ammonia across evaporator shellside (122).
 - .. Elevation head (123).
 - .. Total pressure losses (124).

.. Pumping power requirements (126).

.. Pump cost analysis (127).

. Parasitic pump losses.

In the following section, the basic steps summarized above will be described in detail.

B. ANALYSIS OF PARASITIC LOSSES

1. Hot Pipe Salt Water Pump, P_{HP}

The pressure losses due to piping friction and associated minor losses will be determined using the Darcy-Weisbach correlation [Ref. 10].

$$\Delta P = \sum_{i=1}^n \rho \frac{K_i V^2}{2 g_c} \quad (83)$$

where K_i describes the resistance coefficient.

V = fluid velocity.

$$K_i = f \frac{L}{D} \quad (84)$$

where f = friction factor.

$\frac{L}{D}$ = equivalent length in pipe diameters.

In order to determine the friction factor, the pipe flow Reynolds number must be calculated.

$$Re_d = \frac{\rho_{sw} V_{sw} d_i}{\mu_{sw}}$$

where ρ_{sw}, μ_{sw} = properties of salt water at the hot pipe inlet temperature (assumed constant throughout the pipe).

V_{sw}, d_i = salt water velocity and inner pipe diameter (initialized and treated as design variables by the optimization code); velocity assumed constant over pipe length.

Pipe flow Reynolds number greater than 2300 will be considered turbulent.

for laminar flow

$$f = \frac{64}{Re_d} \quad (85)$$

for turbulent flow

$$f = \frac{1.325}{\left[\ln \left(\epsilon / 3.7 d_i + 5.74 / Re_d^{0.9} \right) \right]^2} \quad (86)$$

where ϵ = absolute roughness corresponding to piping material selected.

Eq. (86) yields a friction factor within one percent of the Colebrook equation and is valid for the following conditions [Ref. 9].

$$\cdot \quad 10^{-6} \leq \frac{\epsilon}{D} \leq 10^{-2}$$

$$\cdot \quad 5000 \leq Re_d \leq 10^8$$

Considering the resistance coefficient for pipe minor losses

- . Assume the inlet duct is the same size as the pipe inner diameter, but it is screened

$$K = 1.5 \quad (87)$$

- . Assume piping enters evaporator through an area which is abruptly changed [Ref. 11]

$$K = \left[1 - \left(d_i / T_{SD} \right)^2 \right]^2 \quad (88)$$

where T_{SD} = evaporator tube sheet diameter (assume tube sheet diameter is twice as large as the inner pipe diameter).

Summing the results of Eqs. (84), (87), and (88) to determine the total resistance coefficient, the pressure losses due to piping can then be determined using Eq. (83).

If a variety of valves or fittings are to be included with Eq. (84), Ref. 11 provides a representative listing of equivalent length-to-pipe-diameter values.

To analyze the pressure drop across the evaporator tubeside, we again use the Darcy-Weisbach correlation, but for different design assumptions.

- . Assume inlets to evaporator tubing are well rounded [Ref. 11]

$$K = 0.5 \quad (89)$$

- . Assume outlets of evaporator tubing expand to an infinite reservoir [Ref. 10]

$$K = 1.0 \quad (90)$$

Using the Reynolds number in the previous chapter, Eq. (5), the corresponding friction factor Eq. (85) or (86), and resistance coefficient can be determined

$$K_{CORE} = f \frac{L_t}{d_i} \quad (91)$$

where L_t, d_i = evaporator tube length and inner tube diameter and are initialized and treated as design variables by the optimization code.

Summing the results of the resistance coefficient in Eqs. (89), (90) and (91), the pressure losses due to the evaporator design may be determined using the Darcy-Weisbach correlation Eq. (83).

The results of the piping losses and core design losses are equivalent to the hot pipe salt water pumping system requirements

$$\Delta P_{pump} = \Delta P_{PIPE SYSTEM} + \Delta P_{EVAP DESIGN} \quad (92)$$

converting to pumping head

$$H = \frac{g_c}{\rho_{sw} g} \Delta P_{pump} \quad (93)$$

Pumping power in terms of horsepower can be determined using the following expression

$$P_{HP} = \frac{\dot{m}_{sw}}{\eta_p} \left(\frac{g H}{g_c} \right) \quad (94)$$

where η_p = pump mechanical efficiency (designer input).

\dot{m}_{sw} = salt water mass flow rate determined in previous chapter, Eq. (2).

To equate parasitic pump losses to power input, Eq. (94) is converted to the motor load requirement in terms of megawatts electrical.

$$P_{HP(MW)} = \frac{P_{HP}}{\eta_M} \times \text{CONVERSION FACTOR} \quad (95)$$

where η_M = pump motor efficiency (designer input).

Because of the high salt water flow rates and relatively low pumping heads, good engineering design would dictate the use of axial flow (propeller) type pumps.

Using the algorithm developed by TRW [Ref. 9] from data provided by Johnston Pump Co., and Process Equipment Co. (distributors of Ingersoll Rank and Johnston Pumps), the cost of salt water pumps can be expressed as

$$C_{pump} = \left[(D/1000) 0.75 + 50 \right] 1.21 \times 10^3 \quad (96)$$

where

$$D = \frac{\pi d_i^2}{4} V_{sw}$$

where d_i, V_{sw} = inner hot pipe diameter, salt water velocity
(initialized for analysis and treated as
design variables by the optimization code).

The above algorithm is valid for the following conditions

- . vertical, wet pit, propeller type pumps with cast iron steel columns with protective epoxy coating, stainless steel shaft and bronze impeller.
- . pump size from 155,000 through 750,000 GPM with total dynamic heads of 8 through 12 feet.

Eq. (96) has been adjusted for current pricing at a 10% annual rate of inflation.

2. Cold Pipe Salt Water Pump, P_{cp}

Using Reynolds number

$$Re_d = \frac{\rho_{sw} V_{sw} d_i}{\mu_{sw}}$$

where ρ_{sw}, μ_{sw} = properties of salt water at the cold pipe inlet temperature (assumed constant throughout the pipe).

V_{sw}, d_i = salt water velocity and inner pipe diameter (initialized and treated as design variable by the optimization code), velocity assumed constant over pipe length.

Pipe flow characteristics and friction factor can be identified. A pumping analysis will be developed for the cold pipe pump using the Darcy-Weisbach correlation, similar to the development in the preceding section.

Considering the resistance coefficient for minor pipe losses

. Assume the inlet duct is well rounded [Ref. 11].

$$K_{INLET} = 0.5 \quad (97)$$

. Assume piping enters condenser through an area which is abruptly changed [Ref. 10].

$$K_{PLENUM} = \left[1 + (d_i / T_{SD})^2 \right]^2 \quad (98)$$

where T_{SD} = condenser tube sheet diameter (assume tube sheet diameter is twice as large as the inner pipe diameter).

. Assume one ninety-degree elbow is required in system [Ref. 11].

$$\frac{L}{D} = 30$$

Summing the results of Eqs. (84), (97), and (98), the total resistance coefficient can be expressed as

$$K = f \left(\frac{L_P}{d_i} + \frac{L}{D} \right) + K_{INLET} + K_{PLENUM} \quad (99)$$

where L_p = length of cold pipe.

d_i = inner diameter of cold pipe.

Pressure losses due to piping can then be determined using the Darcy-Weisbach, Eq. (83).

In analyzing the pressure drop across the condenser tubeside, the Darcy-Weisbach correlation is used again, but for different design assumptions.

- . Assume inlets to evaporator tubing are well rounded.

$$K = 0.5 \quad (100)$$

- . Assume outlet of condenser tubing expands to an infinite reservoir.

$$K = 1.0 \quad (101)$$

Defining Reynolds number for condenser tubeside flow, while assuming

$$T_{BULK} = T_{COLD(INLET)} \quad (102)$$

$$Re_d = \frac{\rho_{sw} V_{sw} d_i}{\mu_{sw}}$$

where ρ_{sw}, μ_{sw} = properties evaluated at condenser tubeside bulk temperature (initially assumed equal to cold pipe inlet temperature).

V_{sw}, d_i = average salt water velocity through tubing, inner condenser tube diameter (both are initialized and treated as design variables by the optimization code).

The corresponding friction factor, Eq. (85) or (86), and resistance coefficient can be determined

$$K_{CORE} = f \frac{L_t}{d_i} \quad (103)$$

where L_t, d_i , the condenser tube length and inner tube diameter are initialized and treated as design variables by the optimization code.

Summing the results of the resistance coefficient in Eqs. (100), (101), and (103), the pressure losses due to the condenser design may be determined using the Darcy-Weisbach correlation, Eq. (83).

A complete analysis of cold pipe losses must also include the effect of density head and a corresponding increase in pumping power requirements.

For most engineering problems involving the flow of liquids through a pipe, where the temperature change in the pipe is small, the density of the fluid is considered to be a constant and the fluid is termed "incompressible." However, the flow problem in OTEC cold pipe systems is unique. We can continue to assume that there is negligible change in the fluid temperature, virtually unaffected by the ocean thermal gradients, because of the system's characteristic high mass

flow rates. However, the height of the water column (1500 to 3000 feet) inside the pipe requires the effect of fluid compressibility to be taken into consideration.

The effect of an increase in density with depth can be expressed by the integral

$$\int_i^e \frac{dP}{\rho g}$$

with a density head defined as²

$$H_\rho = Z_e - Z_i + \int_i^e \frac{dP}{\rho g}$$

Integrating the pressure-density variation, the density head reduces to [Ref. 12]

$$H_\rho = Z_e - Z_i + \frac{1}{\rho_o g} (P_e - P_i) \left[1 - \frac{K_m}{2} (P_e + P_i) \right]$$

where K_m = mean compressibility of salt water, f(salinity, temperature and pressure).

ρ_o = reference density at which K_m is evaluated.

Considering pressure at any depth obtained from the integral,

$$P = -g \int_i^e \rho(z) dz$$

the density head can be rewritten as follows

$$H_\rho = (Z_e - Z_i) - \frac{1}{\rho_o} \int_{Z_i}^{Z_e} \rho(z) dz \left\{ 1 - \frac{K_m}{2} \int_0^{Z_i + Z_e} \rho g dz \right\}$$

²Note that Z is measured as positive upward so that ocean depth values (Z_e, Z_i) are negative and $(Z_e - Z_i)$ is a positive quantity.

Rigorous procedures for calculating the density profile which is a function of temperature, salinity and pressure may be found in Ref. 13; however, they will not be discussed in this document.

For the purposes of simplification, the following solution technique was developed:

(1) If the liquid in the pipe is taken to have a constant density with respect to pressure, the compressibility approaches zero; the density head can then be expressed as

$$H_p = (z_e - z_i) - \frac{1}{\rho_i} \int_{z_i}^{z_e} \rho(z) dz$$

(2) Converting the geometric term for elevation to an equivalent integral expression

$$z_e - z_i = \frac{1}{\rho_i} \int_{z_i}^{z_e} \rho_i dz$$

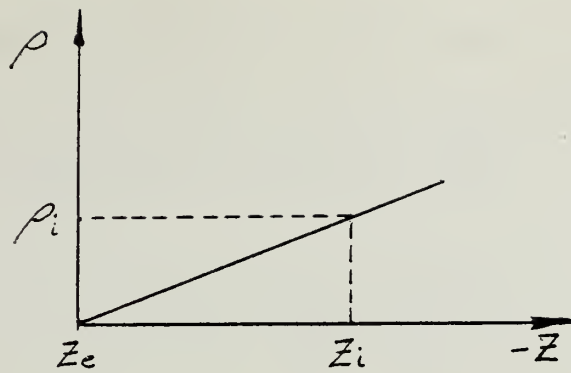
The reference density is taken to be the inlet value so that

$$\rho_i = \rho_o$$

and the density head can be rewritten as follows

$$H_p = \frac{1}{\rho_i} \int_{z_i}^{z_e} (\rho_i - \rho(z)) dz$$

(3) Assuming a linear distribution of density with depth, due to temperature variations, as illustrated below



the following linear expression for density with respect to depth may be formulated, where $Z_e=0$ for convenience.

$$\rho_i - \rho = (\rho_i - \rho_e) \left(1 - Z/Z_i \right)$$

(4) Applying the equation developed in section 3 to the density head integral above and integrating over the range of values for sea water depth (z), the following equation is derived as a linear approximation to the density variation of sea water with respect to depth

$$H_p = \left(\frac{\rho_i - \rho_e}{\rho_i} \right) \left(-\frac{Z_i}{2} \right)$$

where ρ_i, ρ_e = curve fit evaluations of density for specified depths of sea water. Data extracted from Ref. 14.

The results of the piping losses, core design losses, and density head are equivalent to the cold pipe salt water pumping system requirements

$$\Delta P_{pump} = \Delta P_{PIPE SYSTEM} + \Delta P_{COND DESIGN} + \Delta P_{DENSITY} \quad (105)$$

Using Eq. (93), Eq. (105) can be converted to a pumping head. Similarly, pumping power in terms of horsepower can be determined using Eq. (44).

$$P_{CP} = \frac{\dot{m}_{SW}}{\eta_P} \left(\frac{gH}{g_c} \right)$$

where

$$\dot{m}_{SW} = \rho_{SW} \left(\frac{\pi d_i}{4} \right)^2 V_{SW} \quad (106)$$

and ρ_{SW} = density of salt water evaluated for a constant inlet temperature.

V_{SW}, d_i = cold pipe salt water velocity, and inner diameter (initialized and treated as design variables by the optimization code). Note salt water velocity through cold pipe is considered to be constant.

Pumping power can then be expressed in terms of megawatts electrical

$$P_{CP(MW)} = \frac{P_{CP}}{\eta_M} \times \text{CONVERSION FACTOR} \quad (107)$$

where η_M = pump motor efficiency (designer input).

Using the same arguments for the selection of an axial flow (impeller type) pump, as used for the hot pipe salt water pump, the pump cost algorithm developed by TRW can be applied to the cold pipe salt water pump assuming

the required conditions are validated.

$$C_{\text{pump}} = \left[(D/1000) 0.75 + 50 \right] 1.21 \times 10^3 \quad (108)$$

Equation (108) has been adjusted for current pricing at a 10% annual rate of inflation.

3. Ammonia Circulation Pump, P_{CIRC}

The function of the ammonia circulation pump is to circulate and lift saturated liquid ammonia from the condenser hot well at state point 1 and increase its pressure to exceed the operating conditions in the evaporator at state point 2.

In order to evaluate these characteristics, the following pumping elements will be included in the analysis:

- . Piping losses (friction and minor).
- . Heat exchanger shellside pressure drop.
- . Thermodynamic pressure head.
- . Elevation head.

As in the preceding analysis, Reynolds number is used to determine pipe flow characteristics

$$Re_d = \frac{\rho V d_i}{\mu}$$

where ρ, μ = saturated liquid properties of ammonia for the temperature at state point 1 (assume any temperature increase from pump work is negligible).
 d_i = inner pipe diameter (initialized and treated as a design variable by the optimization code).

V = ammonia flow velocity determined from the preceding chapter, Eq. (50).

The ammonia pipe friction factor can then be determined from Eqs. (85) or (86), and the piping friction resistance coefficient can be expressed as

$$K = f \frac{L}{d_i} \quad (109)$$

where L = ammonia circulation pipe length (designer input).

Considering the resistance coefficient for minor pipe losses, assume there are four ninety-degree elbows in the system

$$K = 4 \frac{L}{D} \quad (110)$$

where $\frac{L}{D}$ = equivalent length in pipe diameters for a standard elbow [Ref. 11].

Summing the results of Eqs. (109) and (110), piping losses (friction and minor) can be determined using the Darcy-Weisbach equation (83).

$$\Delta P_{PIPE} = \rho \left[f \frac{L}{d_i} + 4 \frac{L}{D} \right] \frac{V^2}{2g_c} \quad (111)$$

The heat exchanger shellside pressure drop is also included in the pumping head requirement because it serves as a resistance to flow.

Pressure drop across the evaporator shellside was determined using the two-phase flow model (homogeneous) expressed by Eq. (33)

$$\Delta P_{EVAP} = \Delta P_{FRICTION} + \Delta P_{MOMENTUM} + \Delta P_{ELEVATION} \quad (112)$$

Since the pump is required to lift the working fluid to a higher elevation and increase its operating pressure, the following elements must be included in the analysis:

. Thermodynamic head

$$\text{where } \Delta P_{THERMO} = P_2 - P_1 \quad (113)$$

represents the difference in thermodynamic operating pressure between state point 2 and state point 1.

. Elevation head

$$\text{where } \Delta P_{ELEVATION} = Z_2 - Z_1 \quad (114)$$

Z_1 = datum.

Z_2 = elevation of the evaporator inlet above datum (taken to be equal to evaporator tube sheet diameter plus 25).

represents the lift head required to move the working fluid to a higher elevation.

The results of piping losses (111), evaporator pressure drop (112), the thermodynamic head (113) and elevation head (114) are equivalent to the ammonia circulation pump system requirements.

$$\Delta P_{\text{pump}} = \Delta P_{\text{PIPE}} + \Delta P_{\text{EVAP}} + \Delta P_{\text{THERMO}} + \Delta P_{\text{ELEVATION}} \quad (115)$$

Using Eq. (93) with ammonia properties, Eq. (115) can be converted to pumping head and finally expressed as pumping power (horsepower).

$$P_{\text{CIRC}} = \frac{\dot{m}_{\text{NH}_3}}{\eta_p} \left(\frac{gH}{g_c} \right) \quad (116)$$

where \dot{m}_{NH_3} = mass flow rate of ammonia determined by Eq. (20) of the previous chapter.

η_p = pump mechanical efficiency (designer input).

Pumping power can then be expressed in terms of megawatts electrical

$$P_{\text{CIRC(MW)}} = \frac{P_{\text{CIRC}}}{\eta_M} \times \text{CONVERSION FACTOR} \quad (117)$$

where η_M = pump motor efficiency (designer input).

Because of high pumping head and moderate flow rates, good engineering design would dictate the use of a single suction centrifugal flow type pump.

Using the algorithm developed by Westinghouse Electric Co. [Ref. 15] from data provided by Bingham Pump Division, Portland, Oregon, the cost of the ammonia circulation pump can be expressed as

$$C_{\text{pump}} = \left(\frac{\dot{m}_{\text{NH}_3} v_f}{80100} \right)^{0.64} 1.21 \times 10^5 \quad (118)$$

where \dot{m}_{NH_3} = mass flow rate of ammonia (lb_m/hr)

v_f = specific volume of saturated liquid ammonia
at state point 1 (ft^3/lb_m)

Eq. (118) has been adjusted for current pricing at a 10% annual rate of inflation.

4. Ammonia Re-flux Pump, $P_{\text{RE-FLUX}}$

The function of the re-flux pump is to recycle ammonia droplets which are not evaporated in the heat absorption process. Saturated liquid at approximately the heat exchanger's operating pressure is lifted from the evaporator drain to the ammonia feed inlet, for redistribution as droplets across the evaporator tube bundle. (Drainage mass flow rate is assumed to be equal to 30% of the evaporator inlet feed mass flow rate.)

In order to evaluate these characteristics, the following pump elements will be analyzed:

. Piping losses (friction and minor).

- . Thermodynamic pressure head.
- . Elevation head.

As in the preceding analysis, Reynolds number is used to determine pipe flow characteristics

$$Re_d = \frac{\rho V d_i}{\mu}$$

where ρ, μ = saturated liquid properties of ammonia for the average pressure across the evaporator.

d_i = inner pipe diameter (initialized and treated as a design variable by the optimization code).

V = ammonia flow velocity determined from the evaporator drainage mass flow rate assumed equal to 30% of the evaporator inlet feed mass flow rate (assume velocity constant throughout the pipe).

The re-flux pipe friction factor can be determined from Eqs. (85) or (86), and the piping resistance coefficient can be expressed as

$$K = f \frac{L}{d_i} \quad (119)$$

where L = ammonia re-flux pipe length (designer input).

Once again, considering the resistance coefficient for minor pipe losses assume there are four ninety-degree elbows in the system

$$K = 4 \frac{L}{D} \quad (120)$$

where $\frac{L}{D}$ = equivalent length in pipe diameters from a standard elbow.

Summing the results of Eqs. (119) and (120), piping losses (friction and minor) can be determined using the Darcy-Weisbach, equation (83)

$$\Delta P_{PIPE} = \rho \left[f \frac{L}{d_i} + 4 \frac{L}{D} \right] \frac{V^2}{2g_c} \quad (121)$$

In order to determine the thermodynamic pressure head, the pressure drop across the evaporator for the saturated ammonia liquid must be analyzed. Since the saturated vapor and liquid are in thermodynamic equilibrium, the results of Eq. (112) apply. Therefore

$$\Delta P_{LIQ} = P_3 - P_2$$

Therefore, the thermodynamic pressure head is equal to the pressure drop across the evaporator for the saturated ammonia liquid.

$$\Delta P_{THERMO} = \Delta P_{LIQ} \quad (122)$$

Finally, the elevation head is equal to the elevation of the evaporator feed inlet with respect to datum, the drain outlet.

Therefore,

$$\Delta P_{ELEV} = Z_2 - Z_1 \quad (123)$$

where Z_1 = datum, drain outlet.

Z_2 = elevation of the evaporator inlet above datum
(taken to be equal to the evaporator tube
sheet diameter plus 10).

The results of piping losses (121), the thermodynamic pressure head (122), and elevation head (123) are equivalent to the ammonia re-flux pump system requirements.

$$\Delta P_{pump} = \Delta P_{PIPE} + \Delta P_{ELEVATION} + \Delta P_{THERMO} \quad (124)$$

As before, using Eq. (93), Eq. (124) can be converted to a pump head and finally expressed in terms of pumping power (horsepower).

$$P_{RE-FLUX} = \frac{\dot{m}_R}{\eta_p} \left(\frac{gH}{g_c} \right) \quad (125)$$

where \dot{m}_R = drainage mass flow rate.

η_p = pump mechanical efficiency (designer input).

Pumping power can be expressed in terms of megawatts electrical

$$P_{RE-FLUX(MW)} = \frac{P_{RE-FLUX}}{\eta_M} \times \text{CONVERSION FACTOR} \quad (126)$$

where η_M = pump motor efficiency (designer input).

Using the same arguments for the selection of a centrifugal pump, the pump cost algorithm developed by Westinghouse can also be applied to the ammonia re-flux pump.

$$C_{\text{pump}} = \left(\frac{\dot{m}_R v_f}{80100} \right)^{0.64} 1.21 \times 10^5 \quad (127)$$

where \dot{m}_R = mass flow rate of evaporator drainage ammonia
(lb_m/hr)

v_f = specific volume evaluated at the average
evaporator pressure (ft³/lb_m)

Eq. (127) has been adjusted for current pricing at a 10% annual rate of inflation.

5. Parasitic Pump Losses

Parasitic pump losses is the summation of electrical auxiliary pumping requirements (hotel and maintenance loads not included) determined by Eqs. (95), (107), and (126).

$$P_{\text{Loss}} = P_{\text{HP}} + P_{\text{CP}} + P_{\text{CIRC}} + P_{\text{RE-FLUX}} \quad (128)$$

V. TURBINE AND ELECTRICAL POWER

A. INTRODUCTION

The turbine generator is one of the critical elements of the OTEC power system. Its energy conversion efficiency and efficiency of design have a major effect on the overall system performance. To illustrate this point, Ref. 16 reported that a three-point change in turbine efficiency from 85 to 88% results in a 3.6% increase in gross power, and a 5% increase in net power developed.

This chapter will describe the analysis to evaluate the expansion turbine thermodynamic properties and generator output. The use of these properties will determine the internal turbine efficiency and outlet quality subject to design and thermodynamic constraints. The relationship between the condenser operating pressure (design variable) and the turbine outlet quality will be used to initialize the heat rejection characteristics of the condenser.

General literature on turbomachinery designed for OTEC closed cycle systems indicates that a turbine having the following characteristics

- . Double flow, axial inflow,
- . Four stages of expansion,
- . Operating at 1800 RPM,

provides the optimum aerodynamic design [Ref. 16]. However, it is not the intent of this thesis to analyze the geometry

and performance parameters of the turbine. Turbine geometry such as

- . Specific speed and specific diameter,
- . Wheel diameter,
- . Rotational speed,
- . Blade height,
- . Blade stresses,

should be treated as a separate systems problem using optimization to improve state-of-the-art design.

Parasitic losses due to the following generator turbine inefficiencies will be evaluated in this section.

- . Generator mechanical and electrical.
- . Turbine mechanical.

As an overview of the turbine-generator analysis, the following major steps of the algorithm are listed in order of their execution:

- . Gross electrical output with no parasitic losses (129).
- . Enthalpy at state point 5 (130).
- . Turbine outlet quality (131).
- . Entropy at state point from a specified outlet quality (132).
- . Quality and enthalpy at state point 5s (133, 134).
- . Internal (adiabatic) turbine efficiency (135).
- . Turbine cost analysis (137).
- . Generator cost analysis (138).

In the following section, the basic steps summarized above will be described in detail.

B. ANALYSIS OF THE TURBINE AND ELECTRICAL POWER REQUIREMENTS

1. Gross Electrical Output and Inefficiency Losses

If the net electrical output required is indicated by (in terms of megawatts), the gross electrical load at the turbine shaft can be expressed as

$$\dot{E}_g = \frac{\dot{E}}{\eta_{TM} \eta_{GEN}} + P_{Loss} \quad (129)$$

where P_{Loss} = parasitic pump losses determined by Eq. (128).

η_{TM} = turbine mechanical efficiency (designer input).

η_{GEN} = generator mechanical and electrical efficiency (designer input).

The loss of electrical output due to generator-turbine inefficiencies is equal to

$$\dot{E}_{Loss} = \dot{E} \left(\frac{1}{\eta_{TM} \eta_{GEN}} \right)$$

2. Turbine Efficiency

The power developed across the turbine is

$$\dot{E}_g = \dot{m} (h_5 - h_4)$$

where \dot{m} = mass flow rate of ammonia given by Eq. (48).

h_4 = enthalpy at state point 4, Eq. (42).

From this, the enthalpy at state point 5 can be calculated.

If we initialize the operating pressure of the condenser in terms of P_5 , the following relations may be expressed

$$h_{5g} = h_g \big|_{p_5} \quad h_{5f} = h_f \big|_{p_5} \quad (130)$$

Therefore, it follows that the turbine outlet quality, x_5 , can be determined from

$$h_5 = h_{5f} + x_5 (h_{5g} - h_{5f}) \quad (131)$$

Having established the moisture separator outlet pressure and temperature, Eqs. (40) and (41), the entropy at state point 4 can be determined for a known separator outlet quality (designer input) using the following relations

$$\begin{aligned} S_{4f} &= S_f \big|_{T_4} & S_{4g} &= S_g \big|_{T_4} \\ S_4 &= S_{4f} + x_4 (S_{4g} - S_{4f}) \end{aligned} \quad (132)$$

For isentropic turbine work,

$$S_4 = S_{5s} \quad (133)$$

the quality at state point 5s may be determined using the following relations

$$\begin{aligned} S_{5g} &= S_g \big|_{T_5} & S_{5f} &= S_f \big|_{T_5} \\ S_{5s} &= S_{5f} + x_{5s} (S_{5g} - S_{5f}) \end{aligned} \quad (134)$$

Having determined the quality at state point 5s, the enthalpy can now be determined.

$$h_{5s} = h_{5f} + X_{5s} (h_{5g} - h_{5f}) \quad (135)$$

Using the results of Eqs. (41), (130), and (132), the internal turbine efficiency (adiabatic) can be determined, expressed by

$$\eta_T = \frac{h_4 - h_5}{h_4 - h_{5s}} \quad (136)$$

To ensure a realistic selection of internal efficiency, the following constraints are attached to the optimization code

- $h_5 < h_{5g}$
- $X_{5s} < X_5$
- $\eta_T \leq 90\%$

3. Turbine Cost Analysis

The ammonia turbine cost is based on an algorithm developed by Westinghouse to estimate manufacturing costs [Ref. 15].

$$C_{TURB} = 2.42 \times 10^6 \left(0.375 + \dot{E}_g / 136000 N_f \right) F_f \quad (137)$$

where \dot{E}_g = gross electrical output in KW.

N_f = 2 (for a double flow turbine).

F_f = flow price factor (1.0 for single-flow, 1.447 for double-flow).

The above algorithm is valid for the following conditions:

- . Double flow, axial inflow.
- . Multi-stage.
- . Operating at 1800 RPM.

The generator cost will be based on an algorithm developed by TRW from data provided by selected manufacturers,

$$C_{GEN} = (0.023 \dot{E}_G + 0.3) 1.21 \times 10^6 \quad (138)$$

and is valid for the following conditions

- . 1800 RPM rotor speed.
- . power factor 0.8.

Eqs. (137) and (138) have been adjusted for current pricing at a 10% annual rate of inflation.

VI. CONDENSER

A. INTRODUCTION

As indicated in the introduction to Chapter III, several heat exchanger concepts have been proposed for the closed-cycle OTEC system, with variations in their design.

The analysis to be presented for the condensing heat exchanger will be based upon the following design characteristics:

- . Single-pass shell and tube heat exchanger.
- . Horizontal/vertical orientation of tubes with an equilateral triangle or square tube profile.
- . Smooth plain-tube configuration (no enhancements).
- . Tube material (titanium or aluminum based on a 30-year life-cycle criterion).
- . Biofouling control based upon an achievable fouling factor.
- . Heat exchanger centerline located on sea surface.

As an overview of the condenser analysis, the following major steps in the algorithm are listed in order of their execution:

- . Initialization of design variables (DV).
 - .. Tube length.
 - .. SW velocity through condenser tubes.
 - .. Outer tube diameter.
 - .. Tube profile pitch ratio.
- . Amount of heat rejection (139).
- . Tubeside bulk temperature (142).

- . Total number of tubes (143).
- . Log mean temperature difference (144).
- . Conductance (146).
- . Number of transfer units (145).
- . Heat exchanger effectiveness (147).
- . Initially assume a value for ammonia heat transfer coefficient (151).
- . Single tube conductance (148).
- . Average heat rejection per tube (152).
- . Film temperature (153).
- . Revised ammonia heat transfer coefficient (154, etc.); iterate with (151).
- . Tube profile, flow parameters across the tube bank (158, etc.).
- . Tube sheet diameter (163).
- . Condenser shellside pressure drop for two-phase flow (166).
- . Revised properties at state point 1 (171, 172); iterate with (21).
- . Overall heat transfer coefficient (173).
- . Total heat transfer surface area (174).
- . Revised condenser tube length (175).
- . Heat exchanger cost analysis.

In the following section, the basic steps summarized above will be described in detail.

B. ANALYSIS OF THE CONDENSER

1. Amount of Heat Rejection, \dot{Q}

Using the calculated value for enthalpy at state point 5, equation (131) from the previous chapter, the ideal

values at state point 1, Eq. (21), and the steady-state mass flow rate of ammonia, Eq. (48), the amount of heat rejected by the condenser can be expressed as

$$\dot{Q} = \dot{m}_{\text{NH}_3} (h_5 - h_1) \quad (139)$$

2. Tubeside Bulk Temperature

As in condenser tubeside Reynolds number, salt water properties will be evaluated at bulk temperature, initially assumed equal to the cold pipe inlet temperature.

Using this premise, the condenser salt water capacity rate can be evaluated

$$C_{min} = \dot{m}_{cp} c_{p_{sw}} \quad (140)$$

where $c_{p_{sw}}$ = specific heat of salt water initially evaluated at the cold pipe inlet temperature.

\dot{m}_{cp} = mass flow rate of salt water through the cold pipe previously evaluated by Eq. (107).

Using the results of Eqs. (139) and (140), and the known cold pipe inlet temperature, the condenser salt water outlet temperature may be evaluated from the basic expression

$$\dot{Q} = C_{min} (T_{co} - T_{ci}) \quad (141)$$

where T_{co}, T_{ci} = condenser salt water outlet and inlet temperatures, respectively.

Having determined the condenser salt water outlet temperature, the revised bulk temperature can be expressed as

$$T_B = \frac{T_{c_c} + T_{c_i}}{2} \quad (142)$$

Using the revised condenser bulk temperature and iterating with Eq. (102) corrects the operating temperature for salt water properties which are essential to the analysis.

3. Total Number of Condenser Tubes, N_t

Since the mass flow rate of salt water through the cold pipe is equivalent to the mass flow rate through the condenser, according to the law of continuity,

$$\dot{m}_{cp} = \dot{m}_{cond}$$

it follows that the number of condenser tubes for a specified tube diameter, can be evaluated using the following expression:

$$\dot{m} = \rho_{sw} \frac{\pi d_i^2}{4} V_t N_t \quad (143)$$

where ρ_{sw} = average salt water density evaluated at bulk temperature.

d_i = inner tube diameter (initialized and treated as a design variable by the optimization code).

V_t = average salt water velocity through the condenser (initialized and treated as a design variable by the optimization code).

4. Log Mean Temperature Difference, LMTD

Using the result of Eq. (141), the known pipe salt water inlet temperature, and the inlet temperature of ammonia evaluated at state point 5, the LMTD of the condenser may be expressed as

$$LMTD = \frac{T_{c_o} - T_{c_i}}{\ln \left(\frac{T_5 - T_{c_i}}{T_5 - T_{c_o}} \right)} \quad (144)$$

5. NTU-Effectiveness Relations

The number of transfer units which is a measure of the condenser size can be determined from the basic expression

$$NTU = \frac{U_o A_o}{C_{min}} \quad (145)$$

where the conductance ($U_o A_o$) of the heat exchanger is a function of the heat absorbed and the LMTD.

$$\dot{Q} = (U_o A_o) LMTD \quad (146)$$

The condenser effectiveness can then be expressed as

$$\epsilon = 1 - e^{(-NTU)} \quad (147)$$

for a two-phase flow, regardless of the flow geometry.

6. Single-Tube Conductance, $U_o A_o$

Using the resistance analysis derived in Chapter III, Section 4 for an initialized tube length

$$L = L_i$$

the heat exchanger conductance for a single tube can be expressed as

$$U_o A_o = \frac{1}{\frac{1}{\eta_i h_{sw} A_i} + \frac{1}{A_i} R_{fsw} + \frac{\ln d_o/d_i}{2\pi K L} + \frac{1}{A_o} R_{fNH_3} + \frac{1}{\eta_o h_{NH_3} A_o}} \quad (148)$$

where h_{sw} = tubeside heat transfer coefficient.

R_{fsw} = salt water fouling heat transfer resistance.

K = thermal conductivity of the tube material.

A_o, A_i = total outer and inner tube surface areas (including fin and bare tube); tube length is initialized and treated as a design variable by the optimization code).

R_{fNH_3} = ammonia fouling heat transfer resistance

η_o, η_i = outer and inner total fin efficiency

a. Tubeside Reynolds Number

Since the salt water heat transfer correlation is dependent on tubeside flow, Reynolds number must be evaluated

$$Re_d = \frac{\rho_{sw} V_{sw} d_i}{\mu_{sw}}$$

where ρ_{sw}, μ_{sw} = salt water density and viscosity are evaluated for the fluid's bulk temperature.

d_i, V_{sw} = inner diameter and average salt water tube velocity.

Reynolds numbers greater than 2300 will be indicative of turbulent flow [Ref. 3].

b. Salt Water Heat Transfer Coefficient, h_{sw}

Once again the empirical relationship proposed by Sieder and Tate [Ref. 3] will be used for laminar heat transfer in tubes and as defined by

$$Nu_d = 1.86 (Re_d Pr)^{1/3} \left(\frac{d_i}{L} \right)^{1/3} \left(\frac{\mu}{\mu_w} \right)^{0.14}$$

Nusselt and Prandtl numbers are defined as

$$Nu_d = \frac{h_{sw} d_i}{k_{sw}} \quad (149)$$

$$Pr = \frac{C_{p_{sw}} \mu_{sw}}{k_{sw}} \quad (150)$$

where dynamic viscosity, specific heat, and thermal conductivity of salt water are evaluated at the salt water bulk temperature.

The effect of the viscosity ratio in the Sieder-Tate equation is considered negligible, and will hereafter be dropped from the expression. The assumptions and validity condition associated with the Sieder-Tate equation were stated in Chapter III, Section 4, and will not be repeated here.

For fully developed turbulent flow, again the Dittus=Boelter correlation [Ref. 3] was used.

$$Nu_d = 0.023 Re_d^{0.8} Pr^{0.3}$$

Nusselt and Prandtl numbers are previously defined by Eqs. (149) and (150). Assumptions and conditions for validity were stated in Chapter III, Section 4.

c. Salt Water Fouling Heat Transfer Resistance

As indicated previously, it will be assumed that the fouling resistance for tubeside salt water can be maintained at $.00025 \text{ (hr.ft}^2\text{.F/BTU)}$.

d. Ammonia Shellside Heat Transfer Coefficient, h_{NH_3}

Initially, h_{NH_3} will be assumed

$$h_{NH_3} = 1000 \text{ (BTU/hr.ft}^2\text{.F)} \quad (151)$$

since its value cannot be directly calculated during this phase of the analysis.

Using the following single-tube thermal resistance

$$R_1 = \frac{1}{\eta_i h_{sw} \pi d_i L}$$

$$R_2 = \frac{1}{\eta_i h_{fsw} \pi d_i L}$$

$$R_3 = \frac{\ln d_o/d_i}{2\pi K L}$$

$$R_5 = \frac{1}{\eta_o h_{NH_3} \pi d_o L}$$

an initial value for single tube conductance (outer tube surface) may be calculated

$$U_o A_o = \frac{1}{R_1 + R_2 + R_3 + R_5}$$

7. Film Temperature for Property Evaluation, T_f

In order to evaluate the shellside ammonia heat transfer coefficient, working fluid properties must be evaluated at the film temperature.

This can be accomplished by using the results of the single tube conductance, the tube side bulk temperature and the working fluid saturation temperature, expressed in the following equation for single tube heat transfer rate (average).

$$\dot{Q} = U_o A_o (T_5 - T_{BULK}) \quad (152)$$

Again using the resistance analysis as in Chapter III, the shellside wall temperature may be expressed as

$$T_{W2} = T_{BULK} + \dot{Q} (R_1 + R_2 + R_3)$$

Knowing the shellside wall temperature and the free-stream temperature, the film temperature can be derived from their arithmetic mean

$$T_f = \frac{T_{W2} + T_5}{2} \quad (153)$$

For purposes of this calculation, saturated temperature conditions at state point 5 are taken to represent

free-stream conditions, when in fact the two-phase process will experience a pressure drop and a corresponding drop in temperature.

8. Revised Shellside Ammonia Heat Transfer Coefficient,
 \bar{h}_{NH_3}

This analysis will include correlations for both horizontal and vertical heat exchangers.

In the horizontal-tubed condenser, Nusselt's correlation was used as a predictor [Refs. 7 and 17],
 for laminar flow

$$\bar{h} = 0.95 \left(\frac{K_f^3 \rho_f^2 g L}{\mu_f w} \right)^{1/3} \quad (154)$$

where w = estimate of ammonia mass flow rate across each tube.

K_f, ρ_f, μ_f = properties evaluated at film temperature.

L = tube length (initialized and treated as a design variable by the optimization code).

This correlation is probably conservative, since it does not consider turbulence due to high vapor velocity or splashing of condensate [Ref. 7].

For turbulent flow, Nusselt's correlation is increased by 10% as recommended by Jakob [Ref. 17]

$$\bar{h} = 1.045 \left(\frac{K_f^3 \rho_f^2 g L}{\mu_f w} \right)^{1/3} \quad (155)$$

The laminar-turbulent transition point is defined by a Reynolds number of 2100, where the pseudo-Reynolds number for film-type condensation on horizontal tubes is defined as [Ref. 7]

$$Re = \frac{2\Gamma}{\mu_f}$$

where Γ = mass flow rate of condensate per tube over its length.

In the vertical tubed condenser, both Nusselt's and Kirkbride's correlations were used as predictors [Ref. 7].

For laminar flow, Nusselt's correlation is increased by a factor of 1.28 as recommended by McAdams [Ref. 7]:

$$\bar{h} = 1.28 \left[1.47 \left(\frac{\mu_f}{K_f^3 \rho_f^2 g} \right)^{-1/3} \left(\frac{4\Gamma}{\mu_f} \right)^{-1/3} \right] \quad (156)$$

where Γ = mass flow rate of condensate per tube over its diameter.

For turbulent flow, Kirkbride's correlation is applied

$$\bar{h} = 0.0077 \left(\frac{\mu_f^2}{K_f^3 \rho_f^2 g} \right)^{-1/3} \left(\frac{4\Gamma}{\mu_f} \right)^{0.4} \quad (157)$$

The laminar-turbulent transition point is defined by a Reynolds number of 1800, where the pseudo-Reynolds number for film-type condensation on vertical tubes is defined as [Ref. 7]

$$Re = \frac{4\Gamma}{\mu_f}$$

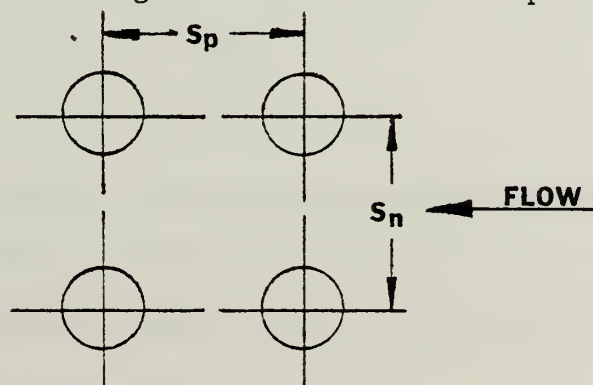
After using the pseudo-Reynolds number to establish the flow in which regime the system is operating, the revised heat transfer coefficient for film-type condensation may be calculated and then iterated with the initial assumption for the shellside heat transfer coefficient, Eq. (151). Once again this will have a convergence effect on variables in which the shellside heat transfer coefficient is a function, moving closer to actual OTEC system operating point characteristics.

9. Tube Profile, Flow across Tube Bank, and Tube Sheet Diameter

Since the condenser tube bundle involves multiple rows of tubes, the geometry of the tube profile arrangement is important to determine the shellside heat transfer coefficient, the tube sheet diameter and the shellside pressure drop associated with the "homogenous" two-phase flow model [Ref. 4].

Using the same arrangements shown in Chapter III, Section 2,

IN-LINE



$$S_n = P_R d_o \quad (158)$$

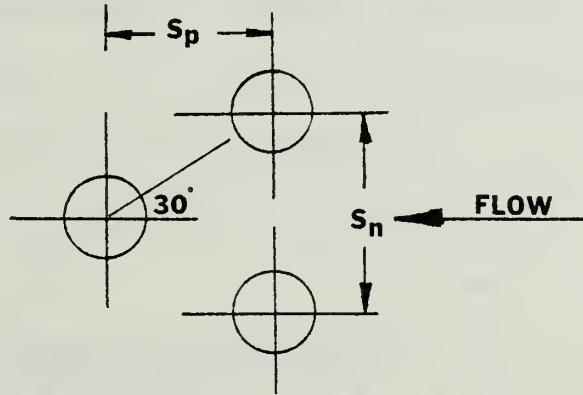
$$A_p = S_n^2 \quad (159)$$

where S_n = pitch ratio x outer tube diameter.

P_R = pitch ratio (initialized and treated as a design variable for the optimization code).

A_p = tube profile area per tube

STAGGERED



where

$$S_n = 2 P_R d_o \sin 30^\circ \quad (160)$$

$$S_p = P_R d_o \cos 30^\circ \quad (161)$$

$$A_p = S_n S_p \quad (162)$$

the ratio of minimum flow area to the frontal area can be expressed as

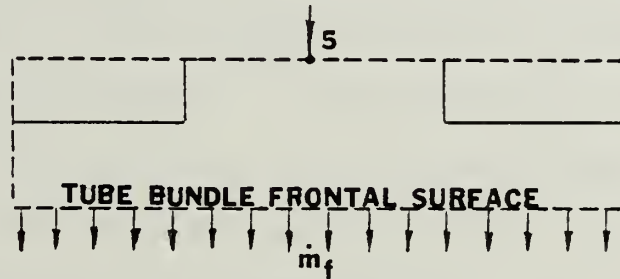
$$\frac{A_{ff}}{A_f} = \frac{S_n - d_o}{S_n} \quad (163)$$

Using the selected tube profile geometry and knowing the number of condenser tubes by Eq. (143), the tube sheet diameter for the condenser design can be evaluated from the following expression

$$N_t A_p = \frac{\pi T_{SD}^2}{4} \quad (164)$$

where T_{SD} = Tube sheet diameter.

To analyze the shellside ammonia flow velocity, the following control volume is introduced (turbine generator discharge and top portion of the condenser).



Since the mass flow rate remains unchanged across any boundary

$$\dot{m}_5 = \dot{m}_f$$

Furthermore, if we assume the condenser has the capability to evenly distribute vapor across the tube bundle (distribution baffles), the following development applies to the vapor coverage:

Let $(A_f)_{VAP} = A_f \eta$

where η = percent of tube frontal area which is covered by vapor.

$$\dot{m}_5 = \rho_5 A_5 V_5$$

$$\dot{m}_f = \rho_f A_f V_f \eta$$

where A_5 = condenser inlet cross-sectional area.

V_5 = turbine discharge ammonia velocity.

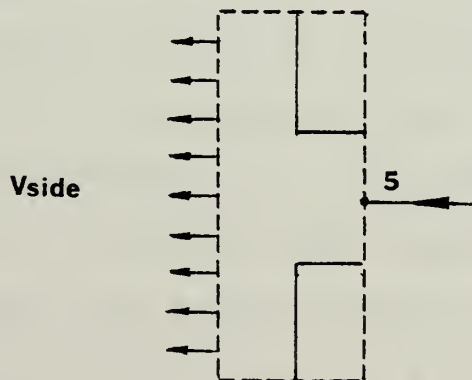
Therefore

$$V_f = \frac{\rho_5 A_5}{\rho_f A_f \eta} V_5$$

If $\eta = \rho_5 A_5 / A_f \rho_f$, it follows that the turbine discharge velocity is equal to the average velocity of ammonia at the tube frontal area boundary. A determination of the distribution fraction η requires a detailed knowledge of the design of the turbine/condenser interface. In the absence of this information it is assumed that

$$V_f = V_5$$

A similar argument could be presented for a vertical tubed condenser where turbine discharge is admitted to a distribution ring that bands the condenser tube bank. Exhaust vapor would travel radially through the tube bundle and then collect at the bottom after vertical film-condensation.



Again, in the absence of a detailed design, it is assumed that

$$V_{SIDE} = V_5$$

Considering the minimum free-flow area for a horizontal tubed condenser, A_{ff} can be derived using Eq. (163) and the projected frontal area.

$$A_f = T_{SD} L_t$$

$$A_{ff} = A_f \left(\frac{S_n - d_o}{S_n} \right) \quad (165)$$

where A_f = the flow frontal area.

L_t = tube length.

For vertical condensers

$$A_f = \pi T_{SD} \times \text{FRONTAL LENGTH OF VAPOR INLET FLOW}$$

Using the previously calculated value of the ammonia flow rate and Eq. (165), mass velocity for the minimum free flow area can be expressed as

$$G = \frac{\dot{m}_4}{A_{ff}} \quad (166)$$

10. Pressure Drop of Two-Phase Flow across a Bank of Tubes, ΔP

The pressure drop in the two-phase flow condensing heat exchanger will be determined using the homogeneous model introduced in Chapter III. The model will consist of three components -- friction loss, momentum change, and elevation pressure drop arising from the effects of gravity.

The local pressure drop for a two-phase flow may be expressed as

$$\Delta P_{COND} = \Delta P_{FRICTION} + \Delta P_{MOMENTUM} + \Delta P_{ELEVATION} \quad (167)$$

For a given channel length, L_c , the pressure drop components can be expressed by

$$\Delta P_{FRICTION} = \frac{f G^2 \bar{v}}{D_e 2 g_c} L_c \quad (168)$$

$$\Delta P_{MOMENTUM} = \frac{G^2 \bar{v}}{g_c} \quad (169)$$

$$\Delta P_{ELEVATION} = \frac{g}{\bar{v} g_c} L_c \quad (170)$$

where f = single phase friction factor by Jakob expressed in Eq. (35) or (36).

G = mass flow velocity determined from Eq. (166).

L_c = channel flow length, defined for horizontal tubed condensers as $L_c = T_{SD}$ (tube sheet diameter) and for vertical tubed condensers as $L_c = L_t$ (tube length).

D_e = equivalent diameter of flow channel, defined by

$$D_e = P_R d_o - d_o$$

\bar{v} = mean specific volume defined by

$$\bar{v} = v_f \left[1 + \frac{x}{v_f} (v_g - v_f) \right]$$

where X = quality of mixture (state point 5).

v_f = specific volume of liquid (state point 1)

v_g = specific volume of vapor (state point 5).

All components of the pressure drop model Eqs. (168, 169, and 170) can be determined using the preceding information.

11. Revised Properties at State Point 1

Since Eq. (167) represents the pressure drop across the condenser shellside, the actual pressure at state point 1 or condenser outlet may be determined from

$$P_1(NEW) = P_1 - \Delta P_{COND} \quad (171)$$

where P_1 is previously described as the condenser operating pressure for the ideal cycle.

Operating on the saturated liquid line on the Temperature-Entropy diagram, the following properties are defined:

$$h_1(NEW) = h_f \big|_{P_1(NEW)} \quad T_1(NEW) = T_{SAT} \big|_{P_1(NEW)} \quad (172)$$

The subscript (NEW) representing a revised property will hereafter be dropped from the expression in Eq. (172).

Until now, we assumed the condenser outlet temperature and pressure were designed to operate as an ideal system, without a pressure drop. Therefore, using the revised temperature at state point 1 and iterating over the range from Eq. (21) until an acceptable convergence criterion is achieved, all the preceding variables as function of T_1

will be reevaluated to complete the closed-loop cycle of the simulated OTEC power system.

12. Overall Heat Transfer Coefficient, U_o

The quantity "U" represents a measure of the total thermal resistances in the flow path. Therefore, using the tube conductance expressed in Eq. (148) which is divided by the outer heat transfer surface area of a single tube, the overall heat transfer coefficient for the condenser can be determined.

The thermal resistances are now expressed as

$$R_1 = \frac{d_o}{\eta_i h_{sw} d_i}$$

$$R_2 = \frac{d_o}{\eta_i h_{fsw} d_i}$$

$$R_3 = \frac{d_o \ln d_o / d_i}{2K}$$

$$R_5 = \frac{1}{\eta_o h_{NH_3}}$$

and the overall heat transfer coefficient for the condenser may be calculated using

$$U_o = \frac{1}{R_1 + R_2 + R_3 + R_5} \quad (173)$$

13. Total Condenser Heat Transfer Surface Area, A_t

Having determined the corrected number of condenser transfer units (145), salt water capacity rate (140) and overall heat transfer rate (173), the total condenser heat transfer area can be calculated from the NTU expression

$$NTU = \frac{U_o A_t}{C_{min}} \quad (174)$$

14. Revised Condenser Tube Length

Using the total heat transfer surface area calculated from Eq. (174) and the total number of condenser tubes (143), the revised condenser tube length can be determined from the basic expression

$$A_t = N_t \pi d_o L_t (REVISED) \quad (175)$$

At this time, it is necessary to iterate the condenser design until the two values (initial and revised) of the tube length converge. This iteration may be accomplished by the COPES routine if the following constraint is defined

$$L_{DIFF} = L_t (REVISED) - L_t (INITIAL)$$

Minimization of this difference will cause continual adjustment of the required tube length, already treated as a design variable by the optimization code.

15. Condenser Heat Exchanger Cost Analysis

As indicated in Chapter III, TRW developed sets of equations to represent the costs of various heat exchanger component parts for shell diameters ranging from 10-35 feet and 35-50 feet [Ref. 9].

The following are the TRW component cost equations for the condensing heat exchanger. Prior equation reference numbers will be substituted where equalities exist with the evaporative heat exchanger component cost expressions.

for tube sheet diameter 10-35 feet

. Drilling time/tube sheet thickness. (58)

. Thickness of the tube sheet. (59)

. Tube sheet labor cost. (60)

. Tube sheet material cost. (61)

. Tube installation cost. (62)

. Heat exchanger drill cost. (63)

. Ammonia distribution plate and baffles cost.

$$C_{DPB} = 1.539 \times 10^{-2} t_d N_t T_{SD}^{2.0} \quad (176)$$

. Bustle, flanges, channels and flow plate cost.

$$C_{BFCF} = 1185.286 T_{SD}^{2.0} \quad (177)$$

. Tube material cost.

$$C_{TH} = (C_1 L_t + C_2) N_t d_o / 1.5 \quad (178)$$

where C_1 = curve fit of tube material cost
per foot.

C_2 = tube machining cost if required.

. Heat exchanger header cost. (67)

. Water inlet, nozzles and support cost.

$$C_{WINS} = 10106.475 T_{SD} \quad (179)$$

. Tube welding costs (Titanium tubes). (69)

The sum of the preceding costs would equal the cost to fabricate one OTEC condenser with a tube sheet diameter of 10-35 feet (all the preceding component costs have been adjusted for current pricing at a 10% annual rate of inflation).

If our analysis is based on a 30-year life-cycle criterion, no adjustments are necessary to any component cost equation if titanium tubing is selected. However, using Al 5052-0, the expense of retubing must be considered to meet the 30-year life-cycle criterion, as in the case of the evaporation. For convenience, and possible subsequent modification, these considerations are repeated here.

Based upon the utility of Al 5052-0, two complete condenser retubings will be required to meet the basic 30-year criterion. This implies Eqs. (62) and (178) must be modified to reflect the costs of retubing at the 10 and 20 year point in the cycle.

. Aluminum tube installation cost.

$$C_{ATI} = C_{TI} \left[1 + (1+i)^{10} + (1+i)^{20} \right] \quad (180)$$

where i = projected annual inflationary rate (input by customer).

. Aluminum tube material cost.

$$C_{ATM} = C_{TM} \left[1 + (1+i)^{10} + (1+i)^{20} \right] \quad (181)$$

for tube sheet diameter 35-50 feet.

. Drilling time/tube sheet thickness (58)

. Thickness of the tube sheet. (59)

. Tube sheet labor and material costs (titanium). (72, 73)

. Tube sheet labor and material costs (aluminum). (74, 75)

. Tube installation cost. (76)

. Tube material cost. (178)

. Heat exchanger shell cost. (77)

. Ammonia distribution plate and baffles cost.

$$C_{DPB} = 9.825 N_t^{0.979} t_d \quad (182)$$

. Bustle, flanges, channels and flow plate.

$$C_{BFCF} = 382.824 T_{SD}^{2.184} \quad (183)$$

. Heat exchange head cost.

$$C_{HxH} = 939.62 T_{SD}^{1.43} \quad (184)$$

- . Water inlet, nozzles, and supporters cost.

$$C_{WINS} = 7453.6 T_{SD}^{1.056} \quad (185)$$

- . Tube welding cost (titanium tubes). (82)

As indicated previously, the cost to fabricate one OTEC condenser with a tube sheet diameter of 35 to 50 feet is equal to the sum of component costs (note, all the preceding component costs have been adjusted for current pricing at a 10% annual inflation rate).

For an analysis based on a 30-year life-cycle criterion, the additional costs for replacing aluminum tubing must be considered and Eqs. (180) and (181) apply.

VII. NUMERICAL OPTIMIZATION

A. INTRODUCTION

Nearly all design processes attempt the minimization or maximization of some parameter or design objective. For the design to be acceptable, it must satisfy a set of constraints which impose limits or bounds on design parameters.

For the stated problem a computer program can be written to perform the basic analysis of the proposed design. If any parameters fall outside the prescribed bounds, the design engineer changes the parameters and re-runs the program. In effect, the computer code provides the analysis with the engineering making the actual design decisions.

A logical extension to the computer-aided approach is a fully automated design, where the computer also makes the actual design decisions and performs trade-off studies. The COPES program provides this automated design and trade-off capability by the use of the optimization program COPES/CONMIN [Ref. 18]. COPES is an acronym for Control Program for Engineering Synthesis, and CONMIN is an acronym for CONstrained function MINimization. Subsequently, a FORTRAN analysis program simulating a closed-cycle OTEC power system can be coupled to the COPES program for automated design, using some basic programming guidelines [Ref. 18].

B. COPES/CONMIN

There are many numerical optimization schemes available to the engineer. Methods employed by these schemes fall into four basic categories: random search, sequential unconstrained minimization, optimality criteria, and direct constrained optimization. The optimization program, selected for automated design analysis of the simulated OTEC power system, is based upon direct constrained optimization.

Before any discussion of the optimization technique, basic definitions are summarized for convenient reference [Ref. 19]:

- . Design variables - those parameters which the optimization program is permitted to change in order to improve the program.
- . Objective function - the parameter which is to be minimized or maximized during the optimization process.
- . Inequality constraint - one-sided conditions which must be satisfied for an acceptable design.
- . Equality constraint - condition which must be equaled for the design to be acceptable.

. Side constraints - upper and lower bounds in a design variable.

Assuming that the FORTRAN analysis program has been developed and a particular objective function has been selected, the general optimization problem can be stated as [Ref. 20]:

Find the vector of design variables, \bar{X} , to

$$\text{Minimize } F(\bar{X}) \quad (186)$$

Subject to the constraints:

$$G_j(\bar{X}) \leq 0 \quad j=1, NCON \quad (187)$$

$$H_j(\bar{X}) = 0 \quad j=1, NEQ \quad (188)$$

$$VLB_i \leq \bar{X}_i \leq VUB_i \quad i=1, NDV \quad (189)$$

where \bar{X} = the vector containing the set of independent design variables.

$F(\bar{X})$ = the objective function to be minimized.

$G_j(\bar{X})$ = inequality constraint (NCON is the number of such constraints).

$H_j(\bar{X})$ = equality constraint (NEQ is the number of such constraints).

VLB_i/VUB_i = lower and upper bounds, respectively, on the design variables.

If all inequalities of Eqs. (187) and (189) are satisfied, the design is said to be feasible if any constraint is not satisfied, the design is infeasible. If the objective function

is a minimum and the design is feasible, it is said to be the optimal design.

In order to start the optimization algorithm, the initial set of design variables, \bar{X} , must be specified. It is desirable, but not essential, that the initial design variables provide a feasible solution. The optimization algorithm will then proceed in an iterative fashion using the following relationship

$$\bar{X}^{q+1} = \bar{X}^q + \alpha * \bar{S}^q$$

where q = the iteration number.

α = scalar quantity which defines the move in the search direction.

\bar{S} = vector search direction which will reduce the objective function (useable direction) without violating constraints (feasible direction).

To solve this problem, the optimization program COPES/CONMIN is used [Ref. 18]. CONMIN uses the Fletcher-Reeves algorithm for locally unconstrained problems [Ref. 20] and Zoutendijk's method of feasible directions (modified to improve efficiency and reliability and to deal with designs which do not initially satisfy all the constraints) for locally constrained problems [Ref. 21].

However, CONMIN does not handle equality constraints directly, but rather by means of penalty parameters. To achieve this, the objective function is augmented as follows

[Ref. 19]:

$$F'(\bar{X}) = F(\bar{X}) - K \sum_{j=1}^{N \in Q} H_j \quad (190)$$

and the equality condition of Eq. (188) is treated as an inequality constraint

$$H_j(\bar{X}) \leq 0 \quad j=1, N \in Q$$

The penalty function approach effectively satisfies the equality constraint while maintaining the rapid convergence characteristics of the CONMIN program.

The numerical optimization problems of equations (186) through (190) are very general, allowing for any number of design variables and constraints. In assessing the value of optimization, the automated design provides a very attractive approach to numerical optimization; however, there are both advantages and limitations to these techniques [Ref. 20].

Advantages:

- . Reduction in design time.
- . Systematic design procedure.
- . Applicable to a wide variety of design variables and constraints.
- . Virtually always yields some design improvement.
- . Not biased by engineering experience.
- . Requires a minimal amount of man-machine interface.

Limitations:

- . Computer times may increase dramatically as the number of design variables increases. A practical limit imposed by the current state of the art for most problems is 30 design variables.

- . Optimization techniques have no stored experience to draw upon; the validity of the result is limited to the validity of the analysis program.
- . The results of the optimization are as correct as the analysis program is theoretically precise.
- . Optimization algorithms used here cannot deal with discontinuous functions.
- . The optimization program will not always obtain a global design optimum and may require restarting from several different points to acquire reasonable assurance of obtaining the global optimum.
- . The analysis program must be properly structured to couple with the COPES/CONMIN optimization code.

C. DESIGNATED DESIGN VARIABLES, CONSTRAINTS AND OBJECTIVE FUNCTION

To assist in the interpretation of the enclosed OTEC power system FORTRAN analysis, the following summary identifies the design variables, constraint functions and objective function used in the analysis and subsequently operated upon by the COPES/CONMIN optimization code. These parameters are all contained in a labeled COMMON block in the computer code, referred to here as "GLOBAL COMMON." Specific GLOBAL COMMON location numbers and upper/lower bounds for operating parameters summarized below can be located in Appendix C.

Design Variables

- . Inner cold pipe diameter
- . Inner hot pipe diameter
- . Inner ammonia circ pipe diameter
- . Inner ammonia re-flux pipe diameter

- . Evaporator operating pressure
- . Condenser operating pressure
- . Outer condenser tube diameter
- . Outer evaporator tube diameter
- . Evaporator tube length
- . Condenser tube length
- . Condenser tube salt water velocity
- . Cold pipe salt water velocity
- . Evaporator tube salt water velocity
- . Hot pipe salt water velocity
- . Evaporator tube profile pitch ratio
- . Condenser tube profile pitch ratio

Constraint Functions

- . Operating system pressure ratio
- . Upper temperature bound of ammonia
- . Lower temperature bound of ammonia
- . Satisfactory enthalpy at state point 5
- . Satisfactory quality at state point 5
- . Satisfactory condenser tube length
- . Internal turbine efficiency
- . Evaporator tube sheet diameter
- . Condenser tube sheet diameter

Objective Function

- . Cost of major power system components

VIII. CONCLUSIONS AND RECOMMENDATIONS

A. CONCLUSIONS

1. The use of an analysis code for OTEC power systems coupled to COPES/CONMIN optimization code provides a powerful tool to design an optimum power system for the desired net electrical output, measured against the objective function. Such a design could permit construction of higher capacity systems using the optimized modules as substations of the total power plant.

2. The analysis code coupled to COPES/CONMIN provides an excellent vehicle to evaluate proposed designs relative to a true optimum. Tables 1 through 4 illustrate the result of preliminary calculations using the analysis code with an objective function to minimize system cost. From these, the following conclusions can be drawn concerning horizontally oriented aluminum (Al-5052) and titanium-tubed heat exchanger power systems:

a. The cost/KW output is nearly constant over the range of optimum designs for both titanium and aluminum tube heat exchangers.

b. During testing for feasible plant designs in increments of 5 MW (net) electrical output, it was observed that a higher megawatt output plant could be achieved with titanium-tubed heat exchangers than for aluminum (Al-5052). For titanium-tubed heat exchangers, a 25 MW (net) power

system is a feasible design; however, aluminum-tubed systems could not provide a feasible design for the same output. Titanium tubed plants failed to produce a feasible design for a 30 MW (net) output power system. In both cases of infeasible design, the constraint which was consistently violated was turbine internal efficiency, set at 90% for current state-of-the-art design.

c. The energy conversion and efficiency of design of a turbine-generator has a major effect on the overall system performance as indicated in paragraph b above.

d. The cost/KW output for titanium-tubed heat exchangers is one third the cost/KW output for aluminum-tubed heat exchangers using a 30-year life-cycle criterion, with a 10% annual inflation rate and retubing at 10 and 20 year marks with AL-5052 tubing.

e. Aluminum-tubed heat exchangers have larger tube bundle volumes, with volumetric differences between aluminum and titanium varying from 26.1 to 11.8% for evaporators and 23.2 to 7.4% for condensers over the range of net power levels considered. In both cases volumetric differences diminish as the system's net electrical output increases to 20 megawatts.

f. COPES/CONMIN has provided optimum designs for each incremental output power level. By manipulating the specified design variables, subject to imposed constraints, COPES/CONMIN has created designs whose geometry and operating

parameters cannot be scaled on the basis of net power output (10 MW). Therefore, designs for component geometry at increasing power levels based upon such simplistic scaling criteria will not achieve an optimum design with respect to the cost objective function.

B. RECOMMENDATIONS

1. Evaluate additional objective functions including:

- a. Minimize heat exchanger volumes.
- b. Minimize parasitic power losses.
- c. Maximize thermodynamic efficiency.
- d. Maximize net electrical output.

2. Perform a sensitivity analysis on power system design variables to evaluate their influence on component and system performance. This allows the designer to prioritize system components which can provide improvement in the objective function for a corresponding improvement in component design.

3. Considerable uncertainties are associated with the expressions used to estimate component performances (two-phase pressure drops, film coefficients, etc.). The code should be tested to determine the sensitivity of system design to these uncertainties.

4. Expand the code to include the use of enhanced heat transfer techniques and evaluate the influence of increased piping friction factors on pumping power requirements.

5. Evaluate proposed OTEC designs using proposed system parameter inputs, comparing both the basic analysis and the optimization output.

6. Select other analytical expressions for heat transfer coefficients to validate the performance and output of the existing code.

7. Evaluate the effect of a smaller thermal difference seen by the power system and its influence on a feasible design for a specific net electrical output.

8. Evaluate the cost aspects of using variable-pitch pumps versus fixed-blade for a variable thermal gradient environment.

9. Evaluate and verify the influence of incremental improvements (percent) in turbine internal/adiabatic efficiency with respect to gross and net electrical outputs and compare with the results reported in Ref. 16.

TABLE 1: OTEC Power System Comparisons (Titanium Tubed Heat Exchangers)

EVAPORATOR	10 MW	15 MW	20 MW	25 MW
HT ABSORB (BTU/HR)	1.44 EØ9	2.01 EØ9	2.80 EØ9	3.46 EØ9
SW FLOW (LB _m /HR)	2.27 EØ8	3.34 EØ8	4.14 EØ8	4.86 EØ8
NH ₃ FLOW (LB _m /HR)	2.73 EØ6	3.78 EØ6	5.29 EØ6	6.53 EØ6
OPER PRESS (LB _f /IN ²)	129.	130.0	127.7	127.1
OVL HT COEF (BTU/ HR·FT ² ·F)	623.19	612.97	601.47	595.73
HT SURFACE (FT ²)	387,598	572,405	743,093	922,075
TUBE OUTER DIA (IN)	0.947	0.952	0.945	0.929
TUBE WALL THICK (IN)	0.025	0.025	0.025	0.025
TUBE PROFILE - STAGGERED EQUILATERAL TRIANGLE				
PITCH RATIO	1.4	1.4	1.47	1.52
TUBE LENGTH (FT)	43.66	42.18	42.27	42.56
TUBE SHEET DIA (FT)	21.96	27.21	32.45	36.76
TOT NR OF TUBES	35,806	54,449	71,034	89,105

TABLE 1. OTEC Power System Comparisons (Continued)

CONDENSER	10 MW	15 MW	20 MW	25 MW
HT REJECT (BTU/HR)	1.39 E09	1.94 E09	2.71 E09	3.34 E09
SW FLOW (LB _m /HR)	2.23 E08	3.35 E08	4.72 E08	5.69 E08
NH ₃ FLOW (LB _m /HR)	2.73 E06	3.79 E06	5.29 E06	6.53 E08
OPER PRESS (LB _f /IN ²)	88.16	88.15	87.46	87.49
OVL HT COEF (BTU/ HR·FT ² ·F)	454.4	446.8	438.4	435.7
HT SURFACE (FT ²)	552,314	762,190	1,168,239	1,483,762
TUBE OUTER DIA (IN)	0.935	0.972	0.957	0.940
TUBE WALL THICK (IN)	0.025	0.025	0.025	0.025
TUBE PROFILE - STAGGERED EQUILATERAL TRIANGLE				
PITCH RATIO	1.4	1.4	1.48	1.51
TUBE LENGTH (FT)	58.57	57.42	58.32	59.09
TUBE SHEET DIA. (FT)	22.48	27.194	35.16	39.734
TOT NR OF TUBES	38,524	52,179	79,956	102,054

TABLE 1: OTEC Power System Comparisons (Continued)

PIPING SYSTEMS	10 MW	15 MW	20 MW	25 MW
SW HOT PIPE (300 FT LENGTH)				
INNER DIA (FT)	17.20	20.08	21.86	23.30
SW VEL (FT/SEC)	4.26	4.6	4.80	4.97
PRESS DROP (LB_f/IN^2)	0.280	0.322	0.348	0.371
SW COLD PIPE (3000 FT LENGTH)				
INNER DIA (FT)	16.1	18.62	21.35	22.97
SW VEL (FT/SEC)	4.94	5.33	5.72	5.95
PRESS DROP (LB_f/IN^2)	0.49	0.508	0.526	0.539
NH_3 CIRC PIPE (150 FT LENGTH)				
INNER DIA (FT)	2.0	2.0	2.0	2.0
PRESS DROP (LB_f/IN^2)	8.46	9.87	11.33	12.53
NH_3 RE-FLUX PIPE (50 FT LENGTH)				
INNER DIA (FT)	2.0	2.0	2.0	2.0
PRESS DROP (LB_f/IN^2)	8.46	9.87	11.33	12.53

TABLE 1: OTEC Power System Comparisons (Continued)

PUMP SYSTEMS	10 MW	15 MW	20 MW	25 MW
EVAP SW PUMP (EFFICIENCY 85 PCT)				
HEAD (FT)	11.0	9.89	9.42	9.26
CAPACITY (GAL/MIN)	444,338	653,260	808,625	930,352
COND SW PUMP (EFFICIENCY 85 PCT)				
HEAD (FT)	22.23	20.75	20.04	20.03
CAPACITY (GAL/MIN)	452,026	652,119	920,116	1,107,382
NH ₃ CIRC PUMP (EFFICIENCY 75 PCT)				
HEAD (FT)	200.9	217.33	214.93	220.52
CAPACITY (GAL/MIN)	8709.3	12,101.7	16,880.2	20,586.8
NH ₃ RE-FLUX PUMP (EFFICIENCY 75 PCT)				
HEAD (FT)	32.4	38.02	43.53	48.13
CAPACITY (GAL/MIN)	2684.3	3732.4	5201.4	6424.3

TABLE 1: OTEC Power System Comparisons (Continued)

EFFICIENCY OF OPERATION	10 MW	15 MW	20 MW	25 MW
TURBINE-GENERATOR (TURB MECH 99.8 PCT, GEN MECH AND ELECT 96.6 PCT)				
TURB INTERNAL (PCT)	87.16	89.88	88.22	89.80
OUTLET QUALITY (PCT)	96.6	96.77	96.9	96.9
POWER REQUIREMENTS (MEGAWATTS)				
TURB EFFIC LOSSES	0.373	0.559	0.745	0.932
EVAP SW PUMP	1.131	1.496	1.762	2.034
COND SW PUMP	2.334	3.143	4.283	5.151
NH ₃ CIRC PUMP	0.281	0.412	0.583	0.738
NH ₃ RE-FLUX PUMP	0.014	0.022	0.035	0.048
TURB-GEN GROSS	14.132	20.633	27.409	33.904
PCT PARASITIC POWER	26.6	24.6	24.31	23.51
THERMO CYCLE EFFIC (PCT)	2.45	2.65	2.53	2.56

TABLE 1: OTEC Power System Comparisons (Continued)

COMPONENT COSTS (\$)	10 MW	15 MW	20 MW	25 MW
EVAPORATOR	5,134,322.	8,223,672.	11,501,680.	13,026,794.
CONDENSER	5,952,658.	8,667,154.	13,011,939.	16,558,713.
GEN-TURBINE	1,495,085.	1,578,776.	1,666,011.	1,749,636.
GENERATOR	756,287.	937,205.	1,125,782.	1,306,554.
EVAP SW PUMP	463,736.	653,333.	794,355.	922,944.
COND SW PUMP	470,714.	652,298.	895,505.	1,065,449.
NH ₃ CIRC PUMP	110,849.	136,825.	169,303.	193,848.
NH ₃ RE-FLUX PUMP	52,190.	64,449.	79,701.	91,233.
OPTIMUM COST (\$)	14,383,650.	20,849,216.	29,164,560.	34,823,904.
COST/KW (NET) OUTPUT (\$/KW)	1438.36	1389.95	1458.23	1392.96

TABLE 2: OTEC Power System Comparisons (Aluminum Tubed Heat Exchanger)

EVAPORATOR	10 MW	15 MW	20 MW	25 MW
HT ABSORB (BTU/HR)	1.51 E09	1.97 E09	2.80 E09	
SW FLOW (LB _m /HR)	2.53 E08	3.42 E08	3.89 E08	
NH ₃ FLOW (LB _m /HR)	2.86 E06	3.72 E06	5.29 E06	
OPER PRESS (LB _f /IN ²)	129.57	131.98	128.01	
OVL HT COEF (BTU/ HR·FT ² ·F)	646.7	643.2	625.5	
HT SURFACE (FT ²)	391,370	610,261	777,553	
TUBE OUTER DIA (IN)	1.221	1.046	0.982	
TUBE WALL THICK (IN)	0.065	0.065	0.065	
TUBE PROFILE - STAGGERED EQUILATERAL TRIANGLE				
PITCH RATIO	1.4	1.46	1.6	
TUBE LENGTH (FT)	47.68	42.42	41.63	
TUBE SHEET DIA (FT)	23.97	30.73	34.68	
TOT NR OF TUBES	25,669	52,512	72,662	

INFEASIBLE DESIGN

TABLE 2: OTEC Power System Comparisons (Continued)

CONDENSER	10 MW	15 MW	20 MW	25 MW
HT REJECT (BTU/HR)	1.47 EØ9	1.89 EØ9	2.71 EØ9	INFEASIBLE DESIGN
SW FLOW (LB _m /HR)	2.44 EØ8	3.04 EØ8	4.38 EØ8	
NH ₃ FLOW (LB _m /HR)	2.86 EØ6	3.72 EØ6	5.30 EØ6	
OPER PRESS (LB _f /IN ²)	88.52	89.18	87.85	
OVL HT COEF (BTU/ HR•FT ² •F)	454.57	453.54	446.48	
HT SURFACE (FT ²)	554,011	690,395	1,173,216	
TUBE OUTER DIA (IN)	1.176	1.092	1.001	
TUBE WALL THICK (IN)	0.065	0.065	0.065	
TUBE PROFILE - STAGGERED EQUILATERAL TRIANGLE				
PITCH RATIO	1.4	1.46	1.5	
TUBE LENGTH (FT)	64.04	57.46	57.24	
TUBE SHEET DIA (FT)	24.15	28.61	36.82	
TOT NR OF TUBES	28,091	42,035	78,198	

TABLE 2: OTEC Power System Comparisons (Continued)

PIPING SYSTEMS	10 MW	15 MW	20 MW	25 MW
SW HOT PIPE (300 FT LENGTH)				
INNER DIA (FT)	17.89	20.25	21.33	
SW VEL (FT/SEC)	4.38	4.63	4.74	
PRESS DROP (LB_f/IN^2)	0.295	0.326	0.341	
SW COLD PIPE (3000 FT LENGTH)				
INNER DIA (FT)	16.53	17.93	20.7	
SW VEL (FT/SEC)	4.93	5.23	5.64	
PRESS DROP (LB_f/IN^2)	0.478	0.504	0.523	
NH_3 CIRC PIPE (150 FT LENGTH)				
INNER DIA (FT)	1.99	2.0	2.0	
PRESS DROP (LB_f/IN^2)	13.78	15.94	17.89	
NH_3 RE-FLUX PIPE (50 FT LENGTH)				
INNER DIA (FT)	2.0	2.0	2.0	
PRESS DROP (LB_f/IN^2)	8.996	10.788	11.916	

INFEASIBLE DESIGN

TABLE 2: OTEC Power System Comparisons (Continued)

PUMP SYSTEMS	10 MW	15 MW	20 MW	25 MW
EVAP SW PUMP (EFFICIENCY 85 PCT)				
HEAD (FT)	10.42	10.27	10.06	
CAPACITY (GAL/MIN)	494,239	669,211	760,748	
COND SW PUMP (EFFICIENCY 85 PCT)				
HEAD (FT)	21.32	20.80	21.05	
CAPACITY (GAL/MIN)	474,918	592,656	851,978	
NH ₃ CIRC PUMP (EFFICIENCY 75 PCT)				
HEAD (FT)	203.5	218.32	216.63	
CAPACITY (GAL/MIN)	9144.3	11,895.6	16,911.6	
NH ₃ RE-FLUX PUMP (EFFICIENCY 75 PCT)				
HEAD (FT)	34.33	41.27	45.66	
CAPACITY (GAL/MIN)	2818.4	3669.9	5210.5	

INFEASIBLE DESIGN

TABLE 2: OTEC Power System Comparisons (Continued)

EFFICIENCY OF OPERATION	10 MW	15 MW	20 MW	25 MW
TURBINE-GENERATOR (TURB MECH 99.8 PCT, GEN MECH AND ELECT 96.6 PCT)				
TURB INTERNAL (PCT)	83.37	89.76	88.05	
OUTLET QUALITY (PCT)	97.06	96.73	96.93	
POWER REQUIREMENTS (MEGAWATTS)				
TURB EFFIC LOSSES	0.373	0.559	0.745	
EVAP SW PUMP	1.191	1.590	1.770	
COND SW PUMP	2.351	2.863	4.166	
NH ₃ CIRC PUMP	0.299	0.416	0.588	
NH ₃ RE-FLUX PUMP	0.015	0.024	0.037	
TURB-GEN GROSS	14.229	20.452	27.306	
PCT PARASITIC POWER	27.10	23.92	24.03	
THERMO CYCLE EFFIC (PCT)	2.34	2.70	2.53	

INFEASIBLE DESIGN

TABLE 2: OTEC POWER SYSTEM COMPARISONS (CONTINUED)

COMPONENT COSTS (\$)	10 MW	15 MW	20 MW	25 MW
EVAPORATOR	20,848,960.	34,297,296.	44,203,408.	
CONDENSER	24,633,360.	31,812,640.	55,404,448.	
GEN-TURBINE	1,496,339.	1,576,449.	1,664,688.	
GENERATOR	758,998.	932,173.	1,122,921.	
EVAP SW PUMP	509,021.	667,809.	750,878.	
COND SW PUMP	491,487.	598,335.	833,670.	
NH ₃ CIRC PUMP	114,361.	135,329.	169,505.	
NH ₃ RE-FLUX PUMP	53,845.	63,756.	79,790.	
OPTIMUM COST (\$)	48,852,480.	70,020,000.	104,149,488.	

INFEASIBLE DESIGN

COST/KW (NET) OUTPUT (\$/KW)	4885.25	4668.00	5207.47
------------------------------	---------	---------	---------

TABLE 3: Heat Exchanger Comparisons (Titanium Tubed)

EVAPORATOR	10 MW	15 MW	20 MW	25 MW
HT ABSORB (BTU/HR)	1.44 E09	2.01 E09	2.80 E09	3.46 E09
SW FLOW (LB _m /HR)	2.27 E08	3.34 E08	4.14 E08	4.86 E08
SW TEMP IN (DEG F)	80.0	80.0	80.0	80.0
SW TEMP OUT (DEG F)	73.36	73.72	72.92	72.56
NH ₃ FLOW (LB _m /HR)	2.73 E06	3.78 E06	5.29 E06	6.53 E06
OPER PRESS (LB _f /IN ²)	129.0	130.1	127.72	127.1
SAT TEMP (DEG F)	70.11	70.59	69.54	69.27
OUTLET TEMP (DEG F)	70.06	70.51	69.47	69.19
OUTLET QUALITY (PCT)	92	92	92	92
NH ₃ PRESS DROP (LB _f /IN ²)	0.105	0.162	0.165	0.174
TUBE CHARACTERISTICS				
OUTER DIA (IN)	0.947	0.952	0.945	0.929
WALL THICK (IN)	0.025	0.025	0.025	0.025
LENGTH (FT)	43.66	42.18	42.27	42.56

TABLE 3: Heat Exchanger Comparisons (Continued)

EVAPORATOR	10 MW	15 MW	20 MW	25 MW
TUBE PROFILE - STAGGERED EQUILATERAL TRIANGLE				
PITCH RATIO	1.4	1.4	1.47	1.52
ENHANCEMENT - PLAIN TUBE				
SW VEL (FT/SEC)	6.3	6.03	5.80	5.64
T WALL (DEG F)	71.09	71.47	70.51	70.22
FILM TEMP (DEG F)	70.57	70.99	69.99	69.71
DELTA T BOILING (DEG F)	1.027	0.952	1.041	1.032
LMTD	6.00	5.76	6.31	6.34
EFFECTIVENESS	0.671	0.667	0.677	0.693
NTU	1.112	1.098	1.13	1.182
OVL HT COEF (BTU/ HR·FT ² ·F)				
h (WATER)	623.19	612.97	601.47	595.73
h (FOULING)	1156.01	1115.97	1081.6	1059.15
	3787.7	3788.5	3787.35	3784.37

TABLE 3: Heat Exchanger Comparisons (Continued)

EVAPORATOR	10 MW	15 MW	20 MW	25 MW
h (METAL)	4413.77	4404.7	4415.43	4429.66
h (AMMONIA)	4015.73	4088.4	4040.26	4090.74
SW PRESS DROP (LB_f/IN^2)	4.593	4.061	3.824	3.727
MOISTURE SEPARATOR				
OPER PRESS (LB_f/IN^2)	128.9	129.94	127.55	126.92
OUTLET TEMP (DEG F)	69.92	70.33	69.22	68.89
OUTLET QUALITY (PCT)	99.5	99.5	99.5	99.5
NH_3 PRESS DROP (LB_f/IN^2)	0.311	0.416	0.578	0.681
CONDENSER				
HT REJECT (BTU/HR)	1.44 E09	2.01 E09	2.80 E09	3.46 E09
SW FLOW (LB_m/HR)	2.27 E08	3.34 E08	4.14 E08	4.86 E08

TABLE 3: Heat Exchanger Comparisons (Continued)

CONDENSER	10 MW	15 MW	20 MW	25 MW
SW TEMP IN (DEG F)	40.0	40.0	40.0	40.0
SW TEMP OUT (DEG F)	46.29	46.06	46.00	46.16
NH ₃ FLOW (LB _m /HR)	2.73 EØ6	3.79 EØ6	5.29 EØ6	6.53 EØ6
OPER PRESS (LB _f /IN ²)	88.16	88.15	87.46	87.49
SAT TEMP (DEG F)	49.36	49.36	49.95	48.97
OUTLET TEMP (DEG F)	49.3	49.24	49.84	48.85
NH ₃ PRESS DROP (LB _f /IN ²)	0.127	0.206	0.173	0.195
TUBE CHARACTERISTICS				
OUTER DIA (IN)	0.935	0.972	0.957	0.940
WALL THICK (IN)	0.025	0.025	0.025	0.025
LENGTH (FT)	58.57	57.42	58.32	59.09
TUBE PROFILE - STAGGERED EQUILATERAL TRIANGLE				
PITCH RATIO	1.4	1.4	1.48	1.51

TABLE 3: Heat Exchanger Comparisons (Continued)

CONDENSER	10 MW	15 MW	20 MW	25 MW
ENHANCEMENT - PLAIN TUBE				
SW VEL (FT/SEC)	6.12	6.02	5.72	5.60
T WALL (DEG F)	48.39	48.33	48.04	48.07
FILM TEMP (DEG F)	48.84	48.79	48.44	48.46
DELTA T COND (DEG F)	0.895	0.901	0.808	0.781
LMTD	5.56	5.68	5.29	5.17
EFFECTIVENESS	0.678	0.655	0.679	0.696
NTU	1.133	1.065	1.136	1.191
OVL HT COEF (BTU/ HR·FT ² ·F)	454.4	446.83	438.4	435.73
h (WATER)	719.6	704.4	678.0	669.3
h (FOULING)	3785.5	3792.0	3789.4	3786.4
h (METAL)	4424.2	4393.6	4405.6	4420.1
h (AMMONIA)	3118.9	3058.6	3171.5	3219.8
SW PRESS DROP (LB _f /IN ²)	6.31	5.64	5.30	5.28

TABLE 4: Heat Exchanger Comparisons (Aluminum Tubed)

EVAPORATOR	10 MW	15 MW	20 MW	25 MW
HT ABSORB (BTU/HR)	1.51 E09	1.97 E09	2.80 E09	
SW FLOW (LB _m /HR)	2.53 E08	3.42 E08	3.89 E08	
SW TEMP IN (DEG F)	80.0	80.0	80.0	
SW TEMP OUT (DEG F)	73.74	73.99	72.47	
NH ₃ FLOW (LB _m /HR)	2.86 E06	3.72 E06	5.29 E06	
OPER PRESS (LB _f /IN ²)	129.57	131.98	128.01	
SAT TEMP (DEG F)	70.35	71.4	69.67	
OUTLET TEMP (DEG F)	70.32	71.4	69.61	
OUTLET QUALITY (PCT)	92.0	92.0	92.0	
NH ₃ PRESS DROP (LB _f /IN ²)	0.070	0.087	0.136	
TUBE CHARACTERISTICS				
OUTER DIA (IN)	1.221	1.046	0.982	
WALL THICK (IN)	0.065	0.065	0.065	

INFEASIBLE DESIGN

TABLE 4: Heat Exchanger Comparisons (Continued)

EVAPORATOR	10 MW	15 MW	20 MW	25 MW
LENGTH (FT)	47.68	42.42	41.63	
TUBE PROFILE - STAGGERED EQUILATERAL TRIANGLE				
PITCH RATIO	1.4	1.46	1.50	
ENHANCEMENT - PLAIN TUBE				
SW VEL (FT/SEC)	6.6	6.2	5.89	
T WALL (DEG F)	71.49	72.25	70.63	
FILM TEMP (DEG F)	70.90	71.80	70.12	
DELTA T BOILING (DEG F)	1.163	0.885	1.02	
LMTD	6.0	5.03	5.8	
EFFECTIVENESS	0.649	0.699	0.729	
NTU	1.047	1.199	1.307	
OVL HT COEF (BTU/ HR·FT ² ·F)	646.7	643.2	625.5	
h (WATER)	1090.0	1052.5	1011.5	

INFEASIBLE DESIGN

TABLE 4: Heat Exchanger Comparisons (Continued)

EVAPORATOR	10 MW	15 MW	20 MW	25 MW
h (FOULING)	3574.3	3503.1	3470.5	
h (METAL)	13,444.8	13,312.9	13,252.2	
h (AMMONIA)	3640.3	4097.4	4058.5	
SW PRESS DROP (LB_f/IN^2)	4.32	4.22	4.11	
MOISTURE SEPARATOR				
OPER PRESS (LB_f/IN^2)	129.5	131.89	127.88	
OUTLET TEMP (DEG F)	70.22	71.23	69.38	
OUTLET QUALITY (PCT)	99.5	99.5	99.5	
NH_3 PRESS DROP (LB_f/IN^2)	0.24	0.307	0.522	
CONDENSER				
HT REJECT (BTU/HR)	1.47 E09	1.89 E09	2.71 E09	

INFEASIBLE DESIGN

TABLE 4: Heat Exchanger Comparisons (Continued)

CONDENSER	10 MW	15 MW	20 MW	25 MW
SW FLOW (LB _m /HR)	2.44 EØ8	3.04 EØ8	4.38 EØ9	
SW TEMP IN (DEG F)	40.0	40.0	40.0	
SW TEMP OUT (DEG F)	46.30	46.53	46.49	
NH ₃ FLOW (LB _m /HR)	2.86 EØ6	3.72 EØ6	5.30 EØ6	
OPER PRESS (LB _f /IN ²)	88.52	89.18	87.83	
SAT TEMP (DEG F)	49.52	49.97	49.17	
OUTLET TEMP (DEG F)	49.52	49.90	49.08	
NH ₃ PRESS DROP (LB _f /IN ²)	0.088	0.111	0.148	
TUBE CHARACTERISTICS				
OUTER DIA (IN)	1.176	1.092	1.001	
WALL THICK (IN)	0.065	0.065	0.065	
LENGTH (FT)	64.04	57.46	57.24	
TUBE PROFILE - STAGGERED EQUILATERAL TRIANGLE				

INFEASIBLE DESIGN

TABLE 4: Heat Exchanger Comparisons (Continued)

CONDENSER	10 MW	15 MW	20 MW	25 MW
PITCH RATIO	1.4	1.46	1.5	
ENHANCEMENT - PLAIN TUBE				
SW VEL (FT/SEC)	6.31	6.23	5.87	
T WALL (DEG F)	48.51	48.85	48.25	
FILM TEMP (DEG F)	49.02	49.38	48.67	
DELTA T COND (DEG F)	1.020	1.055	0.832	
LMTD	5.820	6.062	5.175	
EFFECTIVENESS	0.661	0.660	0.715	
NTU	1.082	1.078	1.254	
OVL HT COEF (BTU/ HR·FT ² ·F)	454.57	453.56	446.48	
h (WATER)	670.0	668.56	641.97	
h (FOULING)	3557.0	3523.7	3480.59	
h (METAL)	13,414.54	13,351.18	13,271.11	
h (AMMONIA)	2842.96	2853.65	3131.0	
SW PRESS DROP (LB _f /IN ²)	5.92	5.66	5.74	

INFEASIBLE DESIGN

APPENDIX A

SAMPLE INPUT DATA FOR OTEC ANALYSIS

EVAPORATOR - HORIZONTAL

TUBE O.D.	1.000(IN)	25.400(MM)
TUBE LENGTH	40.000(FT)	12.192(M)
SW TUBE VEL	6.000(FT/S)	1.829(M/S)
OPER PRESSURE	130.000(LBF/IN ²)	0.896(MPA)
TUBE MATERIAL - TITANIUM		
THERMAL COND(K)	9.500(BTU/HR.FT.F)	16.502(W/M.C)
TUBE PROFILE - STAGGERED EQUI-LATERAL		
PITCH RATIO	1.50	
ENHANCEMENT - PLAIN TUBE		

CONDENSER - HORIZONTAL

TUBE O.D.	1.000(IN)	25.400(MM)
TUBE LENGTH	56.500(FT)	17.221(M)
SW TUBE VEL	6.000(FT/S)	1.829(M/S)
OPER PRESSURE	89.000(LBF/IN ²)	0.614(MPA)
TUBE MATERIAL - TITANIUM		
THERMAL COND(K)	9.500(BTU/HR.FT.F)	16.502(W/M.C)
TUBE PROFILE - STAGGERED EQUI-LATERAL		
PITCH RATIO	1.50	
ENHANCEMENT - PLAIN TUBE		

SALT WATER HOT PIPE

PIPE I.D.	19.300(FT)	5.883(M)
PIPE LENGTH	300.000(FT)	91.440(M)
SW PIPE VEL	4.500(FT/S)	1.372(M/S)
SW INLET TEMP	80.000(DEG F)	26.667(DEG C)
SW SALINITY	35.0/000	

SALT WATER COLD PIPE

PIPE I.D.	19.600(FT)	5.974(M)
PIPE LENGTH	3000.000(FT)	914.400(M)
SW PIPE VEL	5.500(FT/S)	1.676(M/S)
SW INLET TEMP	40.000(DEG F)	4.444(DEG C)
SW SALINITY	35.0/000	

AMMONIA CIRC PIPE

PIPE I.D.	2.000(FT)	0.610(M)
PIPE LENGTH	150.000(FT)	45.720(M)

AMMONIA RE-FLUX PIPE

PIPE I.D.	2.000(FT)	0.610(M)
PIPE LENGTH	50.000(FT)	15.240(M)

PUMP AND GEN-TURB PERFORMANCE

EVAP SW PUMP

EFFICIENCY MECH	95.00(PCT)	MOTOR 98.00(PCT)
-----------------	------------	------------------

COND SW PUMP

EFFICIENCY MECH	85.00(PCT)	MOTOR 98.00(PCT)
-----------------	------------	------------------

AMMONIA CIRC PUMP

EFFICIENCY MECH	75.00(PCT)	MOTOR 98.00(PCT)
-----------------	------------	------------------

GEN-TURB EFFICIENCIES

GEN MECH&ELECT	96.60(PCT)
----------------	------------

TURB MECH	99.80(PCT)
-----------	------------

POWER REQUIREMENTS

NET POWER OUTPUT	15.000(MW)
------------------	------------

APPENDIX B

SAMPLE OTEC ANALYSIS OPTIMIZATION OUTPUT DATA

EVAPORATOR - HORIZONTAL

HT ABSORB	2005013760.0(BTU/HR)	587.601(MW)
SW FLOW	334081280.0(LBM/HR)	151535904.0(KG/HR)
SW TEMP IN	80.000(DEG F)	26.667(DEG C)
SW TEMP OUT	73.724(DEG F)	23.130(DEG C)
NH3 FLOW	3788703.0(LBM/HR)	1718519.0(KG/HR)
OPER PRESSURE	130.097(LBF/IN2)	396.987(KPA)
EVAP SAT TEMP	70.585(DEG F)	21.436(DEG C)
OUTLET TEMP	70.514(DEG F)	21.397(DEG C)
OUTLET QUALITY	92.00(PCT)	
NH3 PRESS DROP	0.162(LBF/IN2)	1.115(KPA)

TUBE CHARACTERISTICS

OUTTER DIA	0.952(IN)	24.180(MM)
WALL THICK	0.025(IN)	0.639(MM)
LENGTH	42.182(FT)	12.857(M)

MATERIAL - TITANIUM

TUBE PROFILE - STAGGERED EQUI-LATERAL

PITCH RATIO 1.40

ENHANCEMENT - PLAIN TUBE

SW VELOCITY	6.026(FT/S)	1.337(M/S)
T WALL(SHELLSIDE)	71.466(DEG F)	21.926(DEG C)
FILM TEMP	70.990(DEG F)	21.661(DEG C)
DELTA T BOILING	0.952(DEG F)	0.529(DEG C)
L.M.T.D.	5.757(DEG F)	3.198(DEG C)
EVAP EFFECTIVENESS	0.667	
NR OF TRANSFER UNITS	1.093	
OVL HT COEF	612.97(BTU/HR.FT2.F)	3480.58(W/M2.C)
H(WATER)	1115.97(BTU/HR.FT2.F)	6336.71(W/M2.C)
H(FOULING)	3738.54(BTU/HR.FT2.F)	21512.09(W/M2.C)
H(METAL)	4409.72(BTU/HR.FT2.F)	25039.29(W/M2.C)
H(AMMONIA)	4088.44(BTU/HR.FT2.F)	23215.00(W/M2.C)

HT SURFACE	572405.00(FT2)	53178.12(M2)
TUBE SHEET DIA	27.213(FT)	8.294(M)
TOT NR OF TUBES	54449.	
SW PRESS DROP	4.061(LBF/IN2)	23.003(KPA)
MOISTURE SEPARATOR-INSIDE EVAP SHELL		
OPER PRESSURE	129.935(LBF/IN2)	395.872(KPA)
OUTLET TEMP	70.333(DEG F)	21.296(DEG C)
OUTLET QUALITY	99.50(PCT)	
NH3 PRESS DROP	0.416(LBF/IN2)	2.868(KPA)
CONDENSER - HORIZONTAL		
HT REJECT	1935472896.0(BTU/HR)	567.221(MW)
SW FLOW	334871552.0(LBM/HR)	151894363.0(KG/HR)
SW TEMP IN	40.000(DEG F)	4.444(DEG C)
SW TEMP OUT	46.055(DEG F)	7.308(DEG C)
NH3 FLCW	3788708.0(LBM/HR)	1718519.0(KG/HR)
OPER PRESSURE	83.151(LBF/IN2)	607.781(KPA)
COND SAT TEMP	49.351(DEG F)	9.645(DEG C)
OUTLET TEMP	49.238(DEG F)	9.577(DEG C)
NH3 PRESS DROP	0.206(LBF/IN2)	1.423(KPA)
TUBE CHARACTERISTICS		
OUTTER DIA	0.972(IN)	24.683(MM)
WALL THICK	0.025(IN)	0.642(MM)
LENGTH	57.416(FT)	17.500(M)
MATERIAL - TITANIUM		
TUBE PROFILE - STAGGERED EQUI-LATERAL		
PITCH RATIO	1.40	
ENHANCEMENT - PLAIN TUBE		
SW VELOCITY	6.017(FT/S)	1.834(M/S)
T WALL(SHELLSIDE)	48.331(DEG F)	9.073(DEG C)
FILM TEMP	48.785(DEG F)	9.325(DEG C)
DELTA T COND	0.907(DEG F)	0.504(DEG C)
L.M.T.D.	5.683(DEG F)	3.157(DEG C)
COND EFFECTIVENESS	0.655	
NR OF TRANSFER UNITS	1.065	

CVL HT COEF	446.83(BTU/HR.FT2.F)	2537.13(W/M2.C)
H(WATER)	704.35(BTU/HR.FT2.F)	3999.47(W/M2.C)
H(FOULING)	3792.00(BTU/HR.FT2.F)	21531.75(W/M2.C)
H(METAL)	4393.63(BTU/HR.FT2.F)	24947.90(W/M2.C)
H(AMMONIA)	3053.65(BTU/HR.FT2.F)	17367.63(W/M2.C)
HT SURFACE	762190.25(F2)	70809.69(M2)
TUBE SHEET DIA	27.194(FT)	8.289(M)
TOT NR OF TUBES	52179.	
SW PRESS DROP	5.636(LBF/IN2)	33.361(KPA)

SALT WATER HOT PIPE

PIPE I.D.	20.077(FT)	6.120(M)
PIPE LENGTH	300.000(FT)	91.440(M)
SW PIPE VEL	4.597(FT/S)	1.401(M/S)
SW FLOW	334081280.0(LBM/HR)	151535904.0(KG/HR)
SW INLET TEMP	80.000(DEG F)	26.667(DEG C)
SW SALINITY	35. 0/000	
SW PRESS DROP	0.322(LBF/IN2)	2.217(KPA)

SALT WATER COLD PIPE

PIPE I.D.	18.622(FT)	5.676(M)
PIPE LENGTH	3000.000(FT)	914.400(M)
SW PIPE VEL	5.334(FT/S)	1.625(M/S)
SW FLOW	334871552.0(LBM/HR)	151894368.0(KG/HR)
SW INLET TEMP	40.000(DEG F)	4.444(DEG C)
SW SALINITY	35. 0/000	
SW PRESS DROP	0.508(LBF/IN2)	3.501(KPA)

AMMONIA CIRC PIPE

PIPE I.D.	2.001(FT)	0.610(M)
PIPE LENGTH	150.000(FT)	45.720(M)
NH3 FLOW	3788708.0(LBM/HR)	1718519.0(KG/HR)
NH3 PRESS DROP	15.033(LBF/IN2)	103.650(KPA)

AMMONIA RE-FLUX CIRC PIPE

PIPE I.D.	2.000(FT)	0.610(M)
PIPE LENGTH	50.000(FT)	15.240(M)
NH3 FLOW	1136612.0(LBM/HR)	515555.3(KG/HR)
NH3 PRESS DROP	9.874(LBF/IN2)	68.079(KPA)

PUMP AND GEN-TURB PERFORMANCE

EVAP SW PUMP

HEAD PRESS	9.898(FT)	3.017(M)
CAPACITY	653259.6(GAL/MIN)	2472587.0(LIT/MIN)
EFFICIENCY MECH	85.00(PCT)	MOTOR 98.00(PCT)

COND SW PUMP

HEAD PRESS	20.753(FT)	9.227(M)
CAPACITY	652119.2(GAL/MIN)	2468271.0(LIT/MIN)
EFFICIENCY MECH	85.00(PCT)	MOTOR 98.00(PCT)

AMMONIA CIRC PUMP

HEAD PRESS	212.327(FT)	64.717(M)
CAPACITY	12101.7(GAL/MIN)	45805.0(LIT/MIN)
EFFICIENCY MECH	75.00(PCT)	MOTOR 98.00(PCT)

AMMONIA RE-FLUX PUMP

HEAD PRESS	33.016(FT)	11.537(M)
CAPACITY	3732.4(GAL/MIN)	14127.1(LIT/MIN)
EFFICIENCY MECH	75.00(PCT)	MOTOR 98.00(PCT)

GEN-TURB EFFICIENCIES

GEN MECH&ELECT	96.60(PCT)
TURB MECH	99.80(PCT)
TURB INTERNAL	89.83(PCT)

TURB OUTLET QUALITY 96.77(PCT)

POWER REQUIREMENTS

TURB-GEN GROSS	27663.313(HP)	20.633(MW)
EFFICIENCY LOSSES		0.559(MW)
EVAP SW PUMP	1964.851(HP)	1.496(MW)
COND SW PUMP	4129.313(HP)	3.143(MW)
NH3 CIRC PUMP	541.714(HP)	0.412(MW)
NH3 RE-FLUX PUMP	29.097(HP)	0.022(MW)

NET POWER OUTPUT

15.000(MW)

PERCENT PARASITIC POWER

24.59(PCT)

THERMODYNAMIC CYCLE EFFICIENCY

2.65(PCT)

COST OF COMPONENTS

EVAPORATOR	8223672.00 (DOLLARS)
CONDENSER	8667154.00 (DOLLARS)
GEN-TURBINE	1578776.00 (DOLLARS)
GENERATOR	937205.06 (DOLLARS)
EVAP SW PUMP	653332.94 (DOLLARS)
COND SW PUMP	652298.06 (DOLLARS)
NH3 CIRC PUMP	136824.94 (DOLLARS)
NH3 RE-FLUX PUMP	64448.34 (DOLLARS)

OPTIMUM COST	20849216.00 (DOLLARS)
COST PER NET KW OUTPUT	1389.95 (DOLLARS)

APPENDIX C

SAMPLE COPEs OPTIMIZATION AND SENSITIVITY ANALYSIS DATA

```

$BLOCK A (TITLE CARD)
OCEAN THERMAL ENERGY CONVERSION (OTEC) POWER SYSTEM
$BLOCK B (PROGRAM CONTROL PARAMETERS)
2,16,16
      2      16      16
$BLOCK C (INTEGER OPT CONTROL PARAMETERS)
5,0,0,5
      5      0      0      5
$BLOCK D (FLOATING PT OPT PROG PARAMETERS)
0.0
      0.0
0.0
      0.0
$BLOCK E (TOT NR DESIGN VAR, DESIGN OBJ IDENT AND SIGN)
16,27,-1.0
      16      27      -1.0
$BLOCK F (DESIGN VARIABLE BOUNDS, INIT VALJES & SCALE FACTOR)
1.0,1.0+20
      1.0      1.0+20
1.0,1.0+20
      1.0      1.0+20
1.0,1.0+20
      1.0      1.0+20
1.0,1.0+20
      1.0      1.0+20
85.0,148.0
      85.0      148.0
85.0,148.0
      85.0      148.0
0.5,2.5
      0.5      2.5
0.5,2.5
      0.5      2.5
10.0,1.0+20
      10.0      1.0+20
10.0,1.0+20
      10.0      1.0+20
2.0,10.0
      2.0      10.0
2.0,10.0
      2.0      10.0
2.0,10.0
      2.0      10.0
2.0,10.0
      2.0      10.0
2.0,10.0
      2.0      10.0
1.4,3.0
      1.4      3.0
1.4,3.0
      1.4      3.0
$BLOCK G (DESIGN VARIABLE IDENT)
1,1,1.0
      1      1      1.0
2,2,1.0
      2      2      1.0
3,3,1.0
      3      3      1.0
4,4,1.0
      4      4      1.0
5,5,1.0
      5      5      1.0

```


6,6,1.0			1.0
7,7,1.0	6	6	1.0
8,8,1.0	7	7	1.0
9,9,1.0	8	8	1.0
10,10,1.0	9	9	1.0
11,11,1.0	10	10	1.0
12,12,1.0	11	11	1.0
13,13,1.0	12	12	1.0
14,14,1.0	13	13	1.0
15,15,1.0	14	14	1.0
16,16,1.0	15	15	1.0
	16	16	1.0

\$BLOCK H (NR OF CONSTRAINED PARAMETERS)

5
\$BLOCK I (CONSTRAINT IDENT AND BOUNDS)

17				
1.,0.0,3.,0.0	17			
18,20	1.	0.0	3.	0.0
0.1,0.0,1.0+20,0.0	18			
21,23	0.1	0.0	1.0+20	0.0
0.,0.0,1.0+20,0.0	21			
24	0.	0.0	1.0+20	0.0
30.,0.0,90.,0.0	24			
25,26	30.	0.0	90.	0.0
10.,0.0,1.0+20,0.0	25			
\$BLOCK P (SENSITIVITY OBJECTIVES)	10.	0.0	1.0+20	0.0

27,0
1,2,3,4,5,6,7,8,9,10,11,12,13,14,15,16,17,18,19,20,
1 2 3 4 5
9 10 11 12 13
17 18 19 20 21
25 26 27
21,22,23,24,25,26,27
6 7 8
14 15 16
22 23 24

\$BLOCK Q (SENSITIVITY VARIABLE BOUNDS)

1,6				
18.,10.,15.,18.,20.,25.	1			
2,6	13.	10.	15.	18.
			20.	25.
18.,10.,15.,18.,20.,25.	2			
3,6	18.	10.	15.	18.
			20.	25.

2.,0.5,1. ³ ,2.,3.,4. ⁰				
4,6	2.	0.5	1.	2.
				3.
				4.
2.,0.5,1. ⁴ ,2.,3.,4. ⁶				
5,6	2.	0.5	1.	2.
				3.
				4.
130.,128. ⁵ ,129.,130. ⁶ ,131.,132.				
6,6	130.	128.	129.	130.
				131.
				132.
89.,87. ⁶ ,88.,89. ⁶ ,90.,91.				
7,6	89.	87.	88.	89.
				90.
				91.
1.,.5,.75, ⁷ 1.,1.25,1. ⁶ .5				
8,6	1.	.5	.75	1.
				1.25
				1.5
1.,.5,.75, ⁸ 1.,1.25,1. ⁶ .5				
9,6	1.	.5	.75	1.
				1.25
				1.5
40.,30. ⁹ ,35.,40. ⁶ ,45.,50.				
10,6	40.	30.	35.	40.
				45.
				50.
55.,45. ¹⁰ ,50.,55. ⁶ ,60.,65.				
11,6	55.	45.	50.	55.
				60.
				65.
7.,5.,6. ¹¹ ,7.,8.,9. ⁶				
12,6	7.	5.	6.	7.
				8.
				9.
4.,2.,3. ¹² ,4.,5.,6. ⁶				
13,6	4.	2.	3.	4.
				5.
				6.
7.,5.,6. ¹³ ,7.,8.,9. ⁶				
14,6	7.	5.	6.	7.
				8.
				9.
4.,2.,3. ¹⁴ ,4.,5.,6. ⁶				
15,6	4.	2.	3.	4.
				5.
				6.
1.6,1.4, ¹⁵ 1.5,1.6,1.7, ⁶ 1.8				
16,6	1.6	1.4	1.5	1.6
				1.7
				1.8
1.6,1.4, ¹⁶ 1.5,1.6,1.7, ⁶ 1.8				
END	1.6	1.4	1.5	1.6
				1.7
				1.8

[illegible]

NP004410
NP002500
NP000910
NP004010
NP003460

NP004030
NP004120
NP004070
NP004110
NP004080
NP005660
NP001500
NP004930
NP004090
NP004020
NP000850
NP003370
NP004130
NP004140
NP001730
NP001740
NP002100
NP001120
NP001080
NP002330
NP005420
NP002380
NP006510
NP002320
NP005410
NP000630
NP001830
NP006180
NP001720
NP001810
NP001470
NP002540
NP000620
NP001750
NP002340
NP005430
NP002300

NP004410
NP002500
NP000910
NP004010
NP003460

NP004030
NP004120
NP004070
NP004110
NP004080
NP005660
NP001500
NP004930
NP004090
NP004020
NP000850
NP003370
NP004130
NP004140
NP001730
NP001740
NP002100
NP001120
NP001080
NP002330
NP005420
NP002380
NP006510
NP002320
NP005410
NP000630
NP001830
NP006180
NP001720
NP001810
NP001470
NP002540
NP000620
NP001750
NP002340
NP005430
NP002300

NP005400
NP001050
NP000840
NP001150
NP002530
NP000700
NP004670
NP001820
NP003400
NP006720
NP000270
NP001210
NP003380
NP003390
NP002060
NP006260
NP006250
NP001110
NP001100

NP005110
NP003660
NP000680
NP004650
NP000810
NP004660
NP006360
NP006350
NP005280
NP001090
NP002290
NP005390
NP002280
NP005380
NP001390
NP001410
NP001960
NP001430
NP004940
NP004950
NP004960
NP004970
NP002260
NP005360
NP002270
NP005370
NP000610
NP001450

C	CTW2	-	CONDENSER SHELLSIDE WALL	TEMPERATURE(DEG F)	NPU01460
C	CTW2C	-	CONVERSION OF CTW2 TO S.I.	UNITS(DEG C)	NPU02550
C	CTWC	-	CONDENSER TUBE WELDING COST	(\$)	NPU02370
C	CTWE	-	EVAP TUBE WELDING COST	(\$)	NPU05450
C	CWINSE	-	EVAP WATER INLET, NOZZLES AND SUPPORTS	COST(\$)	NPU05440
C	CWINSC	-	COND WATER INLETS, NOZZLES & SUPPORTS	COST(\$)	NPU02360
C	DBLKT	-	ABSOLUTE DIFFERENCE BETWEEN TBLKE & RTBLKE	(DEG F)	NPU04900
C	DBLKT C	-	DIFFERENCE BETWEEN REVISED AND ASSUMED TBLKE	TEMP	NPU01170
C	DBLKTC	-	TOTAL PRESSURE LOSSES ACROSS CONDENSER	(LBF/IN2)	NPU06430
C	DCOND	-	CONVERSION OF DCOND TO S.I.	UNITS(KPA)	NPU02560
C	DCOREC	-	CONDENSER TUBING FRICTION LOSSES	(LBF/IN2)	NPU06420
C	DCOREE	-	EVAPORATOR TUBING FRICTION LOSSES	(LBF/IN2)	NPU06080
C	DDC	-	PRESSURE LOSSES DUE TO SW DENSITY DIFF.	(LBF/IN2)	NPU06310
C	DDENC	-	LOSSES DUE TO SW DENSITY COMPRESSIBILITY	(LBF/IN2)	NPU00990
C	DDUCTC	-	SW COLD PIPE INLET/OUTLET DUCT LOSSES	(LBF/IN2)	NPU06270
C	DDUCTH	-	SW HOT PIPE INLET DUCT LOSSES	(LBF/IN2)	NPU03110
C	DELB	-	RATIO OF DBLKT TO SCALB		NPU004920
C	DELBC	-	RATIO OF DBLKTC WRT SCALBC		NPU01190
C	DELH	-	RATIO OF DHNH3C WRT SCALC		NPU02090
C	DELH3	-	RATIO OF HNH3ER WITH RESPECT TO HNH3E		NPU05300
C	DELTA3	-	RATIO OF DTEMP3 WITH RESPECT TO SCALT		NPU06000
C	DELTA4	-	RATIO OF DTEMP4 AND SCALT		NPU01880
C	DELTA5	-	CONDENSING TEMPERATURE(DEG F)		NPU01480
C	DELTAEC	-	EVAP DELTA T FOR BOILING(DEG F)		NPU05020
C	DELTAEC	-	CONVERSION OF DELTAE TO S.I.	UNITS(DEG C)	NPU02570
C	DELTEC	-	CONVERSION OF DELTAE TO S.I.	UNITS(DEG C)	NPU02580
C	DELTV	-	RATIO OF DVNH3ER WITH RESPECT TO SCALV		NPU05960
C	DEVAP	-	TOTAL PRESSURE LOSSES ACROSS EVAPORATOR	(LBF/IN2)	NPU06090
C	DEVAPC	-	CONVERSION OF DEVAP TO S.I.	UNITS(KPA)	NPU02590
C	DF	-	GEN-TURB DOUBLE FLOW FACTOR		NPU00830
C	DH5	-	CONSTRAINT DIFFER FOR ENTHALPY AT STATE PT 5		NPU00430
C	DHEAD	-	LOSSES DUE TO SW DENSITY COMPRESSIBILITY	(FT)	NPU00980
C	DHNH3C	-	ABSOLUTE DIFFERENCE BETWEEN HNH3CR AND HTNH3C		NPU02070
C	DHTNH3	-	ABSOLUTE DIFF BET HNH3ER AND HNH3E	(BTU/HR.FT2.F)	NPU05290
C	DICP	-	COLD PIPE INNER DIAMETER(FT)		NPU03490
C	DICPC	-	CONVERSION OF DICP TO S.I.	UNITS(M)	NPU02600
C	DIHP	-	HOT PIPE INNER DIAMETER(FT)		NPU03500
C	DIHPC	-	CONVERSION OF DIHP TO S.I.	UNITS(M)	NPU02610
C	DINH3C	-	AMMONIA CIRC PIPE INNER DIAMETER(FT)		NPU03510
C	DINH3C	-	CONVERSION OF DINH3 TO S.I.	DIAMETER(FT)	NPU02620
C	DINH3R	-	AMMONIA RE-FLUX PIPE INNER DIAMETER(FT)		NPU03520
C	DINHRC	-	CONVERSION OF DINH3R TO S.I.	DIAMETER(FT)	NPU02630
C	DPCORE	-	EVAPORATOR SHELLSIDE PRESSURE LOSSES	(LBF/IN2)	NPU06590
C	DPDM	-	DEMISTER PRESSURE DROP MULTIPLE		NPU03870
C	DPELEC	-	COND CORE PRESS DROP DUE TO ELEV	(LBF/IN2)	NPU00950
C	DPELER	-	PRESSURE LOSS DUE TO RE-FLUX PIPING	EZR(LBF/IN2)	NPU00130
C	DPELEV	-	PRESSURE LOSS DUE TO AMMONIA PIPING	EZ2(LBF/IN2)	NPU06620
C	DPIPC	-	TOTAL SW COLD PIPE FRICTION LOSSES	(LBF/IN2)	NPU066300

CC	DIPICC	-	CONVERSION OF DIPIPC	TO S.I. UNITS(KPA)	NP002640
CC	DPIPEH	-	SW COLD PIPE	FRICITION LOSSES(LBF/IN2)	NP006290
CC	DPIPEH	-	SW HOT PIPE	FRICITION LOSSES(LBF/IN2)	NP003360
CC	DPIPHC	-	TOTAL SW HOT	PIPE FRICTION LOSSES(LBF/IN2)	NP004680
CC	DPIPHN	-	AMMONIA PCIRC	PIPE PRESSURE TO S.I. UNITS(KPA)	NP002650
CC	DPIPNR	-	CONVERSION OF DIPIPN	TO S.I. LOSSES(LBF/IN2)	NP006630
CC	DPIPNR	-	RE-FLUX AMMONIA	PIPE LOSSES(LBF/IN2)	NP002660
CC	DPMCC	-	CONVERSION OF DPMCC	TO S.I. UNITS(M)	NP000140
CC	DPMCC	-	CONVERSION OF DPMCC	TO S.I. UNITS(M)	NP002680
CC	DPMINE	-	MINOR INLET/OUTLET	CONDENSER LOSSES(LBF/IN2)	NP002690
CC	DPMINE	-	MINOR INLET/OUTLET	EVAPORATOR LOSSES(LBF/IN2)	NP006370
CC	DPMNCC	-	CONVERSION OF DPMNCC	TO S.I. UNITS(M)	NP005620
CC	DPMNCC	-	COND. OR SW COLD	PIPE PUMP PRESSURE HEAD(LBF/IN2)	NP002670
CC	DPMNCC	-	COND. OR SW COLD	PIPE PUMP PRESSURE HEAD(LBF/IN2)	NP006440
CC	DPMNCC	-	COND. OR SW COLD	PIPE PUMP PRESSURE HEAD(LBF/IN2)	NP006450
CC	DPMNCC	-	COND. OR SW COLD	PIPE PUMP PRESSURE HEAD(LBF/IN2)	NP006110
CC	DPMNCC	-	COND. OR SW COLD	PIPE PUMP PRESSURE HEAD(LBF/IN2)	NP006120
CC	DPMNCC	-	COND. OR SW COLD	PIPE PUMP PRESSURE HEAD(LBF/IN2)	NP006650
CC	DPMNCC	-	COND. OR SW COLD	PIPE PUMP PRESSURE HEAD(LBF/IN2)	NP006660
CC	DPMNCC	-	COND. OR SW COLD	PIPE PUMP PRESSURE HEAD(LBF/IN2)	NP000160
CC	DPMNCC	-	COND. OR SW COLD	PIPE PUMP PRESSURE HEAD(LBF/IN2)	NP006580
CC	DPMNCC	-	COND. OR SW COLD	PIPE PUMP PRESSURE HEAD(LBF/IN2)	NP000110
CC	DPMNCC	-	COND. OR SW COLD	PIPE PUMP PRESSURE HEAD(LBF/IN2)	NP002700
CC	DPMNCC	-	COND. OR SW COLD	PIPE PUMP PRESSURE HEAD(LBF/IN2)	NP002710
CC	DPMNCC	-	COND. OR SW COLD	PIPE PUMP PRESSURE HEAD(LBF/IN2)	NP000170
CC	DPMNCC	-	COND. OR SW COLD	PIPE PUMP PRESSURE HEAD(LBF/IN2)	NP006640
CC	DPMNCC	-	COND. OR SW COLD	PIPE PUMP PRESSURE HEAD(LBF/IN2)	NP000150
CC	DPMNCC	-	COND. OR SW COLD	PIPE PUMP PRESSURE HEAD(LBF/IN2)	NP005730
CC	DPMNCC	-	COND. OR SW COLD	PIPE PUMP PRESSURE HEAD(LBF/IN2)	NP002720
CC	DPMNCC	-	COND. OR SW COLD	PIPE PUMP PRESSURE HEAD(LBF/IN2)	NP005710
CC	DPMNCC	-	COND. OR SW COLD	PIPE PUMP PRESSURE HEAD(LBF/IN2)	NP002730
CC	DPMNCC	-	COND. OR SW COLD	PIPE PUMP PRESSURE HEAD(LBF/IN2)	NP002230
CC	DPMNCC	-	COND. OR SW COLD	PIPE PUMP PRESSURE HEAD(LBF/IN2)	NP005340
CC	DPMNCC	-	COND. OR SW COLD	PIPE PUMP PRESSURE HEAD(LBF/IN2)	NP004370
CC	DPMNCC	-	COND. OR SW COLD	PIPE PUMP PRESSURE HEAD(LBF/IN2)	NP004380
CC	DPMNCC	-	COND. OR SW COLD	PIPE PUMP PRESSURE HEAD(LBF/IN2)	NP005980
CC	DPMNCC	-	COND. OR SW COLD	PIPE PUMP PRESSURE HEAD(LBF/IN2)	NP001860
CC	DPMNCC	-	COND. OR SW COLD	PIPE PUMP PRESSURE HEAD(LBF/IN2)	NP002220
CC	DPMNCC	-	COND. OR SW COLD	PIPE PUMP PRESSURE HEAD(LBF/IN2)	NP005940
CC	DPMNCC	-	COND. OR SW COLD	PIPE PUMP PRESSURE HEAD(LBF/IN2)	NP004050
CC	DPMNCC	-	COND. OR SW COLD	PIPE PUMP PRESSURE HEAD(LBF/IN2)	NP004060
CC	DPMNCC	-	COND. OR SW COLD	PIPE PUMP PRESSURE HEAD(LBF/IN2)	NP001540
CC	DPMNCC	-	COND. OR SW COLD	PIPE PUMP PRESSURE HEAD(LBF/IN2)	NP001550
CC	DPMNCC	-	COND. OR SW COLD	PIPE PUMP PRESSURE HEAD(LBF/IN2)	NP004620
CC	DPMNCC	-	COND. OR SW COLD	PIPE PUMP PRESSURE HEAD(LBF/IN2)	NP004560
CC	DPMNCC	-	COND. OR SW COLD	PIPE PUMP PRESSURE HEAD(LBF/IN2)	NP003720
CC	DPMNCC	-	COND. OR SW COLD	PIPE PUMP PRESSURE HEAD(LBF/IN2)	NP003750

CC HG(PCOND) - SUBROUTINE FOR ENTHALPY OF A VAPOR(BTU/LBM)
 CC HG(PEVAP) - SUBROUTINE FOR ENTHALPY(BTU/LBM)
 CC HNH3C - PSEUDO HT COEFF COND AMMONIA(BTU/HR.FT2.F)
 CC HNH3CC - PCONVERSION OF HNH3C TO S.I. UNITS(W/M2.C)
 CC HNH3EC - PSEUDO HT COEFF FOR EVAP AMMONIA(BTU/HR.FT2.F)
 CC HNH3EC - PCONVERSION OF HNH3E TO S.I. UNITS(W/M2.C)
 CC HNH3CR - REVISED AMMONIA HT COEFF COND.(BTU/HR.FT2.F)
 CC HNH3ER - REVISED EVAP SHELLSIDE HT COEF(BTU/HR.FT2.F)
 CC HPC - 550 FT.LBF/SEC.HP
 CC HPKI - INLET DUCT TO SW HOT PIPE RESISTANCE COEFFICIENT
 CC HPKE - OUTLET SW HOT PIPE RESISTANCE COEFFICIENT
 CC HSWC - PSEUDO HT COEFF COND TO S.I. UNITS(W/M2.C)
 CC HSWCC - PCONVERSION OF HSWC TO S.I. UNITS(W/M2.C)
 CC HSWEC - PSEUDO HT COEFF FOR EVAP SW(BTU/HR.FT2.F)
 CC HSWEC - PCONVERSION OF HSWE TO S.I. UNITS(W/M2.C)
 CC HTFDR - EVAP NH3 HT COEFF FULLY DEVELOPING REG(BTU/HR.FT2.F)
 CC HTFSWC - EVAP NH3 HT COEFF SW FOUling COEF(BTU/HR.FT2.F)
 CC HTFSWE - HT COEF FOR COND. SW FOUling COEF(BTU/HR.FT2.F)
 CC HTNH3C - INITIAL AMMONIA HT COEFFICIENT-COND. (BTU/HR.FT2.F)
 CC HTNH3E - EVAP SHELLSIDE HT COEFFICIENT(BTU/HR.FT2.F)
 CC HTSWC - HT COEFFICIENT FOR CONDENSER SW(BTU/HR.FT2.F)
 CC HTSWE - EVAP TUBESIDE HT COEFFICIENT(BTU/HR.FT2.F)
 CC HWC - PSEUDO HT COEFF COND WALL THICK.(BTU/HR.FT2.F)
 CC HWCC - PCONVERSION OF HWC TO S.I. UNITS(W/M2.C)
 CC HWEC - PSEUDO HT COEFF FOR EVAP WALL THICK(BTU/HR.FT2.F)
 CC MATL - TUBING MATERIAL SELECTION
 CC OBJ - OBJECTIVE FUNCTION TO MINIMIZE COST
 CC P1 - PRESSURE OF SAT AMMONIA AT STATE PT 1(LBF/IN2)
 CC P3 - PRESSURE OF AMMONIA AT STATE PT 3(LBF/IN2)
 CC P3C - PCONVERSION OF P3 TO S.I. UNITS(KPA)
 CC P4 - PRESSURE OF AMMONIA AT STATE PT 4(LBF/IN2)
 CC PARAL - PARASITIC PUMP REQUIREMENTS(MW)
 CC PAVGD - AVG PRESSURE ACROSS MOISTURE SEPARATOR(LBF/IN2)
 CC PAVGE - AVERAGE EVAPORATOR PRESSURE(LBF/IN2)
 CC PCOND - OPERATION PRESSURE OF THE CONDENSER(LBF/IN2)
 CC PEVAPC - PCONVERSION OF PCOND TO S.I. UNITS(KPA)
 CC PEVAPC - OPERATING PRESSURE OF THE EVAPORATOR(LBF/IN2)
 CC PIE - 3.141592654
 CC PNH3E - PRANDLT NUMBER FOR EVAP SHELLSIDE FLOW
 CC PNSWC - PRANDLT NUMBER FOR CONDENSER SW
 CC PNSWE - PRANDLT NUMBER FOR EVAP TUBESIDE FLOW
 CC PPP - PERCENT OF PARASITIC POWER(PCT)
 CC PRPROF - TUBE PROFILE SELECTION
 CC PRSYST - TUBE CONSTRAINT FOR SAT SYSTEM PRESS RATIO
 CC PWRCP - POWER COND. OR CSW COLD PIPE PUMP(HP)

NP000420
 NP005570
 NP002190
 NP002840
 NP004840
 NP002850
 NP002040
 NP005160
 NP003440
 NP002810
 NP003080
 NP002160
 NP002860
 NP004810
 NP002870
 NP005240
 NP005250
 NP001400
 NP004770
 NP001250
 NP004420
 NP001360
 NP004740
 NP002180
 NP002880
 NP004830
 NP002910
 NP003830
 NP002490
 NP001840
 NP005760
 NP002890
 NP005740
 NP006730
 NP005830
 NP000010
 NP003530
 NP002900
 NP003540
 NP002920
 NP003450
 NP005170
 NP001350
 NP004730
 NP002420
 NP003710
 NP004360
 NP006470

PWRCPM - CONVERSION OF PWRCPC(MW)
 PWREP - POWER EVAP SW PUMP(HP)
 PWREP - CONVERSION OF PWREP(MW)
 PWRNP - POWER OF AMMONIA CIRC PUMP(HP)
 PWRNPC - CONVERSION OF PWRNP(MW)
 PWRRM - POWER AMMONIA RE-FLUX PUMP MOTOR(MW)
 PWRRP - POWER AMMONIA RE-FLUX PUMP(HP)
 PWRTR - GEN-TURBINE OUTLET POWER(HP)
 QC - AMOUNT OF HEAT REJECTION(BTU/LBM)
 QCC - CONVERSION OF QC TO S.I. UNITS(MW)
 QCCMP - DISCHARGE RATE OF QCCMP TO S.I. UNITS(LIT/MIN)
 QCCMCC - CONVERSION OF QCCMCC TO S.I. UNITS(LIT/HR)
 QCT - HEAT TRANSFERED PER TUBE ADDITION(BTU/HR)
 QEC - AMOUNT OF EVAPORATOR HEAT ADDITION(BTU/HR)
 QEC - CONVERSION OF QEC TO S.I. UNITS(MW)
 QECMCC - CONVERSION OF QECMCC TO S.I. UNITS(LIT/MIN)
 QEPMP - DISCHARGE RATE OF EVAP SW PUMP(FT3/SEC)
 QET - HEAT TRANSFERED PER EVAP TUBE(BTU/HR)
 QIN - AMOUNT OF HEAT ADDED TO THE SYSTEM(MW)
 QNPMP - CONVERSION OF QNPMP TO S.I. UNITS(LIT/MIN)
 QNPMP - DISCHARGE RATE OF QNPMP TO S.I. UNITS(FT3/SEC)
 QRPMP - CONVERSION OF QRPMP TO S.I. UNITS(LIT/MIN)
 QRPMP - DISCHARGE RATE OF QRPMP TO S.I. UNITS(FT3/SEC)
 QRPMP - DISCHARGE RATE OF AMMONIA RE-FLUX PUMP(FT3/SEC)
 QRVMP - DISCHARGE RATE OF AMMONIA RE-FLUX PUMP(GAL/MIN)
 RDEPTH - AVG SW DENSITY OVER A SPECIFIED DEPTH(LBM/FT3)
 REMAX - SW DENSITY FOR MAX EVAP SHELLSIDE FLOW
 REMAXC - REYNOLDS NUMBER FOR MAX CONDENSER SHELLSIDE FLOW
 RFNH3(CFT) - SUBROUTINE FOR AMMONIA DENSITY(LBM/FT3)
 RFNH3(EFT) - SUBROUTINE FOR AMMONIA DENSITY(LBM/FT3)
 RFNH3(TI) - SUBROUTINE SAT LIQ AMMONIA DENSITY(LBM/FT3)
 RGNH3(PEVAP) - SUBROUTINE AMMONIA VAPOR DENSITY(LBM/FT3)
 RKCP - SW COLD PIPE RESISTANCE COEFFICIENT
 RKHE - EVAPORATOR OUTLET RESISTANCE COEFFICIENT
 RKHE - EVAPORATOR TUBING RESISTANCE COEFFICIENT
 RKHC - CONDENSER TUBING RESISTANCE COEFFICIENT
 RKHP - SW HOT PIPE RESISTANCE COEFFICIENT
 RKI - EVAPORATOR INLET RESISTANCE COEFFICIENT
 RKNH3P - PIPED AMMONIA RESISTANCE COEFFICIENT
 RKNHRP - PIPED RE-FLUX AMMONIA RESISTANCE COEFFICIENT
 RHOSWC - DENSITY OF CONDENSER SW(LBM/FT3)
 RHOSWE - EVAPORATOR SW DENSITY(LBM/FT3)
 RHOSW(TBLKC) - SUBROUTINE SW DENSITY(LBM/FT3)
 RHOSW(TCIC) - SUBROUTINE FOR DENSITY OF SW(LBM/FT3)
 RHOSW(THIE) - SUBROUTINE SW DENSITY(LBM/FT3)
 RHOSWD(TLCP) - SUBROUTINE SW DENSITY(DEPTH) (LBM/FT3)
 RHOSWR - REVISED CONDENSER SW DENSITY(LBM/FT3)
 RNH3CH - PSEUDO REYNOLDS NO.FOR HORIZ. CONDENSER

NPU006490
 NPU006140
 NPU006160
 NPU006680
 NPU000230
 NPU000200
 NPU000860
 NPU000670
 NPU002930
 NPU006500
 NPU002950
 NPU001440
 NPU005030
 NPU002940
 NPU002960
 NPU006170
 NPU004980
 NPU002440
 NPU002970
 NPU006710
 NPU002980
 NPU000240
 NPU000250
 NPU000970
 NPU000960
 NPU005630
 NPU001900
 NPU001970
 NPU005510
 NPU005060
 NPU005700
 NPU006280
 NPU005500
 NPU006070
 NPU006410
 NPU003330
 NPU005480
 NPU006570
 NPU000100
 NPU000730
 NPU000790
 NPU000740
 NPU000890
 NPU000880
 NPU001280
 NPU002010

CC	RNH3CV	-	PSEUDO	REYNOLDS	NO.	FOR	VERT.	CONDENSER	NP002020
CC	RNH3EH	-	PSEUDO	REYNOLDS	NR	FOR	THIN	FILM EVAPORATION	NP005150
CC	RNH3EV	-	PSEUDO	REYNOLDS	NR	FOR	CONVECTIVE	EVAPORATION	NP005230
CC	RNH3P	-	REYNOLDS	NUMBER OF	PIPED	AMMONIA	FLOW		NP006550
CC	RNH3RP	-	REYNOLDS	NUMBER OF	RE-FLUX	AMMONIA	PIPE FLOW		NP000080
CC	RNSWC	-	REYNOLDS	NUMBER OF	CONDENSER	TUBESIDE	FLOW		NP006390
CC	RNSWC	-	REYNOLDS	NUMBER OF	COLD PIPE	SW FLOW			NP006230
CC	RNSWE	-	REYNOLDS	NUMBER OF	EVAPORATOR	TUBESIDE	FLOW		NP005720
CC	RNSWHP	-	REYNOLDS	NUMBER OF	HOT PIPE	SW FLOW			NP002310
CC	RONH3C	-	CONDENSER	AMMONIA	DENSITY	(LBM/FT3)			NP001950
CC	RONH3E	-	DENSITY OF	EVAP	AMMONIA	DENSITY	(LBM/FT3)		NP005490
CC	RONH3P	-	EVAP	SHELLSIDE	AMMONIA	DENSITY	(LBM/FT3)		NP005590
CC	RONH3R	-	RE-FLUX	AMMONIA	DENSITY	(LBM/FT3)			NP000030
CC	RONH3S	-	NH3	DENSITY	AT	MOISTURE	SEPARATOR	INLET	(LBM/FT3)
CC	RONH3T	-	CONDENSER	SHELLSIDE	VAPOR	DENSITY	(LBM/FT3)		NP001030
CC	RONH3V	-	EVAPORATOR	AMMONIA	VAPOR	DENSITY	(LBM/FT3)		NP001670
CC	ROSACP	-	DENSITY OF	COLD PIPE	SW	(LBM/FT3)			NP005680
CC	ROSHP	-	HOT PIPE	SW	DENSITY	(LBM/FT3)			NP006190
CC	RTBLKC	-	REVISED	COND	BULK	TEMPERATURE	(DEG F)		NP004430
CC	RTBLKE	-	REVISED	EVAP	TBLKE	TEMPERATURE	(DEG F)		
CC	RTNCT	-	REVISED	NJMBER	OF	CONDENSER	TUBES		
CC	S4	-	ENTROPY	AT	STATE	PT 4	(BTU/LBM.R)		NP004890
CC	S4G	-	ENTROPY	OF	LIQ	AT	STATE	PT 4	(BTU/LBM.R)
CC	S4G	-	ENTROPY	OF	VAPOR	AT	STATE	PT 4	(BTU/LBM.R)
CC	S5F	-	ENTROPY	OF	A LIQ	AT	STATE	PT 5	(BTU/LBM.R)
CC	S5G	-	ENTROPY	OF	A VAPOR	AT	STATE	PT 5	(BTU/LBM.R)
CC	SCALBC	-	ABSOLUTE	TE	TBLKE	TEMPERATURE	(DEG F)		NP000550
CC	SCALBC	-	ABSOLUTE	CONDENSER	BULK	TEMPERATURE	(DEG F)		NP000560
CC	SCALC	-	ABSOLUTE	COAMMONIA	HT	COEFF	(BTU/HR.FT2.F)		NP004910
CC	SCALH	-	ABSOLUTE	VALUE	OF	HNH3ER	(BTU/HR.FT2.F)		NP001180
CC	SCALH	-	ABSOLUTE	VALUE	OF	TR3	(DEG F)		NP002080
CC	SCALT1	-	ABSOLUTE	VALUE	OF	T1R	(DEG F)		NP005330
CC	SCALT1	-	ABSOLUTE	VALUE	FOR	VNH3ER	(FT/SEC)		NP005990
CC	SF(T1)	-	SUBROUTINE	FOR	ENTROPY	OF	A LIQ	(BTU/LBM.R)	NP005950
CC	SF(T4)	-	SUBROUTINE	FOR	ENTROPY	OF	A LIQ	(BTU/LBM.R)	NP000530
CC	SF(T5)	-	SUBROUTINE	FOR	ENTROPY	OF	SAT LIQ	NH3(BTU/LBM.R)	NP000500
CC	SG(T1)	-	SUBROUTINE	FOR	ENTROPY	OF	A VAPOR	(BTU/LBM.R)	NP001640
CC	SG(T4)	-	SUBROUTINE	FOR	ENTROPY	OF	A VAPOR	(BTU/LBM.R)	NP000540
CC	SG(T5)	-	SUBROUTINE	FOR	ENTROPY	OF	A VAPOR	(BTU/LBM.R)	NP000510
CC	SN	-	VERTICAL	HEIGHT	BE	TWEEN	TUBES	SAT VAP	NH3(BTU/LBM.R)
CC	SNC	-	HORIZONTAL	HEIGHT	BE	TWEEN	TUBES	CENTER	(IN)
CC	SPEC	-	HORIZONTAL	DISTANCE	BE	TWEEN	TUBES	CONDENSER	TUBES(IN)
CC	SWFC	-	CONVERSION	OF	SPE	(FT)			NP004550
CC	SWFC	-	SALT	WATER	FOULING	COEFFICIENT	(HR.FT.F/BTU)		NP001660
CC	T1	-	SAT	LIQ	AMMONIA	TEMPERATURE	AT	STATE	PT 1(DEG F)
CC	T1C	-	CONVERSION	OF	T1	TO	S.I.	UNITS	(DEG C)
CC	T1R	-	REVISED	TEMPERATURE	OF	AMMONIA	AT	STATE	PT 1(DEG F)
CC	T3	-	AMMONIA	VAPOR	TEMPERATURE	AT	STATE	PT 3	(DEG F)

T3A	- SAT VAPOR AMMONIA TEMP AT STATE PT 3A(DEG F)	NP004270
T3AC	- CONVERSION OF T3A TO S.I. UNITS(DEG C)	NP003030
T3C	- CONVERSION OF T3 TO S.I. UNITS(DEG C)	NP003040
T3R	- REVISED TEMPERATURE AT STATE PT 3(DEG F)	NP005970
T4	- TEMPERATURE OF AMMONIA AT STATE PT 4(DEG F)	NP005820
T4C	- CONVERSION OF T4 TO S.I. UNITS(DEG C)	NP003050
T5	- TEMPERATURE OF AMMONIA AT STATE PT 5(DEG F)	NP001530
T5VGE	- AVERAGE EVAPORATOR TEMPERATURE(DEG F)	NP000020
TBLKCC	- CONDENSER SW BULK TEMPERATURE(DEG F)	NP006320
TBLKCR	- CONVERSION OF TBLKCC(DEG R)	NP006330
TBLKE	- EVAPORATOR SW BULK TEMPERATURE(DEG F)	NP004460
TBLKER	- CONVERSION OF TBLKE(DEG R)	NP004690
TCE	- THERMODYNAMIC CYCLE EFFICIENCY(PCT)	NP002450
TCIC	- CONDENSER SW INLET TEMPERATURE(DEG F)	NP000710
TCICC	- CONVERSION OF TCIC TO S.I. UNITS(DEG C)	NP003060
TCOC	- CONDENSER SW OUTLET TEMPERATURE(DEG F)	NP000720
TCOCC	- CONVERSION OF TCOC TO S.I. UNITS(DEG C)	NP003070
TC(TDOCC)	- SUBROUTINE TO COST COND TI TUBING/FT(\$/FT)	NP004210
TC(TDOE)	- SUBROUTINE TO COST EVAP TI TUBING O/FT(\$/FT)	NP004160
TC(TDOCC)	- SUBROUTINE TO COST COND TI TUBING/FT(\$/FT)	NP004230
TDIC	- CONDENSER TUBE INNER DIAMETER(IN)	NP004290
TDICC	- CONVERSION OF TDIC(FT)	NP001290
TDIE	- EVAPORATOR TUBE INNER DIAMETER(IN)	NP004310
TDIEC	- CONVERSION OF TDIE(FT)	NP004330
TDICC	- CONVERSION OF TDICC(FT)	NP003560
TDODCC	- CONVERSION OF TDODCC(FT)	NP004340
TDODCC	- CONVERSION OF TDODCC(FT)	NP003090
TDODCC	- EVAPORATOR TUBE OUTER DIAMETER(IN)	NP003570
TDODCC	- CONVERSION OF TDODCC(FT)	NP004350
TEC(TDOE)	- SUBROUTINE TO COST ENHANCED EVAP TI TUBE(\$/FT)	NP004180
TENS	- SURFACE TENSION OF AMMONIA(LB/FT)	NP005270
TE(TDOCC)	- SUBROUTINE TO SIZE ENHANCED COND TI TUBING(IN)	NP004220
TE(TDOE)	- SUBROUTINE TO SIZE ENHANCED EVAP TI TUBING(IN)	NP004170
THIACC	- TOTAL CONDENSER HT SURFACE AREA(FT2)	NP002200
THIAEC	- CONVERSION OF THIACC TO S.I. UNITS(M2)	NP003140
THIAEC	- TOTAL EVAP HEAT TRANSFER AREA(FT3)	NP004530
THIAEC	- CONVERSION OF THIAEC TO S.I. UNITS(M2)	NP003150
THIAEC	- REVISED EVAP HEAT TRANSFER AREA(FT2)	NP005310
THIE	- EVAPORATOR INLET SW TEMPERATURE(DEG F)	NP003580
THIEC	- CONVERSION OF THIE TO S.I. UNITS(DEG C)	NP003120
THOEC	- EVAP SW OUTLET TEMP(DEG F)	NP004880
THOEC	- CONVERSION OF THOEC TO S.I. UNITS(DEG C)	NP003130
TKNH3C	- COND AMMONIA THERMAL CONDUCTIVITY(BTU/HR.FT.F)	NP001980
TKNH3C(FT)	- SUBROUTINE FOR NH3 THERMAL CONDUCTIVITY	NP001990
TKNH3E	- THERMAL COND OF AMMONIA IN EVAP(BTU/HR.FT.F)	NP006030
TKNH3E(FT)	- THERMAL COND OF AMMONIA(BTU/HR.FT.F)	NP005470
TKSWC	- CONDENSER SW THERMAL CONDUCTIVITY(BTU/HR.FT.F)	NP001320

TYPE	CONDENSER	TYPE	SELECTION	UNIT	VALUE
C	UAC	CONDENSER	TYPE	SELECTION	UNIT
C	UCC	CONDENSER	TYPE	SELECTION	UNIT
C	UEC	CONDENSER	TYPE	SELECTION	UNIT
C	UAPC	CONDENSER	TYPE	SELECTION	UNIT
C	VAPC	CONDENSER	TYPE	SELECTION	UNIT
C	VAVGC	CONDENSER	TYPE	SELECTION	UNIT
C	VAVGC	CONDENSER	TYPE	SELECTION	UNIT
C	VFI	CONDENSER	TYPE	SELECTION	UNIT
C	VFR	CONDENSER	TYPE	SELECTION	UNIT
C	VHEAD	CONDENSER	TYPE	SELECTION	UNIT
C	VISSWC	CONDENSER	TYPE	SELECTION	UNIT
C	VISSWE	CONDENSER	TYPE	SELECTION	UNIT
C	VISSW(TBLKC)	CONDENSER	TYPE	SELECTION	UNIT
C	VISSW(TBLKE)	CONDENSER	TYPE	SELECTION	UNIT
C	VISSW(THIE)	CONDENSER	TYPE	SELECTION	UNIT
C	VISSWCP	CONDENSER	TYPE	SELECTION	UNIT
C	VISSWHP	CONDENSER	TYPE	SELECTION	UNIT
C	VLIQC	CONDENSER	TYPE	SELECTION	UNIT
C	VLIQC	CONDENSER	TYPE	SELECTION	UNIT
C	VMAXC	CONDENSER	TYPE	SELECTION	UNIT
C	VMAXE	CONDENSER	TYPE	SELECTION	UNIT
C	VNH3C	CONDENSER	TYPE	SELECTION	UNIT
C	VNH3E	CONDENSER	TYPE	SELECTION	UNIT
C	VNH3ER	CONDENSER	TYPE	SELECTION	UNIT
C	VNH3P	CONDENSER	TYPE	SELECTION	UNIT
C	VNH3P	CONDENSER	TYPE	SELECTION	UNIT
C	VNH3C	CONDENSER	TYPE	SELECTION	UNIT
C	VSNH3C	CONDENSER	TYPE	SELECTION	UNIT
C	VSNH3E	CONDENSER	TYPE	SELECTION	UNIT
C	VSNH3E	CONDENSER	TYPE	SELECTION	UNIT
C	VSNH3P	CONDENSER	TYPE	SELECTION	UNIT
C	VSNH3P	CONDENSER	TYPE	SELECTION	UNIT
C	VSWC	CONDENSER	TYPE	SELECTION	UNIT
C	VSWCC	CONDENSER	TYPE	SELECTION	UNIT
C	VSWCP	CONDENSER	TYPE	SELECTION	UNIT
C	VSWCP	CONDENSER	TYPE	SELECTION	UNIT
C	VSWEC	CONDENSER	TYPE	SELECTION	UNIT
C	VSWEC	CONDENSER	TYPE	SELECTION	UNIT
C	VSWHP	CONDENSER	TYPE	SELECTION	UNIT
C	VSWHP	CONDENSER	TYPE	SELECTION	UNIT
C	WC	CONDENSER	TYPE	SELECTION	UNIT
C	WE	CONDENSER	TYPE	SELECTION	UNIT

C WEA - AMMONIA FLOW RATE PER UNIT AXIAL LENGTH(LBM/HR.FT)
 C WELECG - GROSS ELECTRICAL LOADING(MW)
 C WELELOSS - NET ELECT OUTPUT AS A F(EFFICIENCY)(MW)
 C WNET - NET WORK IN THERMODYNAMIC CIRC PUMP WORK(BTU/LBM)
 C WPNH3 - THERMODYNAMIC AMMONIA CIRC PUMP WORK(BTU/LBM)
 C WPSNH3 - ISENTROPIC AMMONIA AT STATE PT 3(DECIMAL)
 C X3A - QUALITY OF AMMONIA AT STATE PT 3(DECIMAL)
 C X3P - QUALITY OF AMMONIA AT STATE PT 3(PERCENT)
 C X4 - QUALITY OF AMMONIA AT STATE PT 4(DECIMAL)
 C X4P - QUALITY OF AMMONIA AT STATE PT 4(PERCENT)
 C X5 - QUALITY AT STATE PT 5(DECIMAL)
 C X5P - CONVERSION OF X5(PCT)
 C X5S - QUALITY AT STATE PT 5S(DECIMAL)
 C X5SP - CONVERSION OF X5S(PCT)

NPU005190
 NPU000380
 NPU000360
 NPU000370
 NPU002430
 NPU005080
 NPU005070
 NPU001560
 NPU005750
 NPU005860
 NPU005850
 NPU005870
 NPU000450
 NPU000460
 NPU000570
 NPU000580

C	TYPEEC=3.	HORIZONTAL EVAPORATOR	BOILING CORRELATION	49	A
C	TYPEEC=1.	HORIZONTAL CONDENSER		50	A
C	TYPEEC=2.	VERTICAL CONDENSER		51	A
C				52	A
	TYPEEC=1.			53	A
	TYPEEC=1.			54	A
				55	A
C	ENHANCEMENT SELECTION			56	A
C				57	A
C	EHFE=1.	PLAIN TUBE EVAPORATOR		58	A
C	EHFC=1.	PLAIN TUBE CONDENSER		59	A
C	EHFE=2.	LINDE-PROMOTER EVAPORATOR(NOT CODED)		60	A
C	EHFC=2.	LINDE-PROMOTER CONDENSER(NOT CODED)		61	A
C				62	A
	EHFC=1.			63	A
	EHFE=1.			64	A
C	TUBE FIN EFFICIENCY			65	A
C				66	A
	EFFIE=1.0			67	A
	EFFOE=1.0			68	A
	EFFOC=1.0			69	A
	EFFIC=1.0			70	A
C	TUBE PROFILE SELECTION			71	A
C	PROF=1.	STAGGERED EQUI-LATERAL		72	A
C	PROF=2.	IN-LINE EQUI-SIDED		73	A
C	PROF=1.			74	A
C	SYSTEM PIPE GEOMETRY AND MATERIAL			75	A
C				76	A
	ECC=150.E-06			77	A
	ECP=500.E-06			78	A
	ECE=150.E-06			79	A
	EHP=500.E-06			80	A
	ELBOW=30.			81	A
	ENH3P=500.E-06			82	A
	TLC=3000.			83	A
	TLHP=300.			84	A
	TLNH3P=150.			85	A
	TLNHRP=50.			86	A
C	TUBING MATERIAL SELECTION			87	A
C	TMATL=1.	ALUMINIUM		88	A
C	TMATL=2.	TITANIUM		89	A
C				90	A
	TMATL=1.			91	A
	TKW=77.			92	A
				93	A
				94	A
				95	A
				96	A

C C PROJECTED INFLATION RATE FOR AL TUBE REINSTALLATION(PCT)
C C
C AINT=10.
C
C EVAP/MOISTURE SEPARATOR QUALITY REQUIREMENTS(PCT)
C C
C X3P=92.
C X4P=99.5
C
C SALT WATER FOULING COEFFICIENT(HR.FT.F/BTU)
C C
C SWFC=.00025
C
C PUMP AND GEN-TURB EFFICIENCIES
C C
C EEP=96.6
C EMC=98.
C EME=98.
C EMNH3=98.
C EMNHR=98.
C EPC=85.
C EPE=85.
C EPNH3=75.
C EPNHR=75.
C ETRP=99.8
C
C NET OUTPUT POWER REQUIRED(MW)
C C
C ELECT=30.
C
C INPUT DATA SI UNIT CONVERSION
C C
C DICPC=.3048*DICP
C DIHPC=.3048*DIHP
C DINH3C=.3048*DINH3
C DINHRC=.3048*DINH3R
C PCONDC=6.89476E-03*PCOND
C PEVAPC=6.89476E-03*PEVAP
C TICCC=5.*(TICIC-32.)/9.
C TDOCCC=25.4*TDOCC
C TDOECC=25.4*TDOE
C THIEC=5.*(THIE-32.)/9.
C TKWC=1.73707*TKW
C TLCC=.3048*TLCC
C TLEC=.3048*TLE
C TLHPC=.3048*TLHP
C TLNHPC=.3048*TLNH3P

A 97
A 98
A 99
A 100
A 101
A 102
A 103
A 104
A 105
A 106
A 107
A 108
A 109
A 110
A 111
A 112
A 113
A 114
A 115
A 116
A 117
A 118
A 119
A 120
A 121
A 122
A 123
A 124
A 125
A 126
A 127
A 128
A 129
A 130
A 131
A 132
A 133
A 134
A 135
A 136
A 137
A 138
A 139
A 140
A 141
A 142
A 143
A 144


```

TLNRPC=.3048*TLNHRP
TLCPC=.3048*TLCP
VSWCC=.3048*VSWC
VSWEC=.3048*VSWE
VSWCPC=.3048*VSWCP
VSWHPC=.3048*VSWHP

```

C SUMMARY OF INPUT DATA

```

10  WRITE (6,1150)
    IF (TYPE.EQ.2.) GO TO 10
    WRITE (6,1160)
    GO TO 20
    CONTINUE
20  WRITE (6,1170)
    CONTINUE
    WRITE (6,1180) TDOE,TDOECC
    WRITE (6,1190) TLE,TLEC
    WRITE (6,1200) VSWC,VSWEC
    WRITE (6,1210) PEVAP,PEVAPC
    IF (TMATL.EQ.2.) GO TO 30
    WRITE (6,1220) TKW,TKWC
    GO TO 40
    CONTINUE
30  WRITE (6,1230) TKW,TKWC
    CONTINUE
40  IF (PROF.EQ.2.) GO TO 50
    WRITE (6,1240)
    GO TO 60
    CONTINUE
50  WRITE (6,1250)
    CONTINUE
60  WRITE (6,1260) EPR
    IF (EHFE.EQ.2.) GO TO 70
    WRITE (6,1270)
    GO TO 80
    CONTINUE
70  WRITE (6,1280)
    CONTINUE
80  IF (TYPEC.EQ.2.) GO TO 90
    WRITE (6,1290)
    GO TO 100
    CONTINUE
90  WRITE (6,1300)
    CONTINUE
100 WRITE (6,1310) TDOC,TDOCCC
    WRITE (6,1320) TLC,TLCC
    WRITE (6,1330) VSWC,VSWCC

```

A 145
A 146
A 147
A 148
A 149
A 150
A 151
A 152
A 153
A 154
A 155
A 156
A 157
A 158
A 159
A 160
A 161
A 162
A 163
A 164
A 165
A 166
A 167
A 168
A 169
A 170
A 171
A 172
A 173
A 174
A 175
A 176
A 177
A 178
A 179
A 180
A 181
A 182
A 183
A 184
A 185
A 186
A 187
A 188
A 189
A 190
A 191
A 192



110	WRITE (6,1340) PCOND,PCONDC IF (TMATL.EQ.2.) GO TO 110 WRITE (6,1350) TKW,TKWC GO TO 120	
120	CONTINUE WRITE (6,1360) TKW,TKWC CONTINUE IF (PROF.EQ.2.) GO TO 130 WRITE (6,1370) GO TO 140	
130	CONTINUE WRITE (6,1380) CONTINUE WRITE (6,1390) EPR IF (EHFC.EQ.2.) GO TO 150 WRITE (6,1400) GO TO 160	
140	CONTINUE WRITE (6,1410) CONTINUE WRITE (6,1420) WRITE (6,1430) DIHP,DIHPC WRITE (6,1440) TLHP,TLHPC WRITE (6,1450) VSWHP,VSWHPC WRITE (6,1460) THIE,THIEC WRITE (6,1470) CONH WRITE (6,1480) WRITE (6,1490) DICP,DICPC WRITE (6,1500) TLCP,TLCP WRITE (6,1510) VSWCP,VSWCPC WRITE (6,1520) TCIC,TCICC WRITE (6,1530) CONC WRITE (6,1540) WRITE (6,1550) DINH3,DINH3C WRITE (6,1560) TLNH3P,TLNHPC WRITE (6,1570) WRITE (6,1580) DINH3R,DINHRC WRITE (6,1590) TLNHRP,TLNRPC WRITE (6,1600) WRITE (6,1610) WRITE (6,1620) EPE,EME WRITE (6,1630) EPC,EMC WRITE (6,1640) WRITE (6,1650) EPNH3,EMNH3 WRITE (6,1660) WRITE (6,1670) EEP WRITE (6,1680) ETRP WRITE (6,1690)	
150		
160		

A	193
A	194
A	195
A	196
A	197
A	198
A	199
A	200
A	201
A	202
A	203
A	204
A	205
A	206
A	207
A	208
A	209
A	210
A	211
A	212
A	213
A	214
A	215
A	216
A	217
A	218
A	219
A	220
A	221
A	222
A	223
A	224
A	225
A	226
A	227
A	228
A	229
A	230
A	231
A	232
A	233
A	234
A	235
A	236
A	237
A	238
A	239
A	240


```

170 WRITE (6,1700) ELECT
171 RETURN
172 CONTINUE
173
174 C *** EXECUTION OF INPUT DATA ***
175 C
176 C TUBE WALL THICKNESS(INCH) AND TUBE COST PER FT($/FT)
177 C ALUMINUM TUBING
178 C
179 IF (TMAIL.GT.1.5) GO TO 210
180 IF (EHFE.GT.1.5) GO TO 180
181 TTE=AP(TDOE)
182 E1=AC(TDOE)
183 E2=0.0
184 GO TO 190
185 CONTINUE
186 TTE=AE(TDOE)
187 E1=AEC(TDOE)
188 E2=0.0
189 CONTINUE
190 IF (EHFC.GT.1.5) GO TO 200
191 TTC=AP(TDOC)
192 C1=AC(TDOC)
193 C2=0.0
194 GO TO 250
195 CONTINUE
196 TTC=AE(TDOC)
197 C1=ACC(TDOC)
198 C2=0.0
199 GO TO 250
200
201 C TITANIUM TUBING
202 C
203 C CONTINUE
204 IF (EHFE.EQ.2.) GO TO 220
205 TTE=TP(TDOE)
206 E1=TC(TDOE)
207 E2=1.21
208 GO TO 230
209 CONTINUE
210 TTE=TE(TDOE)
211 E1=TEC(TDOE)
212 E2=1.21
213 CONTINUE
214 IF (EHFC.EQ.2.) GO TO 240
215 TTC=TP(TDOC)
216 C1=TC(TDOC)

```



```

240 C2=1.21
      GO TO 250
      CONTINUE
      TTC=TE(TDOC)
      C1=ICC(TDOC)
      C2=1.21
      CONTINUE
250 C
      C DESIGN VARIABLE DIMENSION CONVERSION
      C
      P1=PCOND
      H1=HF(PCOND)
      T1=TSAT(PCOND)
      T3A=TSAT(PEVAP)
      T3=TSAT(PEVAP)
      T5=TSAT(PCOND)
      TDIC=TDOC-2.*TTC
      TDICC=TDIC/12.
      TDIE=TDOE-2.*TTE
      TDIEC=TDIE/12.
      TDOCC=TDOC/12.
      TDOEC=TDOE/12.
      C CONSTRAINT FOR SAT SYSTEM PRESSURE RATIO
      C
      PRSYST=PEVAP/PCOND
      C
      C CONSTRAINT FOR SAT UPPER TEMP BOUND
      C
      DTEMP1=THIE-T3A
      C
      C CONSTRAINT FOR SAT LOWER TEMP BOUND
      C
      DTEMP2=T1-TCIC
      C
      C CONSTRAINT FOR CONDENSER OUTLET TEMPERATURE BOUND
      C
      DTEMP5=T1-TCOC
      C
      *****
      *
      * EVAPORATOR SECTION
      *
      *
      *****
      *
      *
      *
      *
      *****

```

```

289 A
290 A
291 A
292 A
293 A
294 A
295 A
296 A
297 A
298 A
299 A
300 A
301 A
302 A
303 A
304 A
305 A
306 A
307 A
308 A
309 A
310 A
311 A
312 A
313 A
314 A
315 A
316 A
317 A
318 A
319 A
320 A
321 A
322 A
323 A
324 A
325 A
326 A
327 A
328 A
329 A
330 A
331 A
332 A
333 A
334 A
335 A
336 A

```



```

C C INITIALLY ASSUME AN EVAP TUBE LENGTH(FT)
C C ASSUME A HT COEF FOR EVAP SHELLSIDE
C C HTNH3E=1000.
C C HOT PIPE SW MASS FLOW RATE(LBM/HR)
C C
C C ROSWHP=RHOSW(THIE)
C C FLOHP=3600.*ROSWHP*PIE*DIHP**2*VSWHP/4.
C C EVAP SW DENSITY(INITIALY ASSUME TBULK=THIE)
C C
C C TBLKE=THIE
C C CONTINUE
C C RHOSWE=RHOSW(TBLKE)
C C TKSWE=TKSW(TBLKE)
C C
C C TOTAL NUMBER OF EVAP TUBES
C C TNET=4.*FLOHP/(3600.*RHOSWE*PIE*TDIEC**2*VSWWE)
C C
C C TUBE SHEET DIAMETER(FT)
C C
C C TUBE PROFILE - STAGGERED
C C
C C IF (PROF.EQ.2.) GO TO 270
C C EHT=EPR*TD0E*0.5
C C EBASE=EPR*TD0E*0.866
C C ETAREA=EHT*EBASE*2.
C C SN=2.*EHT
C C SPE=2.*EBASE-TD0E
C C SPEC=SPE/12.
C C GO TO 280
C C CONTINUE
C C
C C TUBE PROFILE - IN-LINE
C C
C C EPLONG=EPR*TD0E
C C SN=EPLONG
C C EPLAT=EPR*TD0E
C C ETAREA=EPLONG*EPLAT
C C SPE=EPR*TD0E-TD0E
C C SPEC=SPE/12.
C C CONTINUE
C C EAREA=ETAREA*TNET
C C TSDE=((4.*EAREA/PIE)*0.5)/12.
C C
C C TOTAL HT AREA OF EVAP(FT2 OR M2)

```

A 337
 A 338
 A 339
 A 340
 A 341
 A 342
 A 343
 A 344
 A 345
 A 346
 A 347
 A 348
 A 349
 A 350
 A 351
 A 352
 A 353
 A 354
 A 355
 A 356
 A 357
 A 358
 A 359
 A 360
 A 361
 A 362
 A 363
 A 364
 A 365
 A 366
 A 367
 A 368
 A 369
 A 370
 A 371
 A 372
 A 373
 A 374
 A 375
 A 376
 A 377
 A 378
 A 379
 A 380
 A 381
 A 382
 A 383
 A 384


```

C      THTAE=TNET*PIE*TD0EC*TLE
C      CMIN FOR EVAP(BTU/HR.F OR W/C)
C      CPSWE=CPSW(TBLKE)
C      CMINE=FLOHP*CPSWE
C      OVERALL HT COEF(BTU/HR.FT2.F OR W/M2.C)
C      TBLKER=TBLKE*459.69
C      REYNOLDS NUMBER FOR EVAP TUBESIDE
C      VISSWE=VISSW(TBLKE)
C      RNSWE=3600.*RHOSWE*VSWE*TDIEC/VISSWE
C      PRANDTL NUMBER FOR EVAP TUBESIDE
C      PNSWE=CPSWE*VISSWE/TKSWE
C      HT COEF FOR EVAP TUBESIDE
C      IF (RNSWE.GT.2300.) GO TO 290
C      LAMINAR FLOW USING SIEDER-TATE CORRELATION
C      HTSWE=1.86*TKSWE*(RNSWE*PNSWE)**.3333*(TDIEC/TLE)**.3333/TDIEC
C      GO TO 300
C      CONTINUE
C      TURBULENT FLOW USING DITUS-BOELTER CORRELATION
C      (INITIALLY ASSUME TBLKE=THIE)
C      HTSWE=.023*TKSWE*RNSWE**.8*PNSWE**.4/TDIEC
C      CONTINUE
C      THERMAL RESISTANCE FOR SW(HR.FT2.F/BTU)
C      TRIE=TD0EC/(EFFIE*HTSWE*TDIEC)
C      THERMAL RESISTANCE FOR SW FOULING(HR.FT2.F/BTU)
C      HTFSWE=1./SWFC
C      TR2E=TD0EC/(EFFIE*HTFSWE*TDIEC)
C      THERMAL RESISTANCE FOR WALL THICKNESS(HR.FT2.F/BTU)

```

```

A 385
A 386
A 387
A 388
A 389
A 390
A 391
A 392
A 393
A 394
A 395
A 396
A 397
A 398
A 399
A 400
A 401
A 402
A 403
A 404
A 405
A 406
A 407
A 408
A 409
A 410
A 411
A 412
A 413
A 414
A 415
A 416
A 417
A 418
A 419
A 420
A 421
A 422
A 423
A 424
A 425
A 426
A 427
A 428
A 429
A 430
A 431
A 432

```



```

C C TR3E=IDOE*ALOG(IDOE/IDIE)/(2.*TKW) A 433
C C THERMAL RESISTANCE FOR NH3 FOULING(HR.FT2.F/BTU) A 434
C C CONSIDERED NEGLIGIBLE A 435
C C A 436
C C A 437
C C A 438
C C A 439
C C A 440
C C A 441
C C A 442
C C A 443
C C A 444
C C A 445
C C A 446
C C A 447
C C A 448
C C A 449
C C A 450
C C A 451
C C A 452
C C A 453
C C A 454
C C A 455
C C A 456
C C A 457
C C A 458
C C A 459
C C A 460
C C A 461
C C A 462
C C A 463
C C A 464
C C A 465
C C A 466
C C A 467
C C A 468
C C A 469
C C A 470
C C A 471
C C A 472
C C A 473
C C A 474
C C A 475
C C A 476
C C A 477
C C A 478
C C A 479
C C A 480

TR3E=IDOE*ALOG(IDOE/IDIE)/(2.*TKW)
THERMAL RESISTANCE FOR NH3 FOULING(HR.FT2.F/BTU)
CONSIDERED NEGLIGIBLE

THERMAL RESISTANCE FOR NH3
EFFOE=1.
TR5E=1./((EFFOE*HTNH3E)
PSEUDO HT COEF FOR SW(BTU/HR.FT2.; OR W/M2.C)
HSWE=1./TR1E
PSEUDO HT COEF FOR SW FOULING(BTU/HR.FT2.F OR W/M2.C)
HFSWE=1./TR2E
PSEUDO HT COEF FOR WALL THICK(BTU/HR.FT2.F OR W/M2.C)
HWE=1./TR3E
PSEUDO HT COEF FOR AMMONIA(BTU/HR.FT2.F OR W/M2.C)
HNH3E=1./TR5E
OVERALL HT COEF CALCULATION-OUTTER
SURFACE(BTU/HR.FT2.F OR W/M2.C)
UE=1./((TR1E+TR2E+TR3E+TR5E)
NUMBER OF TRANSFER UNITS FOR EVAP(NTU)
ENTU=UE*HTAE/CMINE
EVAP EFFECTIVENESS(EPSILON)
EPSE=1.-EXP(-ENTU)
EVAP SW OUTLET TEMP(F OR C)
THOE=THIE-(THIE-T3A)*(1.-EXP(-ENTU))
REVISED SW AVG BULK TEMP(F)
RTBLKE=(THOE+THIE)/2.

```



```

C TEST FOR A SAT TBULK TEMPERATURE
C
    DBLKT=ABS(TBLKE-RTBLKE)
    SCALB=ABS(TBLKE)
    IF (SCALB.LT.0.1) SCALB=0.1
    DELB=DBLKT/SCALB
    IF (DELB.LT.0.001) GO TO 310
    TBLKE=RTBLKE
    GO TO 260
    CONTINUE
    TBLKE=RTBLKE
310
C FILM TEMP FOR PROPERTY EVALUATION
C INITIALLY ASSUME T3(IDEAL)=T3(ACTUAL)
C
    THERMAL RESISTANCES FOR SINGLE TUBE CONDUCTANCE(UA)
    (BTU/HR.F)
    AO=PIE*IDDEC*TLE
    THERMAL RESISTANCE SW(HR.F/BTU)
    CTR1E=TR1E/AO
    THERMAL RESISTANCE SW FOULING(HR.F/BTU)
    CTR2E=TR2E/AO
    THERMAL RESISTANCE WALL THICKNESS(HR.F/BTU)
    CTR3E=TR3E/AO
    THERMAL RESISTANCE FOR NH3 FOULING(HR.F/BTU)
    NEGLIGIBLE
    THERMAL RESISTANCE NH3(HR.F/BTU)
    CTR5E=TR5E/AO
    HEAT TRANSFERED PER TUBE(BTU/HR)
    QET=(TBLKE-T3)/(CTR1E+CTR2E+CTR3E+CTR5E)
    SHELLSIDE WALL TEMPERATURE(F)
    ETW2=TBLKE-QET*(CTR1E+CTR2E+CTR3E)
C

```

A 481
 A 482
 A 483
 A 484
 A 485
 A 486
 A 487
 A 488
 A 489
 A 490
 A 491
 A 492
 A 493
 A 494
 A 495
 A 496
 A 497
 A 498
 A 499
 A 500
 A 501
 A 502
 A 503
 A 504
 A 505
 A 506
 A 507
 A 508
 A 509
 A 510
 A 511
 A 512
 A 513
 A 514
 A 515
 A 516
 A 517
 A 518
 A 519
 A 520
 A 521
 A 522
 A 523
 A 524
 A 525
 A 526
 A 527
 A 528


```

C C TUBESIDE WALL TEMPERATURE(F) A 529
C C ETW1=TBLKE-QET*(CTR1E+CTR2E) A 530
C C EVAP FILM TEMP CALCULATION(F) A 531
C C EFT=(ETW2+T3)/2. A 532
C C DELTA T TEMPERATURE(F) A 533
C C DELTAE=ETW2-T3 A 534
C C AMOUNT OF HEAT ADDITION(BTU/HR OR W) A 535
C C QE=CMINE*(THIE-THOE) A 536
C C LOG MEAN TEMPERATURE DIFFERENCE OF EVAP(F OR C) A 537
C C INITIALLY ASSUME T3(IDEAL)=T3(ACTUAL) A 538
C C ELMTD=(1.-EXP(-ENTU))*CMINE*(THIE-T3)/(UE*THTAE) A 539
C C ISENTROPIC NH3 PUMP WORK(BTU/LBM) A 540
C C INITIALLY ASSUME P1(IDEAL)=P1(ACTUAL) A 541
C C VF1=1./RFNH3(T1) A 542
C C WPSNH3=VF1*(PEVAP-P1)*144./BTUC A 543
C C THERMODYNAMIC NH3 PUMP WORK(BTU/LBM) A 544
C C EPNH3C=EPNH3/100. A 545
C C WPNH3=WPSNH3/EPNH3C A 546
C C WORKING FLUID PROPERTIES A 547
C C CPNH3E=CPNH3(EFT) A 548
C C VSNH3E=VSNH3(EFT) A 549
C C TKNH3E=TKNH3(EFT) A 550
C C RONH3E=RFNH3(EFT) A 551
C C ENTHALPY AT STATE PT 2(BTU/LBM) A 552
C C H2=H1+WPNH3 A 553
C C ENTHALPY AT STATE PT 3A(BTU/LBM) A 554
C C H3A=HF(PEVAP) A 555
C C INITIALIZE NH3 MASS FLOW RATE(LBM/HR) A 556
C C A 557
C C A 558
C C A 559
C C A 560
C C A 561
C C A 562
C C A 563
C C A 564
C C A 565
C C A 566
C C A 567
C C A 568
C C A 569
C C A 570
C C A 571
C C A 572
C C A 573
C C A 574
C C A 575
C C A 576

```



```

C      H3=HG(PEVAP)
C      FLONH3=QE/(H3-H2)
C      CONTINUE
320 C      PRESS DROP EVAP SHELLSIDE(LBF/IN2)
C      ASSUME VISCOSITY(TWALL)=VISCOSITY(TBULK)
C      MAX VELOCITY THRU MIN-FLOW AREA F(TUBE PROFILE)
C      RONH3P=RFNH3(T1)
C      VNH3E=4.*FLONH3/(3600.*RONH3P*PIE*DINH3**2)
C      VMAXE=VNH3E*(SN/(SN-TDOE))
C      REYNOLDS NO. FOR MAX SHELLSIDE FLOW
C      REMAX=3600.*RONH3E*VMAXE*TDOE/(12.*VSNH3E)
C      EMPIRICAL FRICTION FACTOR USING CORRELATION BY JAKOB
C      IF (PROF.EQ.2.) GO TO 330
C      EFF=(0.25+0.118/((SN-TDOE)/TDOE)**1.08)*REMAX**(-.16)
C      GO TO 340
C      CONTINUE
330 C      EFF=(0.44+(0.08*SN/TDOE)/((SN-TDOE)/TDOE)**(0.43+1.13*TDOE/SN))*RE
C      IMAX**(-.15)
C      CONTINUE
340 C      MASS VELOCITY FOR MIN FREE-FLOW AREA(LBM/FT2.SEC)
C      EAF=TSDE*TLE
C      EAF=EFF*(((SN-TDOE)/SN)
C      EGF=FLONH3/(3600.*EAF)
C      CALCULATION OF PRESS DROP EVAP SHELLSIDE(LBF/IN2)
C      USING THE HOMOGENEOUS TWO-PHASE MODEL
C      X3A=1.0
C      EDE=(EPR*TDOE-TDOE)/12.
C      VLIQE=1./RFNH3(T3A)
C      VAPE=1./RGNH3(PEVAP)
C      VAVGE=VLIQE*(1.+X3A*(VAPE-VLIQE)/VLIQE)
C      EFRIC=(EFF*EGF**2*VAVGE)/(144.*GC)
C      EMOM=(EGF**2*VAVGE)/(144.*GC)
C      EELEV=(EGF*TSDE)/(144.*GC)
C      DSEVAP=EFRICT+EMOM+EELEV
C      ENTHALPY AT STATE PT 3(BTU/LBM)

```



```

C ASSUME QUALITY EVAPORATOR OUTLET X3P
C
X3=X3P/100.
P3=PEVAP-DS*EVAP
H3F=HF(P3)
H3G=HG(P3)
H3=H3F+X3*(H3G-H3F)
C
C PRESSURE DROP ACROSS THE MOISTURE SEPARATOR(LBF/IN2)
C
RONH3S=RGNH3(P3)
ESPACE=0.1*TSDE*ILE
VNH3S=FLOH3/(3600.*RONH3S*ESPACE)
VHEAD=RONH3S*VNH3S**2/(2.*GC*144.)
DSDEM=20.*VHEAD
C
C MOISTURE SEPARATOR DISCHARGE DRAIN ENTHALPY(BTU/LBM)
C
P4=P3-DSDEM
T4=TSAT(P4)
PAVGD=(P3+P4)/2.
HDE=HF(PAVGD)
C
C ENTHALPY AT STATE PT 4(BTU/LBM)
C
ASSUME QUALITY OF MOISTURE SEPARATOR OUTLET X4P
X4=X4P/100.
H4F=HF(P4)
H4G=HG(P4)
H4=H4F+X4*(H4G-H4F)
C
C REVISED AMMONIA FLOW RATE(LBM/HR)
C
FLOH3=QE/((X4/X3)*H3-H2-(X4/X3-1.)*HDE)
C
C REVISED AMMONIA SHELLSIDE VELOCITY(FT/SEC)
C
VNH3ER=4.*FLOH3/(3600.*RONH3P*PIE*DINH3**2)
C
C TEST FOR SAT VNH3E(FT/SEC)
C
DVNH3E=ABS(VNH3ER-VNH3E)
SCALV=ABS(VNH3ER)
IF (SCALV.LT.0.1) SCALV=0.1
DELV=DVNH3E/SCALV
IF (DELV.LT.0.001) GO TO 350
VNH3E=VNH3ER
GO TO 320

```

A 625
A 626
A 627
A 628
A 629
A 630
A 631
A 632
A 633
A 634
A 635
A 636
A 637
A 638
A 639
A 640
A 641
A 642
A 643
A 644
A 645
A 646
A 647
A 648
A 649
A 650
A 651
A 652
A 653
A 654
A 655
A 656
A 657
A 658
A 659
A 660
A 661
A 662
A 663
A 664
A 665
A 666
A 667
A 668
A 669
A 670
A 671
A 672


```

350  CONTINUE
    VNH3E=VNH3ER
C  REVISED TEMP AT STATE PT 3(DEG F)
C
C  T3R=TSAT(P3)
C  TEST FOR SAT T3(DEG F)
C
    DTEMP3=ABS(T3R-T3)
    SCALT=ABS(T3R)
    IF (SCALT.LT.0.1) SCALT=0.1
    DELT3=DTEMP3/SCALT
    IF (DELT3.LT.0.001) GO TO 360
    T3=T3R
    GO TO 260
360  CONTINUE
    T3=T3R
C  PRANDTL NUMBER
C
    PNH3E=CPNH3E*VSNH3E/TKNH3E
C  EVAPORATOR TYPE IDENTIFICATION
C  TYPEE=1:HORIZONTAL OWENS CORRELATION
C  TYPEE=2:HORIZONTAL NON-BOILING CORRELATION
C  TYPEE=3:HORIZONTAL BOILING CORRELATION
C
    IF (TYPEE.GT.1.) GO TO 380
C  HORIZONTAL NON-BOILING USING OWENS CORRELATION
C
    TRANSITION REYNOLDS NUMBER
    TRNE1=1680.*(CPNH3E*VSNH3E/TKNH3E)**(-1.5)
C  REYNOLDS NUMBER(PSEUDO)
C
    WE=FLONH3/TNET
    RNH3EH=4.*WE/(TLE*VSNH3E)
    IF (RNH3EH.GT.TRNE1) GO TO 370
C  LAMINAR FLOW USING OWENS CORRELATION
C
    HNH3ER=2.2*(SPEC/TDOEC)**.1*(VSNH3E**2/(3600.***2*GRONH3E**2*TKNH3
    1E**3))**(-.3333)*RNH3EH**(-.3333)
    GO TO 420
370  CONTINUE

```



```

1RNH3EV**(-.22)*(1.-TLD/TLFD)
C
C LAMINAR FLOW CALCULATIONS
C
390 HNH3ER=HTDR+HTFDR
C GO TO 420
C CONTINUE
C TURBULENT FLOW USING LORENZ AND YUNG CORRELATIONS
C
C CONVECTION IN DEVELOPING REGION
C
C HTDR=3.*CPNH3E*WEA/TLFD
C
C CONVECTION IN FULLY DEVELOPED REGION
C
C HTFDR=3.8E-03*(VSNH3E**2/(3600.**2*RONH3E**2*TKNH3E**3*G))**(-.333
13)*RNH3EV**.4*PNH3E**.65
C
C TURBULENT FLOW CALCULATION
C
C HNH3ER=HTDR+HTFDR
C GO TO 420
C CONTINUE
400
C
C HORIZONTAL BOILING USING LORENZ AND YUNG CORRELATIONS
C
C TRANSITION REYNOLDS NUMBER FOR CORRELATIONS
C
C TRNE3=5800.*(CPNH3E*VSNH3E/TKNH3E)**(-1.06)
C
C REYNOLDS NUMBER(PSEUDO-VERTICAL)
C
C RNH3EV=4.*WE/(PI*TDACC*VSNH3E)
C IF (RNH3EV.GT.TRNE3) GO TO 410
C
C LAMINAR FLOW USING LORENZ AND YUNG CORRELATIONS
C
C CONVECTION IN DEVELOPING REGION
C
C HTDR=3.*CPNH3E*WEA/TLFD
C
C CONVECTION IN FULLY DEVELOPED REGION
C
C HTFDR=.821*(VSNH3E**2/(3600.**2*RONH3E**2*TKNH3E**3*G))**(-.3333)*
1RNH3EV**(-.22)*(1.-TLD/TLFD)
C
C BOILING USING LORENZ AND YUNG CORRELATION
C
C

```

A 769
 A 770
 A 771
 A 772
 A 773
 A 774
 A 775
 A 776
 A 777
 A 778
 A 779
 A 780
 A 781
 A 782
 A 783
 A 784
 A 785
 A 786
 A 787
 A 788
 A 789
 A 790
 A 791
 A 792
 A 793
 A 794
 A 795
 A 796
 A 797
 A 798
 A 799
 A 800
 A 801
 A 802
 A 803
 A 804
 A 805
 A 806
 A 807
 A 808
 A 809
 A 810
 A 811
 A 812
 A 813
 A 814
 A 815
 A 816


```

      HFNH3E=HF(P3)
      HGHNH3E=HG(P3)
      TENS=1.6038998E-03
      CSF=.0154
      HTB=VSNH3E*(HGNH3E-HFNH3E)/(CSF**3*(TENS/RONH3E)**.5)*(CPNH3E/((HG
      INH3E-HFNH3E)*PNH3E))**3*DELTAE**2
      C
      C
      C
      LAMINAR FLOW CORRELATION
      HNH3ER=HTB+HTDR+HTFDR
      GO TO 420
      C
      C
      C
      TURBULENT FLOW USING LORENZ AND YUNG CORRELATIONS
      CONVECTION IN DEVELOPING REGION
      HTDR=3.*CPNH3E*WEA/TLFD
      C
      C
      C
      CONVECTION IN FULLY DEVELOPED REGION
      HTFDR=3.8E-03*(VSNH3E**2/(3600.**2*RONH3E**2*TKNH3E**3*G))**(-.333
      13)*RNH3EV**4*PNH3E**65
      C
      C
      C
      BOILING USING LORENZ AND YUNG CORRELATION
      HGNH3E=HG(P3)
      HFNH3E=HF(P3)
      TENS=1.6038998E-03
      CSF=.0154
      HTB=VSNH3E*(HGNH3E-HFNH3E)/(CSF**3*(TENS/RONH3E)**.5)*(CPNH3E/((HG
      INH3E-HFNH3E)*PNH3E))**3*DELTAE**2
      C
      C
      C
      TURBULENT FLOW CALCULATIONS
      HNH3ER=HTB+HTDR+HTFDR
      C
      C
      C
      420
      C
      C
      C
      TEST FOR SAT HTNH3E
      C
      C
      C
      DHTNH3=ABS(HNH3ER-HTNH3E)
      SCALH=ABS(HNH3ER)
      IF (SCALH.LT.0.1) SCALH=0.1
      DELH=DHTNH3/SCALH
      IF (DELH.LT.0.001) GO TO 430
      HTNH3E=HNH3ER
      GO TO 260
      C
      C
      C
      430
      C
      C
      C

```



```

      HTNH3E=HNH3ER
C    REVISED EVAP HEAT TRANSFER AREA(FT2)
C
C    THTAER=ENTU*CMINE/UE
C    REVISED EVAP TUBE LENGTH(FT)
C
C    TLER=THTAER/(PIE*TDDEC*TNET)
C    TEST FOR SAT TUBE LENGTH
C
C    COST CF EVAPORATOR UNIT($)
C    IF (TSDE.GT.35.) GO TO 480
C
C    EVAPORATOR TUBE SHEET DIAMETER(10-35)FT
C
C    DRILLING TIME/TUBE SHELL THICK(MIN/IN)
C
C    DTE=0.66*(TDOE-.5)
C
C    THICKNESS OF TUBE SHEET(IN)
C
C    TTSE=0.56*TSDE**0.68
C
C    TUBE SHEET LABOR COST($)
C
C    CTSLE=156695.*(TNET/9630.)*(DTE/0.66)*(TTSE/4.)
C
C    TUBE SHEET MATERIAL COST($)
C
C    CTSME=189.486*TSDE**2.3
C    IF (TMATL.EQ.1.) GO TO 440
C
C    TUBE MATERIAL COST($)
C
C    CTME=(E1*TL+E2)*TNET*(TDOE/1.5)
C
C    TUBE INSTALLATION COST($)
C
C    CTIE=34.*TNET*TDOE**0.7
C    GO TO 450
C    CONTINUE
C
C    TUBE MATERIAL COST($)
C
C    CTME=(E1*TL+E2)*TNET*(TDOE/1.5)*(1.+(1.+AINT/100.))*10+(1.+AINT/1
100.))**20)

```


C	TUBE INSTALLATION COST(\$)	913
C	CTIE=34.*TNET*TD0E**0.7*(1.+(1.+AINT/100.))*10+(1.+AINT/100.))**20)	A 914
C	CONTINUE	A 915
450		A 916
C	HEAT EXCH SHELL COST(\$)	A 917
C		A 918
C	CHSE=177265.*(TLE+6.)/31.*(TSDE/18.))**2	A 919
C	NH3 DIST PLATE AND BAFFLES(\$)	A 920
C		A 921
C	CDPBE=93865.75*(TNET/9630.)*(DTE/0.66)*(TSDE/18.))**2	A 922
C	BUSTLE, FLANGES, CHANNELS, AND FLOW PLATES COST(\$)	A 923
C		A 924
C	CBFCFE=308550.*(TSDE/18.))**2	A 925
C	HEAT EXCH HEADS COST(\$)	A 926
C		A 927
C	CHE=53240.*(TSDE/18.))**3	A 928
C	WATER INLET, NOZZLES AND SUPPORTS COST(\$)	A 929
C		A 930
C	CWINSE=220310.75*(TSDE/18.))**2	A 931
C	TUBE WELDING COST(\$)	A 932
C		A 933
C	CTWE=0.0	A 934
C	IF (TMATL.EQ.1.) GO TO 470	A 935
C	IF (TNET.GT.36000) GO TO 460	A 936
C	CTWE=14.73*TNET**1.03*(TD0E/1.5)**0.7	A 937
C	GO TO 470	A 938
C	CONTINUE	A 939
460		A 940
C	CTWE=0.8797*TNET**1.3*(TD0E/1.5)**0.7	A 941
C	CONTINUE	A 942
470		A 943
C	CEVAP=(CTSL+CTSM+CTME+CTIE+CHSE+CBFCFE+CHE+CWINSE+CTWE+CDPBE)	A 944
C	GO TO 550	A 945
C	CONTINUE	A 946
480		A 947
C	EVAPORATOR TUBE SHEET DIAMETER(35-50)FT	A 948
C		A 949
C	DRILLING TIME/TUBE SHEET THICK(MIN/IN)	A 950
C		A 951
C	DTE=0.66*(TD0E-.5)	A 952
C		A 953
C	THICKNESS OF TUBE SHEET(IN)	A 954
C		A 955
C		A 956
C		A 957
C		A 958
C		A 959
C		A 960

C	TTISE=0.56*TSDE**0.68	A 961
C	TUBE SHEET MATERIAL AND LABOR COSTS(\$)	A 962
C		A 963
		A 964
490	IF (TMATL.EQ.1.) GO TO 490	A 965
	CTSLE=55.189*TNET**0.791*TSDE**0.68*DTE	A 966
500	CTSME=29.566*TSDE**2.014*TTISE	A 967
	GO TO 500	A 968
	CONTINUE	A 969
	CTSLE=73.81*TNET**0.791*TSDE**0.68*DTE	A 970
	CTSME=354.3*TSDE**1.61*TTISE	A 971
	CONTINUE	A 972
	IF (TMATL.EQ.1.) GO TO 510	A 973
		A 974
C	TUBE MATERIAL COST(\$)	A 975
C		A 976
C	CTME=(E1*TL+E2)*TNET*(TDOE/1.5)	A 977
C	TUBE INSTALLATION COST(\$)	A 978
C		A 979
	CTIE=36.542*TNET*TDOE**0.7	A 980
510	GO TO 520	A 981
C	CONTINUE	A 982
C		A 983
C	TUBE MATERIAL COST(\$)	A 984
		A 985
	CTME=(E1*TL+C2)*TNET*(TDOE/1.5)*(1.+(1.+AINT/100.))**10+(1.+AINT/1	A 986
	100.))**20)	A 987
C		A 988
C	TUBE INSTALLATION COST(\$)	A 989
C		A 990
	CTIE=36.542*TNET*TDOE**0.7*(1.+(1.+AINT/100.))**10+(1.+AINT/100.))**	A 991
520	120)	A 992
C	CONTINUE	A 993
C		A 994
C	HEAT EXCH SHELL COST(\$)	A 995
C		A 996
	CHSE=12.544*(TLE+6.)*TSDE**2.06	A 997
C	NH3 DIST PLATE AND BAFFLES COST(\$)	A 998
C		A 999
C		A1000
	CDPBE=158.099*TSDE**1.82+72.419*TNET**0.873*DTE	A1001
C		A1002
C	BUSTLE, FLANGE, CHANNELS AND FLOW PLATE COSTS(\$)	A1003
C		A1004
	CBFCFE=472.977*TSDE**2.12	A1005
C		A1006
C	HEAT EXCH HEAD COST(\$)	A1007
		A1008


```

C      CHE=1725.31*TSDE**1.45
C      WATER INLET,NOZZLES AND SUPPORTS COST($)
C      CWINSE=7445.297*TSDE**1.1
C      TUBE WELDING COSTS($)
C      CTWE=0.0
C      IF (TMATL.EQ.1.) GO TO 540
C      IF (TNET.GT.36000) GO TO 530
C      CTWE=14.73*TNET**1.03*(TDOE/1.5)**0.7
C      GO TO 540
C      CONTINUE
530    CTWE=0.8797*TNET**1.3*(TDOE/1.5)**0.7
C      CONTINUE
540    CEVAP=(CTSLE+CTSME+CTME+CTIE+CHSE+CDPBE+CBFCFE+CHE+CWINSE+CTWE)
550    CONTINUE
C      *****
C      *
C      *      PARASITIC LOSS SECTION
C      *
C      *
C      *****
C      EVAPORATOR SALT WATER PUMP OR HOT PIPE PUMP
C      DELTA P EVAP SW PUMP
C      ROSWHP=RHOSW(THIE)
C      THIER=THIE+459.69
C      VISWHP=VISSW(THIE)
C      DELTA P SW HOT PIPE USING DARCEY-WEISBACH CORRELATION
C      (LBF/IN2)
C      REYNOLDS NUMBER FOR HOT PIPE FLOW
C      RNSWHP=3600.*ROSWHP*VSWHP*DIHP/VISWHP
C      FRICTION FACTOR FOR LAMINAR FLOW
C      IF (RNSWHP.GT.2300.) GO TO 560
C      FFHP=64./RNSWHP
C      GO TO 570

```



```

560      CONTINUE
C      FRICTION FACTOR TURBULENT FLOW USING STREETER CORR
C
570      FFHP=1.325/(ALOG(EHP/(3.7*DIHP))+5.74/RNSWHP**.9))**.2
C      CONTINUE
C      INTAKE DUCT LOSSES(ASSUME K=1.5 FOR INLET SCREEN AND
C      ENTERS PLENUM PRIOR TO EVAP WHERE AREA IS ABRUPTLY
C      CHANGED TO 2 TIMES THE PIPE DIAMETER(LBF/IN2))
C      HPKI=1.5
C      HPKE=(1.-(DIHP/(2.*DIHP))**.2)**2
C      DDUCTH=(HPKI+HPKE)*ROSWHP*VSWHP**2/(2.*GC*144.)
C      PIPE FRICTION LOSSES(LBF/IN2)
C      RKHP=FFHP*ILHP/DIHP
C      DPIPEH=RKHP*ROSWHP*VSWHP**2/(2.*GC*144.)
C      OUTLET DUCT LOSSES(ASSUME NO OUTLET PIPING)
C
C      DELTA P PIPE LOSS CALCULATION(LBF/IN2)
C      DPIPH=DDUCTH+DPIPEH
C      DELTA P EVAPORATOR(ASSUME NO OUTLET PIPING) USING DARCEY-
C      WEISBACH CORRELATION(LBF/IN2)
C      MINOR ENTRY/EXIT LOSSES(ASSUME KI=.05 WELL ROUNDED
C      TUBE ENTRANCE AND KE=1. EXPANSION TO AN INFINITE
C      RESEVOIR)(LBF/IN2)
C      RKI=.05
C      RKE=1.
C      DPMINE=(RKI+RKE)*RHOSWE*VSWE**2/(2.*GC*144.)
C      DELTA P EVAPORATOR CORE(LBF/IN2)
C      REYNOLDS NUMBER FOR EVAP(DETERMINED IN EVAP SECTION)
C      FRICTION FACTOR LAMINAR FLOW
C      IF (RNSWE.GT.2300.) GO TO 580
C      FFE=64./RNSWE
C      GO TO 590
C      CONTINUE
580

```

A1057
 A1058
 A1059
 A1060
 A1061
 A1062
 A1063
 A1064
 A1065
 A1066
 A1067
 A1068
 A1069
 A1070
 A1071
 A1072
 A1073
 A1074
 A1075
 A1076
 A1077
 A1078
 A1079
 A1080
 A1081
 A1082
 A1083
 A1084
 A1085
 A1086
 A1087
 A1088
 A1089
 A1090
 A1091
 A1092
 A1093
 A1094
 A1095
 A1096
 A1097
 A1098
 A1099
 A1100
 A1101
 A1102
 A1103
 A1104

C	FRICITION FACTOR TURBULENT FLOW USING STREETER CORR	A1105
C		A1106
C		A1107
590	FFE=1.325/(ALOG(ECE/(3.7*TDIEC))+5.74/RNSWE**.9))**.2	A1108
C	CONTINUE	A1109
C		A1110
C	DELTA P EVAP CORE CALCULATED(LBF/IN2)	A1111
C		A1112
C	RKHE=FFE*TL/TDIEC	A1113
C	DCOREE=RKHE*RHOSWE*VSWE**2/(2.*GC*144.)	A1114
C		A1115
C	DELTA P EVAPORATOR CALCULATED(LBF/IN2)	A1116
C		A1117
C	DEVAP=DPMINE+DCOREE	A1118
C		A1119
C	DELTA P EVAP SW PUMP CALCULATION(LBF/IN2 OR FT)	A1120
C		A1121
C	DPMPE=DDUCTH+DPIPEH+DPMINE+DCOREE	A1122
C	DPMPEC=144.*DPMPE*GC/(ROSWHP*G)	A1123
C		A1124
C	POWER EVAP SW PUMP (HP)	A1125
C		A1126
C	EPEC=EPE/100.	A1127
C	PWREP=FLOHP*DPMPEC*G/(EPEC*HPC*3600.*GC)	A1128
C		A1129
C	POWER EVAP SW PUMP MOTOR (MW)	A1130
C		A1131
C	EMEC=EME/100.	A1132
C	PWREPM=PWREP*CMW/EMEC	A1133
C		A1134
C	DISCHARGE RATE EVAP SW PUMP (FT3/SEC OR GAL/MIN)	A1135
C		A1136
C	QEPMP=PIE*DIHP**2*VSWHP/4.	A1137
C	QEPMPC=QEPMP*60.*GAL	A1138
C		A1139
C	COST OF EVAP SW PUMP (\$)	A1140
C		A1141
C	CESWP=((QEPMPC/1000.)*.75+50.)*1.21E+03	A1142
C		A1143
C	CONDENSER SALT WATER PUMP OR COLD PIPE PUMP	A1144
C		A1145
C	DELTA P CONDENSER SW PUMP (ASSUME TSW(IN)=TSW(OUT), V1=V2)	A1146
C	ROSWCP=RHOSW(TCIC)	A1147
C	TCICR=TCIC+459.69	A1148
C	VISWCP=VISSW(TCIC)	A1149
C	FLOCP=3600.*ROSWCP*PIE*DICP**2*VSWCP/4.	A1150
C		A1151
C	DELTA P SW COLD PIPE (ASSUME V1=V2, TSW(IN)=TSW(OUT) USING	A1152


```

C DARCEY-WEISBACH CORRELATION(LBF/IN2)
C
C REYNOLDS NUMBER FOR COLD PIPE FLOW
C
C RNSWCP=3600.*ROSWCP*VSWCP*DICP/VISWCP
C
C FRICTION FACTOR LAMINAR FLOW
C
C IF (RNSWCP.GT.2300.) GO TO 600
C FFCP=64./RNSWCP
C GO TO 610
C CONTINUE
600
C FRICTION FACTOR TURBULENT FLOW USING STREETER CORR
C
C FFCP=1.325/(ALOG(ECP/(3.7*DICP))+5.74/RNSWCP**9))**2
C CONTINUE
610
C MINOR ENTRY/EXIT LOSSES(ASSUME KI=.05 WELL ROUNDED
C PIPE ENTRANCE AND ENTERS PLENUM PRIOR TO CONDENSER
C WHERE AREA IS ABRUPTLY CHANGED TO 2 TIMES PIPE
C DIAMETER)(LBF/IN2)
C
C CPKI=.05
C CPKE=(1.-(DICP/(2.*DICP))**2)**2
C DDUCTC=(CPKI+CPKE)*ROSWCP*VSWCP**2/(2.*GC*144.)
C
C PIPE FRICTION LOSSES(LBF/IN2)
C
C RKCP=FFCP*(TLCF/DICP+ELBOW)
C DPIPEC=RKCP*ROSWCP*VSWCP**2/(2.*GC*144.)
C
C DELTA P PIPE LOSS CALCULATION(LBF/IN2)
C
C DPIPC=DDUCTC+DPIPEC
C
C DELTA P DUE TO SW DENSITY(LBF/IN2)
C
C RDEPTH=RHOSWD(TLCP)
C RAVG=((RDEPTH+64.184)/2.
C DHEAD=((RDEPTH-64.184)/RDEPTH)*TLCF/2.
C DDENC=G*RAVG*DHEAD/(144.*GC)
C
C DELTA P CONDENSER(ASSUME NO OUTLET PIPING) USING
C DARCEY-WEISBACH CORRELATION(LBF/IN2)
C
C INITIALLY ASSUME TBLK=TSW(IN)
C TBLKC=TCIC

```


620	CONTINUE	AI201
	TBLKCR=TBLKC+459.69	AI202
	RHOSWC=RHOSW(TBLKC)	AI203
C		AI204
C	MINOR ENTRY/EXIT LOSSES(ASSUME KI=.05 WELL ROUNDED	AI205
C	TUBE ENTRANCE AND KE=1. EXPANSION TO AN INFINITE	AI206
C	RESEVOIR(LBF/IN2)	AI207
		AI208
	RKI=.05	AI209
	RKE=1.	AI210
	DPMINC=(RKI+RKE)*RHOSWC*VSWC**2/(2.*GC*144.)	AI211
C		AI212
C	DELTA P CONDENSER CORE(LBF/IN2)	AI213
C		AI214
C		AI215
C	REYNOLDS NUMBER FOR COND TUBESIDE	AI216
		AI217
	VISSWC=VISSW(TBLKC)	AI218
	RNSWC=3600.*RHOSWC*VSWC*TDICC/VISSWC	AI219
C		AI220
C	FRICTION FACTOR LAMINAR FLOW	AI221
		AI222
	IF (RNSWC.GT.2300.) GO TO 630	AI223
	FFC=64./RNSWC	AI224
	GO TO 640	AI225
630	CONTINUE	AI226
	FFC=1.325/(ALOG(ECC/(3.7*TDICC)+5.74/RNSWC**9))**2	AI227
640	CONTINUE	AI228
C		AI229
C	DELTA P COND CORE CALCULATION(LBF/IN2)	AI230
C		AI231
	RKHC=FFC*TLC/TDICC	AI232
	DCOREC=RKHC*RHOSWC*VSWC**2/(2.*GC*144.)	AI233
C		AI234
C	DELTA P CONDENSER DUE TO CORE ELEVATION(LBF/IN2)	AI235
		AI236
	IF (TYPEC.GT.1.) GO TO 650	AI237
	DPELEC=0.	AI238
	GO TO 660	AI239
	CONTINUE	AI240
650		AI241
C	VERTICAL TUBED CONDENSER SW INLET ENTERS AT THE TOP	AI242
C	OF THE HEAT EXCHANGER	AI243
C		AI244
	DPELEC=0.	AI245
	CONTINUE	AI246
660		AI247
C	DELTA P CONDENSER CALCULATION(LBF/IN2)	AI248


```

C      DCOND=DPMINC+DCOREC+DPELEC
C      DELTA P COND SW PUMP CALCULATION(LBF/IN2 OR FT)
C      DPMC=DDUCTC+DDENC+DPMINC+DCOREC+DPIPEC
C      DPMPC=144.*DPMPC*GC/(ROSWCP*G)
C      POWER COND SW PUMP(HP)
C      EPCC=EPCC/100.
C      PWRCP=FLOCP*DPMPC*G/(EPCC*HPC*3600.*GC)
C      POWER COND SW PUMP MOTOR(MW)
C      EMCC=EMCC/100.
C      PWRCPM=PWRCP*CMW/EMCC
C      DISCHARGE RATE OF COND SW PUMP(FT3/SEC OR GAL/MIN)
C      QCPMP=PIE*DICP**2*VSWCP/4.
C      QCPMP=QCPMP*60.*GAL
C      COST OF COND SW PUMP($)
C      CCSWP=((QCPMP/1000.)*0.75+50.)*1.21E+03
C      AMMONIA CIRCULATION PUMP
C      DELTA P NH3 CIRC PUMP
C      VSNH3P=VSNH3(T1)
C      RANH3P=RFNH3(T1)
C      DELTA P NH3 PUMP(ASSUME V1=V2)USING DARCEY-WEISBACH
C      CORRELATION(LBF/IN2)
C      NH3 PIPE FLOW VELOCITY(FT/SEC)
C      VNH3P=4.*FLONH3/(3600.*RANH3P*PIE*DINH3**2)
C      REYNOLDS NUMBER FOR NH3 PIPE FLOW
C      RANH3P=3600.*RANH3P*VNH3P*DINH3/VSNH3P
C      FRICTION FACTOR LAMINAR FLOW
C      IF (RANH3P.GT.2300.) GO TO 670
C      FFNH3P=64./RANH3P

```

A1249
 A1250
 A1251
 A1252
 A1253
 A1254
 A1255
 A1256
 A1257
 A1258
 A1259
 A1260
 A1261
 A1262
 A1263
 A1264
 A1265
 A1266
 A1267
 A1268
 A1269
 A1270
 A1271
 A1272
 A1273
 A1274
 A1275
 A1276
 A1277
 A1278
 A1279
 A1280
 A1281
 A1282
 A1283
 A1284
 A1285
 A1286
 A1287
 A1288
 A1289
 A1290
 A1291
 A1292
 A1293
 A1294
 A1295
 A1296


```

670 GO TO 680
C CONTINUE
C
C FRICTION FACTOR TURBULENT FLOW USING STREETER CORR
C
C FFNH3P=1.325/(ALOG(ENH3P/(3.7*DMINH3)+5.74/RNH3P**2.9))**2
680 CONTINUE
C
C PIPE FRICTION LOSSES(LBF/IN2)
C
C RKNH3P=FFNH3P*(TLNH3P/DINH3+4.*ELBOW)
C DPNH3=RKNH3P*RONH3P*VNH3P**2/(2.*GC*144.)
C
C DELTA P CORE EVAPORATOR
C
C DPCORE=DSEVAP+DSDEM
C
C DELTA P DUE TO PIPING ELEVATION(LBF/IN2)
C
C EZ1=0.
C EZ2=TSDE+25
C DPELEV=RONH3P*G*(EZ2-EZ1)/(GC*144.)
C
C DELTA P PIPE LOSS CALCULATION(LBF/IN2)
C DPIP=DPNH3+DPELEV
C
C DELTA P THERMODYNAMICALLY(LBF/IN2)
C
C DPTHER=PEVAP-PCOND
C
C DELTA P NH3 CIRC PUMP(LBF/IN2 OR FT)
C
C DMPN=DPNH3+DPCORE+DPELEV+DPTHER
C DMPNC=144.*DMPN*GC/(RONH3P*G)
C
C POWER NH3 CIRC PUMP(HP)
C
C EPNH3C=EPNH3/100.
C PWRNP=FLONH3*DMPNC*G/(EPNH3C*HPC*3600.*GC)
C
C POWER NH3 CIRC PUMP MOTOR(MW)
C
C EMNH3C=EMNH3/100.
C PWRNPM=PWRNP*CMW/EMNH3C
C
C DISCHARGE RATE NH3 CIRC PUMP(FT3/SEC OR GAL/MIN)
C

```

A1297
 A1298
 A1299
 A1300
 A1301
 A1302
 A1303
 A1304
 A1305
 A1306
 A1307
 A1308
 A1309
 A1310
 A1311
 A1312
 A1313
 A1314
 A1315
 A1316
 A1317
 A1318
 A1319
 A1320
 A1321
 A1322
 A1323
 A1324
 A1325
 A1326
 A1327
 A1328
 A1329
 A1330
 A1331
 A1332
 A1333
 A1334
 A1335
 A1336
 A1337
 A1338
 A1339
 A1340
 A1341
 A1342
 A1343
 A1344

QNPMPC=PIE*DINH3**2*VNH3P/4.
 QNPMPC=QNPMPC*60.*GAL
 C COST OF NH3 CIRC PUMP(\$)
 C
 VF1=1./RFNH3(T1)
 CNH3P=(FLONH3*VF1/80100.)*0.64*1.21E+05
 C
 C EVAPORATOR RE-FLUX PUMP
 C ASSUME RE-FLUX MASS FLOW RATE=0.3 X FLONH3
 C
 C DELTA P NH3 RE-FLUX PIPING(ASSUME V1=V2)
 C USING DARCEY-WEISBACH CORRELATION(LBF/IN2)
 C PAVGE=(PEVAP+P3)/2.
 C TAVGE=TSAT(PAVGE)
 C RDNH3R=RFNH3(TAVGE)
 C VSNHRP=VSNH3(TAVGE)
 C
 C NH3 FLOW VELOCITY(FT/SEC)
 C
 C FLONHR=0.3*FLONH3
 C VNH3RP=4.*FLONHR/(3600.*RONH3R*PIE*DINH3R**2)
 C
 C REYNOLDS NO FOR NH3 RE-FLUX PIPE FLOW
 C
 C RNH3RP=3600.*RONH3R*VNH3RP*DINH3R/VSNHRP
 C
 C FRICTION FACTOR LAMINAR FLOW
 C
 C IF (RNH3RP.GT.2300.) GO TO 690
 C FNH3RP=64./RNH3RP
 C GO TO 700
 C CONTINUE
 690
 C FRICTION FACTOR TURBULENT FLOW USING STREETEER CORR
 C
 C FNH3RP=1.325/(ALOG(ENH3P/(3.7*DINH3R)+5.74/RNH3RP**0.9))**2
 C CONTINUE
 700
 C PIPE FRICTION LOSSES(LBF/IN2)
 C
 C RKNHRP=FNH3RP*(TLNHRP/DINH3R+4.*ELBOW)
 C DPNHRP=RKNHRP*RONH3R*VNH3RP**2/(2.*GC*144.)
 C
 C DELTA P DUE TO PIPING ELEVATION(LBF/IN2)
 C
 C EZR=TSDE+10
 C DPFLER=RONH3R*G*(EZR-EZ1)/(GC*144.)


```

C C DELTA P PIPE LOSSES(LBF/IN2)
C C
C C DPIPNR=DPNHRP+DPELER
C C
C C DELTA P NH3 RE-FLUX THERMODYNAMICALLY(LBF/IN2)
C C USING A SINGLE PHASE PRESSURE MODEL
C C
C C RONHEV=RGNH3(PEVAP)
C C DPTHRF=2.*EFF*EGF**2*INET**0.5/(144.*RONHEV*GC)
C C
C C DELTA P NH3 RE-FLUX PUMP(LBF/IN OR FT)
C C
C C DPMPNR=DPNHRP+DPELER+DPTHRF
C C DPPNRC=144.*DPMPNR*GC/(RONH3R*G)
C C
C C POWER NH3 RE-FLUX PUMP(HP)
C C
C C EPNHRC=EPNHR/100.
C C PWRRP=FLONHR*DPPNRC*G/(EPNHRC*HPC*3600.*GC)
C C
C C POWER NH3 RE-FLUX PUMP MOTOR(MW)
C C
C C EMNHRC=EMNHR/100.
C C PWRRM=PWRRP*CMW/EMNHRC
C C
C C DISCHARGE RATE NH3 RE-FLUX PUMP(FT3/SEC OR GAL/MIN)
C C
C C QRPMP=PIE*DINH3R**2*VNH3RP/4.
C C QRPMP*PC=QRPMP*60.*GAL
C C
C C COST OF NH3 RE-FLUX PUMP($)
C C
C C VFR=1./RFNH3(TAVGE)
C C CNH3RP=(FLONHR*VFR/80100.)*0.64*1.21E+05
C C
C C PARASITIC PUMP LOSSES(MW)
C C
C C PARAL=PWREPM+PWRC*PM+PWRNPM+PWRRM
C C
C C *****
C C *
C C *
C C *
C C *
C C *
C C *****
C C TURBINE AND ELECTRICAL POWER SECTION
C C *****
C C *
C C *
C C *
C C *
C C *****

```

A1393
 A1394
 A1395
 A1396
 A1397
 A1398
 A1399
 A1400
 A1401
 A1402
 A1403
 A1404
 A1405
 A1406
 A1407
 A1408
 A1409
 A1410
 A1411
 A1412
 A1413
 A1414
 A1415
 A1416
 A1417
 A1418
 A1419
 A1420
 A1421
 A1422
 A1423
 A1424
 A1425
 A1426
 A1427
 A1428
 A1429
 A1430
 A1431
 A1432
 A1433
 A1434
 A1435
 A1436
 A1437
 A1438
 A1439
 A1440

C	GROSS ELECTRICAL LOAD(MW)	A1441
C		A1442
C	NET ELECTRICAL OUTPUT DESIRED(ELECT- PROVIDED IN INITIAL PARAMETERS)(MW)	A1443
C		A1444
C		A1445
C		A1446
C	ELECTRICAL LOADING AS EFFECTED BY EFFICIENCY(MW)	A1447
C		A1448
C		A1449
C		A1450
C		A1451
C		A1452
C		A1453
C		A1454
C		A1455
C		A1456
C		A1457
C		A1458
C		A1459
C		A1460
C		A1461
C		A1462
C		A1463
C		A1464
C		A1465
C		A1466
C		A1467
C		A1468
C		A1469
C		A1470
C		A1471
C		A1472
C		A1473
C		A1474
C		A1475
C		A1476
C		A1477
C		A1478
C		A1479
C		A1480
C		A1481
C		A1482
C		A1483
C		A1484
C		A1485
C		A1486
C		A1487
C		A1488

	GROSS ELECT LOADING INCL PARASITIC LOSSES(MW)
	WELECG=WELECT+PARAL
	POWER GENERATOR-TURBINE(HP)
	PWRTR=1341.*WELECG
	TURBINE EFFICIENCY REQUIREMENT(PCT)
	ENTHALPY AT STATE PT 5(BTU/LBM)
	H5=H4-(3412.2E+03*WELECG/FLONH3)
	CONSTRAINT FOR SAT STATE PT 5
	H5G=HG(PCOND)
	DH5=H5G-H5
	QUALITY OF NH3 AT STATE PT5(PCT)
	H5F=HF(PCOND)
	X5=(H5-H5F)/(H5G-H5F)
	X5P=X5*100.
	QUALITY OF NH3 EXHAUST AT STATE PT 5S(PCT)
	S4F=SF(T4)
	S4G=SG(T4)
	S4=S4F+X4*(S4G-S4F)
	S5F=SF(T5)
	S5G=SG(T5)
	X5S=(S4-S5F)/(S5G-S5F)
	X5SP=X5S*100.


```

C C CONSTRAINT FOR A SAT QUALITY AT STATE PT 5S
C C DX5=X5-X5S
C C ENTHALPY AT STATE PT 5S
C C H5S=H5F+X5S*(H5G-H5F)
C C TURBINE EFFICIENCY CALCULATION(PCT)
C C ETURB=(H4-H5)/(H4-H5S)
C C ETURBP=ETURB*100.
C C COST OF NH3 TURBINE- GENERATOR($ )
C C FPF=1.447
C C DF=2.0
C C CTURB=(0.375+(WELECG*1000.)/(136000*DF))*FPF*2.42E+06
C C CGEN=(WELECG*.023+.3)*1.21E+06
C C CELECT=CGEN+CTURB
C C *****
C C *
C C *
C C *
C C *
C C *
C C *****
C C CONDENSER SECTION
C C *
C C *
C C *
C C *
C C *****
C C AMOUNT OF HEAT REJECTION(BTU/HR OR MW)
C C QC=FLONH3*(H5-H1)
C C CMIN FOR CONDENSER(BTU/HR.F)
C C CPSWC=CPSW(TBLKC)
C C CMINC=FLOCP*CPSWC
C C COND SW OUTLET TEMP(F OR C)
C C TCOC=TCIC+QC/CMINC
C C TOTAL NUMBER OF CONDENSER TUBES
C C RHOSWC=RHOSW(TBLKC)
C C TNCT=4.*FLOCP/(3600.*RHOSWC*PIE*TDICCC**2*VSWC)
C C *****

```

A1489
 A1490
 A1491
 A1492
 A1493
 A1494
 A1495
 A1496
 A1497
 A1498
 A1499
 A1500
 A1501
 A1502
 A1503
 A1504
 A1505
 A1506
 A1507
 A1508
 A1509
 A1510
 A1511
 A1512
 A1513
 A1514
 A1515
 A1516
 A1517
 A1518
 A1519
 A1520
 A1521
 A1522
 A1523
 A1524
 A1525
 A1526
 A1527
 A1528
 A1529
 A1530
 A1531
 A1532
 A1533
 A1534
 A1535
 A1536

C TUBE SHEET DIAMETER(FT)
C
C TUBE PROFILE - STAGGERED
C
IF (PROF.EQ.2.) GO TO 710
CHT=CPR*IDOC*0.5
CBASE=CPR*IDOC*0.866
CTAREA=CHT*CBASE*2.
SNC=2.*CHT
GO TO 720
CONTINUE
710
C
C TUBE PROFILE - IN-LINE
C
CPLONG=CPR*IDOC
CPLAT=CPR*IDOC
CTAREA=CPLONG*CPPLAT
CONTINUE
720
C
C CAREA=CTAREA*INCT
TSDC=((4.*CAREA/PIE)**0.5)/12.
C
C LOG MEAN TEMP DIFFERENCE OF CONDENSER(F OR C)
C
CLMTD=((T1-TCOC)-(T1-TCIC))/ALOG((T1-TCOC)/(T1-TCIC))
C
C COND SW AVG BULK TEMP(F)
C
RTBLKC=(TCOC+TCIC)/2.
C
C TEST FOR SAT TBLKC
C
DBLKTC=ABS(TBLKC-RTBLKC)
SCALBC=ABS(TBLKC)
IF (SCALBC.LT.0.1) SCALBC=0.1
DELBK=DBLKTC/SCALBC
IF (DELBK.LT.0.001) GO TO 730
TBLKC=RTBLKC
GO TO 620
CONTINUE
730
C
C TBLKC=RTBLKC
TBLKCR=TBLKC+459.69
C
C CONDENSER CONDUCTANCE(BTU/HR.F)
C
UAC=QC/CLMTD
C
C NUMBER OF TRANSFER UNITS FOR COND(NTU)
C


```

C CNTU=UAC/CMINC
C COND EFFECTIVENESS(EPSILON)
C EPSC=1.-EXP(-CNTU)
C INITIALLY ASSUME A TLC
C OVERALL HEAT TRANSFER COEFFICIENT(BTU/HR.FT2.F OR W/M2)
C INITIALLY ASSUME HTNH3
C HTNH3C=1000.
C CONTINUE
740
C REYNOLDS NUMBER FOR COND TUBESIDE
C (PROPERTIES EVAL AT TBULK)
C VISSWC=VISSW(TBLKC)
C RHOSWR=RHOSW(TBLKC)
C RNSWC=3600.*RHOSWR*VSWC*TDICC/VISSWC
C PRANDTL NUMBER FOR COND TUBESIDE
C CPSWC=CPSW(TBLKC)
C TKSWC=TKSW(TBLKC)
C PNSWC=CPSWC*VISSWC/TKSWC
C HEAT TRANSFER COEF FOR COND SW TUBESIDE
C (BTU/HR.FT2.F OF W/M2)
C IF (RNSWC.GT.2300.) GO TO 750
C LAMINAR FLOW USING SEIDER-TATE CORRELATION(ASSUME
C VISCOSITY(TBULK)=VISCOSITY(TWALL))
C HTSWC=1.86*TKSWC*((RNSWC*PNSWC)**.3333)*(TDICC/TLC)**.3333/TDICC
C GO TO 760
C CONTINUE
750
C TURBULENT FLOW USING DITTUS-BOELTER CORRELATION
C HTSWC=.023*TKSWC*RNSWC**.8*PNSWC**.3/TDICC
C CONTINUE
760
C FILM TEMP FOR PROPERTY EVALUATION
C THERMAL RESISTANCES FOR SINGLE TUBE CONDUCTANCE
C UA - OUTSIDE(BTU/HR.F)

```


C	$\text{THERMAL RESISTANCE SW}(\text{HR.F/BTU})$	$\text{CTR1C}=1./(\text{EFFIC}*\text{HTSWC}*\text{PIE}*\text{TDICC}*\text{TLC})$	$\text{THERMAL RESISTANCE FOR SW FOULING}(\text{HR.F/BTU})$	$\text{HTFSWC}=1./\text{SWFC}$	$\text{CTR2C}=1./(\text{EFFIC}*\text{HTFSWC}*\text{PIE}*\text{TDICC}*\text{TLC})$	$\text{THERMAL RESISTANCE FOR WALL THICKNESS}(\text{HR.F/BTU})$	$\text{CTR3C}=\text{ALOG}(\text{TDCCC}/\text{TDICC})/(2.*\text{PIE}*\text{TKW}*\text{TLC})$	$\text{THERMAL RESISTANCE FOR NH3 FOULING}(\text{HR.F/BTU})$ (CONSIDERED NEGLIGIBLE)	$\text{THERMAL RESISTANCE FOR NH3}(\text{HR.F/BTU})$	$\text{CTR5C}=1./(\text{EFFOC}*\text{HTNH3C}*\text{PIE}*\text{TDCCC}*\text{TLC})$	$\text{HEAT TRANSFERED PER TUBE}(\text{BTU/HR})$	$\text{QCT}=(\text{T1}-\text{TBLKC})/(\text{CTR1C}+\text{CTR2C}+\text{CTR3C}+\text{CTR5C})$	$\text{TUBE SIDE WALL TEMP}(\text{F})$	$\text{CTW1}=\text{TBLKC}+\text{QCT}*(\text{CTR1C}+\text{CTR2C})$	$\text{SHELLSIDE WALL TEMP}(\text{F})$	$\text{CTW2}=\text{TBLKC}+\text{QCT}*(\text{CTR1C}+\text{CTR2C}+\text{CTR3C})$	$\text{COND FILM TEMP CALCULATION}(\text{F})$	$\text{CFT}=(\text{CTW2}+\text{T1})/2.$	$\text{CONDENSER DELTA T TEMP}(\text{F})$	$\text{DELTA C}=\text{T1}-\text{CTW2}$	$\text{COND SHELLSIDE HEAT TRANSFER COEF}(\text{BTU/HR.FT2.F OR W/M2})$	$\text{VSNH3C}=\text{VSNH3}(\text{CFT})$ $\text{RONH3C}=\text{RFNH3}(\text{CFT})$ $\text{TKNH3C}=\text{TKNH3}(\text{CFT})$	C
---	---	--	---	--------------------------------	---	---	---	---	--	---	--	---	--	---	--	--	---	---	---	--	---	--	---


```

800 1)*RNH3CV**+.4
C CONTINUE
C
C TEST FOR SAT HTNH3C
C
    DHNH3C=ABS(HNH3CR-HTNH3C)
    SCALC=ABS(HNH3CR)
    IF (SCALC.LT.0.1) SCALC=0.1
    DELC=DHNH3C/SCALC
    IF (DELC.LT.0.001) GO TO 810
    HTNH3C=HNH3CR
    GO TO 740
810 CONTINUE
    HTNH3C=HNH3CR
C
C PRESSURE DROP ACROSS CONDENSER SHELLSIDE(LBF/IN2)USING
C TWO-PHASE MODEL(HOMOGENEOUS)
C
C MAX VELOCITY THRU MINIMUM- FLOW AREA F(TUBE PROFILE)
    RONH3T=RGNH3(PCOND)
    VNHC=4.*FLONH3/(3600.*RONH3T*PIE*TSDC**2)
    VMAXC=VNHC*(SNC/(SNC-TDOC))
C
C REYNOLDS NUMBER FOR MAXIMUM SHELLSIDE FLOW
    REMAXC=3600.*RONH3C*VMAXC*TDOC/(12.*VSNH3C)
C
C EMPIRICAL FRICTION FACTOR USING CORRELATION BY JAKOB
C
    IF (PROF.EQ.2.) GO TO 820
    CFF=(0.25+0.118)/((SNC-TDOC)/TDOC)**1.08*REMAXC**(-.16)
    GO TO 830
820 CONTINUE
    CFF=(0.44+(0.08*SNC/TDOC)/((SNC-TDOC)/TDOC)**(0.43+1.13*TDOC/SNC))
    1*REMAXC**(-.15)
830 CONTINUE
C
C MASS VELOCITY FOR MINIMUM FREE-FLOW AREA(LBM/FT2.SEC)
C
    IF (TYPEC.GT.1.) GO TO 840
    CAF=TSDC*TLC
    CL=TSDC
    GO TO 850
840 CONTINUE
    BAND=TLC
    CAF=PIE*TSDC*BAND
    CL=TLC
850 CONTINUE

```



```

      CAFF=CAF*((SNC-TDOC)/SNC)
      CGF=FLONH3/(3600.*CAFF)
C
C  CALCULATION OF CONDENSER SHELLSIDE PRESSURE DROP(LBF/IN2)
C  USING THE HOMOGENEOUS TWO-PHASE MODEL
C
      EDC=((CPR*TDOC-TDOC)/12.
      VLIQC=1./RGNH3(T5)
      VAPC=1./RGNH3(PCOND)
      VAVGC=VLIQC*(1.+X5*(VAPC-VLIQC)/VLIQC)
      CFRICT=((CGF*CGF**2*VAVGC*CL)/(144.*EDC*2.*GC)
      CMOM=((CGF**2*VAVGC)/(144.*GC)
      CELEV=((CGF*CL)/(144.*GC)
      DSCOND=CFRICT+CMOM+CELEV
C
C  PROPERTIES AT STATE PT 1
C
      PI=PCOND-DSCOND
      HI=HF(PI)
      TIR=TSAT(PI)
C
C  TEST FOR SAT T1(DEG F)
C
      DTEMP4=ABS(TIR-T1)
      SCALT1=ABS(TIR)
      IF (SCALT1.LT.0.1) SCALT1=0.1
      DELT4=DTEMP4/SCALT1
      IF (DELT4.LT.0.001) GO TO 860
      T1=TIR
      GO TO 260
860  CONTINUE
      T1=TIR
C
C  THERMAL RESISTANCES FOR OVERALL HEAT TRANSFER COEF - U
C  OUTSIDE(HR.FT2.F/BTU)
C
      OUTSIDE TUBE SURFACE AREA(FT2)
      CAO=PI*EDOCC*TLC
      THERMAL RESISTANCE FOR SW(HR.FT2.F/BTU)
      TRIC=CAO*CTRIC
      THERMAL RESISTANCE FOR SW FOULING(HR.FT2.F/BTU)
      TR2C=CAO*CTR2C
C

```



```

C C THERMAL RESISTANCE FOR WALL THICKNESS(HR.FT2.F/BTU)
C C TR3C=CAO*CTR3C
C C
C C THERMAL RESISTANCE FOR NH3 FOULING(HR.FT2.F/BTU)
C C (CONSIDERED NEGLIGIBLE)
C C
C C THERMAL RESISTANCE FOR NH3(HR.FT2.F/BTU)
C C TR5C=CAO*CTR5C
C C
C C OVERALL HEAT TRANSFER COEF U - OUTSIDE(BTU/HR.FT2.F
C C OR W/M2)
C C UC=1./((TR1C+TR2C+TR3C+TR5C)
C C
C C PSEUDO HT COEF FOR SW(BTU/HR.FT1.F OR W/M2.C)
C C HSWC=1./TR1C
C C
C C PSEUDO HT COEF FOR SW FOULING(BTU/HR.FT2.F OR W/M2.C)
C C HFSWC=1./TR2C
C C
C C PSEUDO HT COEF FOR WALL THICK(BTU/HR.FT2.F OF W/M2.C)
C C HWC=1./TR3C
C C
C C PSEUDO HT COEF FOR NH3(BTU/HR.FT2.F OR W/M2.C)
C C HNH3C=1./TR5C
C C
C C TOTAL CONDENSER HEAT TRANSFER AREA(FT2 OR M2)
C C THTAC=CNTU*CMINC/UC
C C
C C REVISED CONDENSER TUBE LENGTH(FT)
C C TLCCR=THTAC/(PIE*IDOC*TNCT)
C C
C C CONSTRAINT FOR A SAT TUBE LENGTH
C C DTLC=TLC-TLCR
C C
C C COST OF CONDENSER UNIT($ )
C C IF (TSDC.GT.35.) GO TO 910
C C

```

A1825
 A1826
 A1827
 A1828
 A1829
 A1830
 A1831
 A1832
 A1833
 A1834
 A1835
 A1836
 A1837
 A1838
 A1839
 A1840
 A1841
 A1842
 A1843
 A1844
 A1845
 A1846
 A1847
 A1848
 A1849
 A1850
 A1851
 A1852
 A1853
 A1854
 A1855
 A1856
 A1857
 A1858
 A1859
 A1860
 A1861
 A1862
 A1863
 A1864
 A1865
 A1866
 A1867
 A1868
 A1869
 A1870
 A1871
 A1872

C CONDENSER TUBE SHEET DIAMETER(10-35)FT
 C
 C DRILLING TIME/TUBE SHELL THICK(MIN/IN)
 C
 C DTC=0.66*(TDOC-.5)
 C
 C THICKNESS OF TUBE SHEET(IN)
 C
 C TTSC=0.56*TSDC**0.68
 C
 C TUBE SHEET LABOR COSTS(\$)
 C
 C CTSLC=156695.*(TNCT/9630.)*(DTC/0.66)*(TTSC/4.0)
 C
 C TUBE SHEET MATERIAL COST(\$)
 C
 C CTSMC=189.486*TSDC**2.3
 C IF (TMATL.EQ.1.) GO TO 870
 C
 C TUBE MATERIAL COST(\$)
 C
 C CTMC=(C1*TLC+C2)*TNCT*(TDOC/1.5)
 C
 C TUBE INSTALLATION COST(\$)
 C
 C CTIC=34.*TNCT*TDOC**0.7
 C GO TO 880
 C CONTINUE
 C
 C TUBE MATERIAL COST(\$)
 C
 C CTMC=(C1*TLC+C2)*TNCT*(TDOC/1.5)*(1.+(1.+AINT/100.))**10+(1.+AINT/1
 C 100.))**20)
 C
 C TUBE INSTALLATION COST(\$)
 C
 C CTIC=34.*TNCT*TDOC**0.7*(1.+(1.+AINT/100.))**10+(1.+AINT/100.))**20)
 C CONTINUE
 C
 C HEAT EXCH SHELL COST(\$)
 C
 C CHSC=177265.*(TLC*6.)/31.*(TSDC/18.))**2
 C
 C NH3 DIST PLATE AND BAFFLES COST(\$)
 C
 C CDPBC=1.539E-02*DTC*TNCT*TSDC**2
 C
 C BUSTLE, FLANGES, CHANNELS AND FLOW PLATES COST(\$)
 C

C	CBFCFC=1185.286*TSDC**2	Al 921
C	HEAT EXCH HEAD COST(\$)	Al 922
C	CHC=53240.0*(TSDC/18.0)**3	Al 923
C	WATER INLETS,NOZZLES AND SUPPORTS COST(\$)	Al 924
C	CWINSC=10106.475*TSDC	Al 925
C	TUBE WELDING COST(\$)	Al 926
C	CTWC=0.0	Al 927
C	IF (TMATL.EQ.1.0) GO TO 900	Al 928
C	IF (TNCT.GT.36000.0) GO TO 890	Al 929
890	CTWC=14.73*TNCT**1.03*(TDOC/1.5)**0.7	Al 930
900	GO TO 900	Al 931
910	CONTINUE	Al 932
C	CTWC=0.8797*TNCT**1.3*(TDOC/1.5)**0.7	Al 933
C	CONTINUE	Al 934
C	CCOND=(CTSLC+CTSMC+CTMC+CTIC+CHSC+CDPBC+CBFCFC+CHC+CWINSC+CTWC)	Al 935
C	GO TO 980	Al 936
C	CONTINUE	Al 937
C	CONDENSER TUBE SHEET DIAMETER(35-50)FT	Al 938
C	DRILLING TIME/TUBE SHELL THICKNESS(MIN/IN)	Al 939
C	DTC=0.66*(TDOC-0.5)	Al 940
C	THICKNESS OF TUBE SHEET(IN)	Al 941
C	TTSC=0.56*TSDC**0.68	Al 942
C	TUBE SHEET MATERIAL AND LABOR COST(\$)	Al 943
C	IF (TMATL.EQ.1.0) GO TO 920	Al 944
C	CTSLC=55.189*TNCT**0.791*TSDC**0.68*DTC	Al 945
C	CTSMC=29.566*TSDC**2.014*TTSC	Al 946
C	GO TO 930	Al 947
C	CONTINUE	Al 948
C	CTSLC=73.81*TNCT**0.791*TSDC**0.68*DTC	Al 949
C	CTSMC=354.3*TSDC**1.61*TTSC	Al 950
C	CONTINUE	Al 951
C	IF (TMATL.EQ.1.0) GO TO 940	Al 952
C	TUBE MATERIAL COST(\$)	Al 953

C	CTMC=(C1*TLC+C2)*TNCT*(IDOC/1.5)	A1969
C	TUBE INSTALLATION COST(\$)	A1970
C		A1971
C	CTIC=36.542*TNCT*IDOC**0.7	A1972
	GO TO 950	A1973
940	CONTINUE	A1974
C		A1975
C	TUBE MATERIAL COST(\$)	A1976
C		A1977
C		A1978
	CTMC=(C1*TLC+C2)*TNCT*(IDOC/1.5)*(1.+(1.+AINT/100.))**10+(1.+AINT/100.))**20)	A1979
C		A1980
C	TUBE INSTALLATION COST(\$)	A1981
C		A1982
	CTIC=36.542*TNCT*IDOC**0.7*(1.+(1.+AINT/100.))**10+(1.+AINT/100.))**20)	A1983
950	CONTINUE	A1984
C		A1985
C	HEAT EXCH SHELL COST(\$)	A1986
C		A1987
	CHSC=12.544*(TLC+6.)*TSDC**2.06	A1988
C		A1989
C	NH3 DIST PLATE AND BAFFLES COST(\$)	A1990
C		A1991
C	CDPBC=9.8252*TNCT**0.978*DTC	A1992
C		A1993
C	BUSTLE, FLANGES, CHANNELS AND FLOW PLATES COST(\$)	A1994
	CBFCFC=383.824*TSDC**2.184	A1995
C		A1996
C	HEAT EXCH HEAD COST(\$)	A1997
C		A1998
	CHC=938.62*TSDC**1.43	A1999
C		A2000
C	WATER INLET, NOZZLES AND SUPPORTERS COST(\$)	A2001
C		A2002
	CWINSC=7453.6*TSDC**1.056	A2003
C		A2004
C	TUBE WELDING COST(\$)	A2005
C		A2006
	CTWC=0.0	A2007
C	IF (TMATL.EQ.1.) GO TO 970	A2008
C	IF (TNCT.GT.36000.) GO TO 960	A2009
	CTWC=14.73*TNCT**1.03*(IDOC/1.5)**0.7	A2010
960	GO TO 970	A2011
	CONTINUE	A2012
		A2013
		A2014
		A2015
		A2016

1010	GO TO 1020	
	CONTINUE	
1020	WRITE (6, 1900)	
	CONTINUE	
	IF (PROF.EQ.2.) GO TO 1030	
	WRITE (6, 1910)	
	GO TO 1040	
1030	CONTINUE	
	WRITE (6, 1920)	
1040	CONTINUE	
	WRITE (6, 1930) EPR	
	IF (EHFE.EQ.2.) GO TO 1050	
	WRITE (6, 1940)	
	GO TO 1060	
1050	CONTINUE	
	WRITE (6, 1950)	
1060	CONTINUE	
	WRITE (6, 1960) VSWE, VSWEC	
	WRITE (6, 1970) ETW2, ETW2C	
	WRITE (6, 1980) EFT, EFTC	
	WRITE (6, 1990) DELTAE, DELTEC	
	WRITE (6, 2000) ELMTD, ELMTDC	
	WRITE (6, 2010) EPSE	
	WRITE (6, 2020) ENTU	
	WRITE (6, 2030) UE, UEC	
	WRITE (6, 2040) HSWE, HSWEC	
	WRITE (6, 2050) HFSWE, HFSWEC	
	WRITE (6, 2060) HWE, HWEC	
	WRITE (6, 2070) HNH3E, HNH3EC	
	WRITE (6, 2080) THTAE, THTAEC	
	WRITE (6, 2090) TSDE, TSDEC	
	WRITE (6, 2100) TNET	
	WRITE (6, 2110) DEVAP, DEVAPC	
	WRITE (6, 2120)	
	WRITE (6, 2130) P3, P3C	
	WRITE (6, 2140) T4, T4C	
	WRITE (6, 2150) X4P	
	WRITE (6, 2160) DSDEM, DSDEMC	
	IF (TYPEQ.EQ.2.) GO TO 1070	
	WRITE (6, 2170)	
	GO TO 1080	
1070	CONTINUE	
	WRITE (6, 2180)	
1080	CONTINUE	
	WRITE (6, 2190) QC, QCC	
	WRITE (6, 2200) FLOCP, FLOPCPC	
	WRITE (6, 2210) TCIC, TCICC	
	WRITE (6, 2220) TCOC, TCOCC	

A2161
 A2162
 A2163
 A2164
 A2165
 A2166
 A2167
 A2168
 A2169
 A2170
 A2171
 A2172
 A2173
 A2174
 A2175
 A2176
 A2177
 A2178
 A2179
 A2180
 A2181
 A2182
 A2183
 A2184
 A2185
 A2186
 A2187
 A2188
 A2189
 A2190
 A2191
 A2192
 A2193
 A2194
 A2195
 A2196
 A2197
 A2198
 A2199
 A2200
 A2201
 A2202
 A2203
 A2204
 A2205
 A2206
 A2207
 A2208

1090	WRITE (6,2230)	FLONH3,FLNH3C
	WRITE (6,2240)	PCOND,PCONDC
	WRITE (6,2250)	T5,T5C
	WRITE (6,2260)	T1,T1C
	WRITE (6,2270)	DSCOND,DSCONC
	WRITE (6,2280)	
	WRITE (6,2290)	TDOC,TDOCCC
	WRITE (6,2300)	TTC,TTCC
	WRITE (6,2310)	TLCR,TLCRC
	IF (TMATL.EQ.2.) GO TO 1090	
	WRITE (6,2320)	
	GO TO 1100	
	CONTINUE	
1100	WRITE (6,2330)	
	CONTINUE	
	IF (PROF.EQ.2.) GO TO 1110	
	WRITE (6,2340)	
	GO TO 1120	
1110	CONTINUE	
	WRITE (6,2350)	
	CONTINUE	
1120	WRITE (6,2360)	CPR
	IF (EHFC.EQ.2.) GO TO 1130	
	WRITE (6,2370)	
	GO TO 1140	
1130	CONTINUE	
	WRITE (6,2380)	
	CONTINUE	
1140	WRITE (6,2390)	VSWC,VSWCC
	WRITE (6,2400)	CTW2,CTW2C
	WRITE (6,2410)	CFT,CFTC
	WRITE (6,2420)	DELTAC,DELTC
	WRITE (6,2430)	CLMTD,CLMTDC
	WRITE (6,2440)	EPSC
	WRITE (6,2450)	CNTU
	WRITE (6,2460)	UC,UCC
	WRITE (6,2470)	HSWC,HSWCC
	WRITE (6,2480)	HFSWC,HFSWCC
	WRITE (6,2490)	HWC,HWCC
	WRITE (6,2500)	HNH3C,HNH3CC
	WRITE (6,2510)	THTAC,THTACC
	WRITE (6,2520)	TSDC,TSDCC
	WRITE (6,2530)	TNCT
	WRITE (6,2540)	DCOND,DCONDC
	WRITE (6,2550)	
	WRITE (6,2560)	DIHP,DIHPC
	WRITE (6,2570)	TLHP,TLHPC
	WRITE (6,2580)	VSWHP,VSWHPC

A2209
 A2210
 A2211
 A2212
 A2213
 A2214
 A2215
 A2216
 A2217
 A2218
 A2219
 A2220
 A2221
 A2222
 A2223
 A2224
 A2225
 A2226
 A2227
 A2228
 A2229
 A2230
 A2231
 A2232
 A2233
 A2234
 A2235
 A2236
 A2237
 A2238
 A2239
 A2240
 A2241
 A2242
 A2243
 A2244
 A2245
 A2246
 A2247
 A2248
 A2249
 A2250
 A2251
 A2252
 A2253
 A2254
 A2255
 A2256

WRITE	(6, 2590)	FLOHP, FLOHPC	A2257
WRITE	(6, 2600)	THIE, THIEC	A2258
WRITE	(6, 2610)	CONH	A2259
WRITE	(6, 2620)	DPIPH, DPIPHC	A2260
WRITE	(6, 2630)		A2261
WRITE	(6, 2640)	DICP, DICPC	A2262
WRITE	(6, 2650)	TLCP, TLCPC	A2263
WRITE	(6, 2660)	VSWCP, VSWCPC	A2264
WRITE	(6, 2670)	FLOCP, FLOCPC	A2265
WRITE	(6, 2680)	TCIC, TCICC	A2266
WRITE	(6, 2690)	CONC	A2267
WRITE	(6, 2700)	DPIPC, DPIPC	A2268
WRITE	(6, 2710)		A2269
WRITE	(6, 2720)	DINH3, DINH3C	A2270
WRITE	(6, 2730)	TLNH3P, TLNHPC	A2271
WRITE	(6, 2740)	FLONH3, FLNH3C	A2272
WRITE	(6, 2750)	DIPN, DIPNC	A2273
WRITE	(6, 2760)		A2274
WRITE	(6, 2770)	DINH3R, DINHRC	A2275
WRITE	(6, 2780)	TLNHRP, TLNRPC	A2276
WRITE	(6, 2790)	FLONHR, FLNHR	A2277
WRITE	(6, 2800)	DPIPNR, DPNRC	A2278
WRITE	(6, 2810)		A2279
WRITE	(6, 2820)		A2280
WRITE	(6, 2830)	DPMEC, DPMEC	A2281
WRITE	(6, 2840)	QEPMP, QEPMCC	A2282
WRITE	(6, 2850)	EPE, EME	A2283
WRITE	(6, 2860)		A2284
WRITE	(6, 2870)	DPMPCC, DPMPCC	A2285
WRITE	(6, 2880)	QCPMP, QCPMCC	A2286
WRITE	(6, 2890)	EPC, EMC	A2287
WRITE	(6, 2900)		A2288
WRITE	(6, 2910)	DPMPNC, DPMNCC	A2289
WRITE	(6, 2920)	QNPMP, QNPMCC	A2290
WRITE	(6, 2930)	EPNH3, EMNH3	A2291
WRITE	(6, 2940)		A2292
WRITE	(6, 2950)	DPNRC, DPNRCC	A2293
WRITE	(6, 2960)	QRPMP, QRPMPCC	A2294
WRITE	(6, 2970)	EPNHR, EMNHR	A2295
WRITE	(6, 2980)		A2296
WRITE	(6, 2990)	EET	A2297
WRITE	(6, 3000)	ETRP	A2298
WRITE	(6, 3010)	ETURBP	A2299
WRITE	(6, 3020)	X5P	A2300
WRITE	(6, 3030)		A2301
WRITE	(6, 3040)	PWRTR, WELEGG	A2302
WRITE	(6, 3050)	WELOSS	A2303
WRITE	(6, 3060)	PWREP, PWREPM	A2304

WRITE	(6,3070)	PWRCP, PWRCPM	A2305
WRITE	(6,3080)	PWRNP, PWRNPM	A2306
WRITE	(6,3090)	PWRRP, PWRRM	A2307
WRITE	(6,3100)		A2308
WRITE	(6,3110)	ELECT	A2309
WRITE	(6,3120)	PPP	A2310
WRITE	(6,3130)	TCE	A2311
WRITE	(6,3140)		A2312
WRITE	(6,3150)	CEVAP	A2313
WRITE	(6,3160)	CCOND	A2314
WRITE	(6,3170)	CTURB	A2315
WRITE	(6,3180)	CGEN	A2316
WRITE	(6,3190)	CESWP	A2317
WRITE	(6,3200)	CCSWP	A2318
WRITE	(6,3210)	CNH3P	A2319
WRITE	(6,3220)	CNH3RP	A2320
WRITE	(6,3230)		A2321
WRITE	(6,3240)	OBJ	A2322
WRITE	(6,3250)	CPKW	A2323
RETURN			A2324
FORMAT	(1H1,19X,21HINITIAL DESIGN VALUES)		A2325
FORMAT	(1H0,2X,23HEVAPORATOR - HORIZONTAL)		A2326
FORMAT	(1H0,2X,21HEVAPORATOR - VERTICAL)		A2327
FORMAT	(1H0,4X,9HTUBE O.D.,7X,F8.3,4H(IN),12X,F8.3,4H(MM))		A2328
FORMAT	(1H0,4X,11HTUBE LENGTH,5X,F8.3,4H(FT),12X,F8.3,3H(M))		A2329
FORMAT	(1H0,4X,11HSW TUBE VEL,5X,F8.3,6H(FT/S),10X,F8.3,5H(M/S))		A2330
FORMAT	(1H0,4X,13HOPER PRESSURE,3X,F8.3,9H(LBF/IN2),7X,F8.3,5H(MPA		A2331
1)			A2332
FORMAT	(1H0,4X,24HTUBE MATERIAL - ALUMINUM,/,6X,15HTHERMAL COND(K		A2333
1),F8.3,			A2334
FORMAT	(1H0,4X,24HTUBE MATERIAL - TITANIUM,/,6X,15HTHERMAL COND(K		A2335
1),F8.3,			A2336
FORMAT	(1H0,4X,37HTUBE PROFILE - STAGGERED EQUI-LATERAL)		A2337
FORMAT	(1H0,4X,33HTUBE PROFILE - IN-LINE EQUI-SIDED)		A2338
FORMAT	(1H0,6X,11HPITCH RATIO,6X,F5.2)		A2339
FORMAT	(1H0,4X,24HENHANCEMENT - PLAIN TUBE)		A2340
FORMAT	(1H0,4X,28HENHANCEMENT - LINDEN-PROMOTER)		A2341
FORMAT	(1H0,2X,22HCONDENSER - HORIZONTAL)		A2342
FORMAT	(1H0,2X,20HCONDENSER - VERTICAL)		A2343
FORMAT	(1H0,4X,9HTUBE O.D.,7X,F8.3,4H(IN),12X,F8.3,4H(MM))		A2344
FORMAT	(1H0,4X,11HTUBE LENGTH,5X,F8.3,4H(FT),12X,F8.3,3H(M))		A2345
FORMAT	(1H0,4X,11HSW TUBE VEL,5X,F8.3,6H(FT/S),10X,F8.3,5H(M/S))		A2346
FORMAT	(1H0,4X,13HOPER PRESSURE,3X,F8.3,9H(LBF/IN2),7X,F8.3,5H(MPA		A2347
1)			A2348
FORMAT	(1H0,4X,24HTUBE MATERIAL - ALUMINUM,/,6X,15HTHERMAL COND(K		A2349
1),F8.3,			A2350
FORMAT	(1H0,4X,24HTUBE MATERIAL - TITANIUM,/,6X,15HTHERMAL COND(K		A2351
1360			A2352

1370	1)	F8.3,	13H(BTU/HR.FT.F)	3X,F8.3,7H(W/M.C))	A2353
1380	FORMAT	(1H0,4X,37HTUBE	PROFILE -	STAGGERED EQUI-LATERAL)	A2354
1390	FORMAT	(1H0,4X,33HTUBE	PROFILE -	IN-LINE EQUI-SIDED)	A2355
1400	FORMAT	(1H0,6X,11HPITCH	RATIO,6X,F5.2)		A2356
1410	FORMAT	(1H0,4X,24HENHANCEMENT	- PLAIN TUBE)		A2357
1420	FORMAT	(1H0,4X,28HENHANCEMENT	- LINDE-PROMOTER)		A2358
1430	FORMAT	(1H0,2X,19HSALT WATER	HOT PIPE)		A2359
1440	FORMAT	(1H0,4X,9HPPIPE	I.D.,7X,F8.3,4H(FT),12X,F8.3,3H(M))		A2360
1450	FORMAT	(1H0,4X,11HPPIPE	LENGTH,5X,F8.3,4H(FT),12X,F8.3,3H(M))		A2361
1460	FORMAT	(1H0,4X,11HSW PIPE	VEL,5X,F8.3,6H(FT/S),10X,F8.3,5H(M/S))		A2362
	FORMAT	(1H0,4X,13HSW INLET	TEMP,3X,F8.3,7H(DEG F),9X,F8.3,7H(DEG C		A2363
	1)				A2364
1470	FORMAT	(1H0,4X,12HSW SALINITY	7X,F5.0,1X,5H0/000)		A2365
1480	FORMAT	(1H0,2X,20HSALT WATER	COLD PIPE)		A2366
1490	FORMAT	(1H0,4X,9HPPIPE	I.D.,7X,F8.3,4H(FT),12X,F8.3,3H(M))		A2367
1500	FORMAT	(1H0,4X,11HPPIPE	LENGTH,5X,F8.3,4H(FT),12X,F8.3,3H(M))		A2368
1510	FORMAT	(1H0,4X,11HSW PIPE	VEL,5X,F8.3,6H(FT/S),10X,F8.3,5H(M/S))		A2369
1520	FORMAT	(1H0,4X,13HSW INLET	TEMP,3X,F8.3,7H(DEG F),9X,F8.3,7H(DEG C		A2370
	1)				A2371
1530	FORMAT	(1H0,4X,12HSW SALINITY	7X,F5.0,1X,5H0/000)		A2372
1540	FORMAT	(1H0,2X,17HAMMONIA	CIRC PIPE)		A2373
1550	FORMAT	(1H0,4X,9HPPIPE	I.D.,7X,F8.3,4H(FT),12X,F8.3,3H(M))		A2374
1560	FORMAT	(1H0,4X,11HPPIPE	LENGTH,5X,F8.3,4H(FT),12X,F8.3,3H(M))		A2375
1570	FORMAT	(1H0,2X,20HAMMONIA	RE-FLUX PIPE)		A2376
1580	FORMAT	(1H0,4X,9HPPIPE	I.D.,7X,F8.3,4H(FT),12X,F8.3,3H(M))		A2377
1590	FORMAT	(1H0,4X,11HPPIPE	LENGTH,5X,F8.3,4H(FT),12X,F8.3,3H(M))		A2378
1600	FORMAT	(1H0,2X,29HPUMP	AND GEN-TURB PERFORMANCE)		A2379
1610	FORMAT	(1H0,4X,12HEVAP	SW PUMP)		A2380
1620	FORMAT	(1H0,6X,10HEFFICIENCY	1X,4HMECH,2X,F5.2,5H(PCT),7X,5HMOTOR,		A2381
	1X,F5.2,	5H(PCT))			A2382
1630	FORMAT	(1H0,4X,12HCOND	SW PUMP)		A2383
1640	FORMAT	(1H0,6X,10HEFFICIENCY	1X,4HMECH,2X,F5.2,5H(PCT),7X,5HMOTOR,		A2384
	1X,F5.2,	5H(PCT))			A2385
1650	FORMAT	(1H0,4X,17HAMMONIA	CIRC PUMP)		A2386
1660	FORMAT	(1H0,6X,10HEFFICIENCY	1X,4HMECH,2X,F5.2,5H(PCT),7X,5HMOTOR,		A2387
	1X,F5.2,	5H(PCT))			A2388
1670	FORMAT	(1H0,21HGEN-TURB	EFFICIENCIES)		A2389
1680	FORMAT	(1H0,6X,14HGEN	MECH&ELECT,3X,F5.2,5H(PCT))		A2390
1690	FORMAT	(1H0,6X,9HTURB	MECH,8X,F5.2,5H(PCT))		A2391
1700	FORMAT	(1H0,2X,18HPower	REQUIREMENTS)		A2392
1710	FORMAT	(1H0,4X,16HNET	POWER OUTPUT,10X,F8.3,4H(MW))		A2393
1720	FORMAT	(1H1,19HOPTIMIZATION	VALUES)		A2394
1730	FORMAT	(1H0,2X,23HEVAPORATOR	- HORIZONTAL)		A2395
1740	FORMAT	(1H0,2X,21HEVAPORATOR	- VERTICAL)		A2396
1750	FORMAT	(1H0,4X,9HHT	ABSORB,1X,F14.1,8H(BTU/HR),7X,F8.3,4H(MW))		A2397
1760	FORMAT	(1H0,4X,7HHSW	FLOW,3X,F14.1,8H(LBM/HR),1X,F14.1,7H(KG/HR))		A2398
1770	FORMAT	(1H0,6X,10HSW	TEMP IN,4X,F8.3,7H(DEG F),8X,F8.3,7H(DEG C))		A2399
1780	FORMAT	(1H0,6X,11HSW	TEMP OUT,3X,F8.3,7H(DEG F),8X,F8.3,7H(DEG C))		A2400

1790	FORMAT	(1H0,4X,8HNNH3 FLOW,2X,F14.1,8H(LBM/HR),1X,F14.1,7H(KG/HR))	A2401
1800	FORMAT	(1H0,4X,13HOPER PRESSURE,3X,F8.3,9H(LBF/IN2),6X,F8.3,5H(KPA	A2402
	1))		A2403
1810	FORMAT	(1H0,6X,13HEVAP SAT TEMP,1X,F8.3,7H(DEG F),8X,F8.3,7H(DEG C	A2404
	1))		A2405
1820	FORMAT	(1H0,6X,11HOUTLET TEMP,3X,F8.3,7H(DEG F),8X,F8.3,7H(DEG C))	A2406
1830	FORMAT	(1H0,6X,14HOUTLET QUALITY,4X,F5.2,5H(PCT))	A2407
1840	FORMAT	(1H0,4X,14HNNH3 PRESS DROP,2X,F8.3,9H(LBF/IN2),6X,F8.3,5H(KP	A2408
	1A))		A2409
1850	FORMAT	(1H0,4X,20HTUBE CHARACTERISTICS)	A2410
1860	FORMAT	(1H0,6X,10HOUTTER DIA,4X,F8.3,4H(IN),11X,F8.3,4H(MM))	A2411
1870	FORMAT	(1H0,6X,10HWALL THICK,4X,F8.3,4H(IN),11X,F8.3,4H(MM))	A2412
1880	FORMAT	(1H0,6X,6HLENGTH,8X,F8.3,4H(FT),11X,F8.3,3H(M))	A2413
1890	FORMAT	(1H0,6X,19HMTATERIAL - ALUMINUM)	A2414
1900	FORMAT	(1H0,6X,19HMTATERIAL - TITANIUM)	A2415
1910	FORMAT	(1H0,6X,37HTUBE PROFILE - STAGGERED EQUI-LATERAL)	A2416
1920	FORMAT	(1H0,6X,37HTUBE PROFILE - IN-LINE EQUI-SIDED)	A2417
1930	FORMAT	(1H0,8X,11HPITCH RATIO,4X,F5.2)	A2418
1940	FORMAT	(1H0,6X,24HENHANCEMENT - PLAIN TUBE)	A2419
1950	FORMAT	(1H0,6X,28HENHANCEMENT - LINDE-PROMOTER)	A2420
1960	FORMAT	(1H0,6X,11HSW VELOCITY,3X,F8.3,6H(FT/S),9X,F8.3,5H(M/S))	A2421
1970	FORMAT	(1H0,4X,17HT WALL(SHELLSIDE),F7.3,7H(DEG F),8X,F8.3,7H(DEG	A2422
	1C))		A2423
1980	FORMAT	(1H0,4X,9HFILM TEMP,7X,F8.3,7H(DEG F),8X,F8.3,7H(DEG C))	A2424
1990	FORMAT	(1H0,4X,15HDELTA T BOILING,1X,F8.3,7H(DEG F),8X,F8.3,7H(DEG	A2425
	1 C))		A2426
2000	FORMAT	(1H0,4X,8HL.M.T.D.,8X,F8.3,7H(DEG F),8X,F8.3,7H(DEG C))	A2427
2010	FORMAT	(1H0,4X,18HEVAP EFFECTIVENESS,7X,F8.3)	A2428
2020	FORMAT	(1H0,4X,20HNR OF TRANSFER UNITS,5X,F8.3)	A2429
2030	FORMAT	(1H0,4X,11HOVL HT COEF,5X,F8.2,14H(BTU/HR.FT2.F),1X,F8.2,8H	A2430
	1(W/M2.C))		A2431
2040	FORMAT	(1H0,6X,8HH(WATER),6X,F8.2,14H(BTU/HR.FT2.F),1X,F8.2,8H(W/M	A2432
	12.C))		A2433
2050	FORMAT	(1H0,6X,10HH(FOULING),4X,F8.2,14H(BTU/HR.FT2.F),1X,F8.2,8H(A2434
	1W/M2.C))		A2435
2060	FORMAT	(1H0,6X,8HH(METAL),6X,F8.2,14H(BTU/HR.FT2.F),F9.2,8H(W/M2.C	A2436
	1))		A2437
2070	FORMAT	(1H0,6X,10HH(AMMONIA),4X,F8.2,14H(BTU/HR.FT2.F),1X,F8.2,8H(A2438
	1W/M2.C))		A2439
2080	FORMAT	(1H0,4X,10HHT SURFACE,2X,F12.2,5H(FT2),6X,F12.2,4H(M2))	A2440
2090	FORMAT	(1H0,4X,14HTUBE SHEET DIA,2X,F8.3,4H(FT),11X,F8.3,3H(M))	A2441
2100	FORMAT	(1H0,6X,15HTOT NR OF TUBES,7X,F12.0)	A2442
2110	FORMAT	(1H0,4X,13HSW PRESS DROP,3X,F8.3,9H(LBF/IN2),6X,F8.3,5H(KPA	A2443
	1))		A2444
2120	FORMAT	(1H0,2X,36HMOISTURE SEPARATOR-INSIDE EVAP SHELL)	A2445
2130	FORMAT	(1H0,4X,13HOPER PRESSURE,3X,F8.3,9H(LBF/IN2),6X,F8.3,5H(KPA	A2446
	1))		A2447
2140	FORMAT	(1H0,6X,11HOUTLET TEMP,3X,F8.3,7H(DEG F),8X,F8.3,7H(DEG C))	A2448

2150	FORMAT	(1H0,6X,14HOUTLET QUALITY,3X,F5.2,5H(PCT))	A2449
2160	FORMAT	(1H0,6X,14HNNH3 PRESS DROP,F8.3,9H(LBF/IN2),6X,F8.3,5H(KPA))	A2450
2170	FORMAT	(1H1,2X,22HCONDENSER - HORIZONTAL)	A2451
2180	FORMAT	(1H0,2X,20HCONDENSER - VERTICAL)	A2452
2190	FORMAT	(1H0,4X,9HHT REJECT,1X,F14.1,8H(BTU/HR),7X,F8.3,4H(MW))	A2453
2200	FORMAT	(1H0,4X,7HSH FLOW,3X,F14.1,8H(LBM/HR),1X,F14.1,7H(KG/HR))	A2454
2210	FORMAT	(1H0,6X,10HSW TEMP IN,4X,F8.3,7H(DEG F),8X,F8.3,7H(DEG C))	A2455
2220	FORMAT	(1H0,6X,11HSW TEMP OUT,3X,F8.3,7H(DEG F),8X,F8.3,7H(DEG C))	A2456
2230	FORMAT	(1H0,4X,8HNNH3 FLOW,2X,F14.1,8H(LBM/HR),1X,F14.1,7H(KG/HR))	A2457
2240	FORMAT	(1H0,4X,13HOPER PRESSURE,3X,F8.3,9H(LBF/IN2),6X,F8.3,5H(KPA))	A2458
	1)		A2459
2250	FORMAT	(1H0,6X,13HCOND SAT TEMP,1X,F8.3,7H(DEG F),8X,F8.3,7H(DEG C))	A2460
	1)		A2461
2260	FORMAT	(1H0,6X,11HOUTLET TEMP,3X,F8.3,7H(DEG F),8X,F8.3,7H(DEG C))	A2462
2270	FORMAT	(1H0,4X,14HNNH3 PRESS DROP,2X,F8.3,9H(LBF/IN2),6X,F8.3,5H(KP	A2463
	1A))		A2464
2280	FORMAT	(1H0,4X,20HTUBE CHARACTERISTICS)	A2465
2290	FORMAT	(1H0,6X,10HOUTTER DIA,4X,F8.3,4H(IN),11X,F8.3,4H(MM))	A2466
2300	FORMAT	(1H0,6X,10HWALL THICK,4X,F8.3,4H(IN),11X,F8.3,4H(MM))	A2467
2310	FORMAT	(1H0,6X,6HLENGTH,8X,F8.3,4H(FT),11X,F8.3,3H(M))	A2468
2320	FORMAT	(1H0,6X,19HMATERIAL - ALUMINUM)	A2469
2330	FORMAT	(1H0,6X,19HMATERIAL - TITANIUM)	A2470
2340	FORMAT	(1H0,6X,37HTUBE PROFILE - STAGGERED EQUI-LATERAL)	A2471
2350	FORMAT	(1H0,6X,33HTUBE PROFILE - IN-LINE EQUI-SIDED)	A2472
2360	FORMAT	(1H0,8X,11HPITCH RATIO,4X,F5.2)	A2473
2370	FORMAT	(1H0,6X,24HENHANCEMENT - PLAIN TUBE)	A2474
2380	FORMAT	(1H0,6X,28HENHANCEMENT - LINDE-PROMOTER)	A2475
2390	FORMAT	(1H0,6X,11HSW VELOCITY,3X,F8.3,6H(FT/S),9X,F8.3,5H(M/S))	A2476
2400	FORMAT	(1H0,4X,17HT WALL(SHELLSIDE),F7.3,7H(DEG F),8X,F8.3,7H(DEG	A2477
	1C))		A2478
2410	FORMAT	(1H0,4X,9HFILM TEMP,7X,F8.3,7H(DEG F),8X,F8.3,7H(DEG C))	A2479
2420	FORMAT	(1H0,4X,12HDELTA T COND,4X,F8.3,7H(DEG F),8X,F8.3,7H(DEG C))	A2480
	1)		A2481
2430	FORMAT	(1H0,4X,8HL-M.T.D.,8X,F8.3,7H(DEG F),8X,F8.3,7H(DEG C))	A2482
2440	FORMAT	(1H0,4X,18HCOND EFFECTIVENESS,7X,F8.3)	A2483
2450	FORMAT	(1H0,4X,20HNR OF TRANSFER UNITS,5X,F8.3)	A2484
2460	FORMAT	(1H0,4X,11HOVL HT COEF,5X,F8.2,14H(BTU/HR.FT2.F),1X,F8.2,8H	A2485
	1(W/M2.C))		A2486
2470	FORMAT	(1H0,6X,8HH(WATER),6X,F8.2,14H(BTU/HR.FT2.F),1X,F8.2,8H(W/M	A2487
	12.C))		A2488
2480	FORMAT	(1H0,6X,10HH(FOULING),4X,F8.2,14H(BTU/HR.FT2.F),1X,F8.2,8H(A2489
	1W/M2.C))		A2490
2490	FORMAT	(1H0,6X,8HH(METAL),6X,F8.2,14H(BTU/HR.FT2.F),F9.2,8H(W/M2.C	A2491
	1))		A2492
2500	FORMAT	(1H0,6X,10HH(AMMONIA),4X,F8.2,14H(BTU/HR.FT2.F),1X,F8.2,8H(A2493
	1W/M2.C))		A2494
2510	FORMAT	(1H0,4X,10HHT SURFACE,2X,F12.2,5H(FT2),6X,F12.2,4H(M2))	A2495
2520	FORMAT	(1H0,4X,14HTUBE SHEET DIA,2X,F8.3,4H(FT),11X,F8.3,3H(M))	A2496

2530	FORMAT	(1H0,6X,15HTOT NR OF TUBES,7X,F12.0)	A2497
2540	FORMAT	(1H0,4X,13HSW PRESS DROP,3X,F8.3,9H(LBF/IN2),6X,F8.3,5H(KPA	A2498
	1))		A2499
2550	FORMAT	(1H1,2X,19HSALT WATER HOT PIPE)	A2500
2560	FORMAT	(1H0,4X,9HPIPE I.D.,7X,F8.3,4H(FT),11X,F8.3,3H(M))	A2501
2570	FORMAT	(1H0,4X,11HPIPE LENGTH,5X,F8.3,4H(FT),11X,F8.3,3H(M))	A2502
2580	FORMAT	(1H0,4X,11HSW PIPE VEL,5X,F8.3,6H(FT/S),9X,F8.3,5H(M/S))	A2503
2590	FORMAT	(1H0,4X,7HSW FLOW,3X,F14.1,8H(LBM/HR),1X,F14.1,7H(KG/HR))	A2504
2600	FORMAT	(1H0,4X,13HSW INLET TEMP,3X,F8.3,7H(DEG F),8X,F8.3,7H(DEG C	A2505
	1))		A2506
2610	FORMAT	(1H0,4X,12HSW SALINITY,7X,F5.0,1X,5H0/000)	A2507
2620	FORMAT	(1H0,4X,13HSW PRESS DROP,3X,F8.3,9H(LBF/IN2),6X,F8.3,5H(KPA	A2508
	1))		A2509
2630	FORMAT	(1H0,2X,20HSALT WATER COLD PIPE)	A2510
2640	FORMAT	(1H0,4X,9HPIPE I.D.,7X,F8.3,4H(FT),11X,F8.3,3H(M))	A2511
2650	FORMAT	(1H0,4X,11HPIPE LENGTH,5X,F8.3,4H(FT),11X,F8.3,3H(M))	A2512
2660	FORMAT	(1H0,4X,11HSW PIPE VEL,5X,F8.3,6H(FT/S),9X,F8.3,5H(M/S))	A2513
2670	FORMAT	(1H0,4X,7HSW FLOW,3X,F14.1,8H(LBM/HR),1X,F14.1,7H(KG/HR))	A2514
2680	FORMAT	(1H0,4X,13HSW INLET TEMP,3X,F8.3,7H(DEG F),8X,F8.3,7H(DEG C	A2515
	1))		A2516
2690	FORMAT	(1H0,4X,12HSW SALINITY,7X,F5.0,1X,5H0/000)	A2517
2700	FORMAT	(1H0,4X,13HSW PRESS DROP,3X,F8.3,9H(LBF/IN2),6X,F8.3,5H(KPA	A2518
	1))		A2519
2710	FORMAT	(1H0,2X,17HAMMONIA CIRC PIPE)	A2520
2720	FORMAT	(1H0,4X,9HPIPE I.D.,7X,F8.3,4H(FT),11X,F8.3,3H(M))	A2521
2730	FORMAT	(1H0,4X,11HPIPE LENGTH,5X,F8.3,4H(FT),11X,F8.3,3H(M))	A2522
2740	FORMAT	(1H0,4X,8HMH3 FLOW,2X,F14.1,8H(LBM/HR),1X,F14.1,7H(KG/HR))	A2523
2750	FORMAT	(1H0,4X,14HMH3 PRESS DROP,2X,F8.3,9H(LBF/IN2),6X,F8.3,5H(KP	A2524
	1A))		A2525
2760	FORMAT	(1H0,2X,25HAMMONIA RE-FLUX CIRC PIPE)	A2526
2770	FORMAT	(1H0,4X,9HPIPE I.D.,7X,F8.3,4H(FT),11X,F8.3,3H(M))	A2527
2780	FORMAT	(1H0,4X,11HPIPE LENGTH,5X,F8.3,4H(FT),11X,F8.3,3H(M))	A2528
2790	FORMAT	(1H0,4X,8HMH3 FLOW,2X,F14.1,8H(LBM/HR),1X,F14.1,7H(KG/HR))	A2529
2800	FORMAT	(1H0,4X,14HMH3 PRESS DROP,2X,F8.3,9H(LBF/IN2),6X,F8.3,5H(KP	A2530
	1A))		A2531
2810	FORMAT	(1H1,2X,29HPUMP AND GEN-TURB PERFORMANCE)	A2532
2820	FORMAT	(1H0,4X,12HEVAP SW PUMP)	A2533
2830	FORMAT	(1H0,6X,10HHEAD PRESS,4X,F8.3,4H(FT),11X,F8.3,3H(M))	A2534
2840	FORMAT	(1H0,6X,8HCAPACITY,2X,F12.1,9H(GAL/MIN),2X,F12.1,9H(LIT/MIN	A2535
	1))		A2536
2850	FORMAT	(1H0,6X,10HEFFICIENCY,1X,4HMECH,2X,F5.2,5H(PCT),7X,5HMOTOR,	A2537
	11X,F5.2,5H(PCT))		A2538
2860	FORMAT	(1H0,4X,12HCOND SW PUMP)	A2539
2870	FORMAT	(1H0,6X,10HHEAD PRESS,4X,F8.3,4H(FT),11X,F8.3,3H(M))	A2540
2880	FORMAT	(1H0,6X,8HCAPACITY,2X,F12.1,9H(GAL/MIN),2X,F12.1,9H(LIT/MIN	A2541
	1))		A2542
2890	FORMAT	(1H0,6X,10HEFFICIENCY,1X,4HMECH,2X,F5.2,5H(PCT),7X,5HMOTOR,	A2543
	11X,F5.2,5H(PCT))		A2544


```

2900 FORMAT (1H0,4X,17HAMMONIA CIRC PUMP)
2910 FORMAT (1H0,6X,10HHEAD PRESS,4X,F8.3,4H(FT),11X,F8.3,3H(M))
2920 FORMAT (1H0,6X,8HCAPACITY,2X,F12.1,9H(GAL/MIN),2X,F12.1,9H(LIT/MIN
1))
2930 FORMAT (1H0,6X,10HEFFICIENCY,1X,4HMECH,2X,F5.2,5H(PCT),7X,5HMOTOR,
11X,F5.2,5H(PCT))
2940 FORMAT (1H0,4X,20HAMMONIA RE-FLUX PUMP)
2950 FORMAT (1H0,6X,10HHEAD PRESS,4X,F8.3,4H(FT),11X,F8.3,3H(M))
2960 FORMAT (1H0,6X,8HCAPACITY,2X,F12.1,9H(GAL/MIN),2X,F12.1,9H(LIT/MIN
1))
2970 FORMAT (1H0,6X,10HEFFICIENCY,1X,4HMECH,2X,F5.2,5H(PCT),7X,5HMOTOR,
11X,F5.2,5H(PCT))
2980 FORMAT (1H0,4X,21HGEN-TURB EFFICIENCIES)
2990 FORMAT (1H0,6X,14HGEN MECH&ELECT,4X,F5.2,5H(PCT))
3000 FORMAT (1H0,6X,9HTURB MECH,9X,F5.2,5H(PCT))
3010 FORMAT (1H0,6X,13HTURB INTERNAL,5X,F5.2,5H(PCT))
3020 FORMAT (1H0,4X,19HTURB OUTLET QUALITY,1X,F5.2,5H(PCT))
3030 FORMAT (1H1,2X,18HPOWER REQUIREMENTS)
3040 FORMAT (1H0,4X,14HTURB-GEN GROSS,10.3,4H(HP),12X,F8.3,4H(MW))
3050 FORMAT (1H0,6X,17HEFFICIENCY LOSSES,21X,F8.3,4H(MW))
3060 FORMAT (1H0,4X,12HEVAP SW PUMP,4X,F8.3,4H(HP),12X,F8.3,4H(MW))
3070 FORMAT (1H0,4X,12HCOND SW PUMP,4X,F8.3,4H(HP),12X,F8.3,4H(MW))
3080 FORMAT (1H0,4X,13H3H3 CIRC PUMP,3X,F8.3,4H(HP),12X,F8.3,4H(MW))
3090 FORMAT (1H0,4X,16H3H3 RE-FLUX PUMP,F8.3,4H(HP),12X,F8.3,4H(MW))
3100 FORMAT (1H0,42X,10H)
3110 FORMAT (1H0,10X,16HNET-POWER-OUTPUT,18X,F8.3,4H(MW))
3120 FORMAT (1H0,2X,23HPERCENT PARASITIC POWER,10X,F5.2,5H(PCT))
3130 FORMAT (1H0,2X,29HTHEMODYNAMIC CYCLE EFFICIENCY,4X,F5.2,5H(PCT))
3140 FORMAT (1H0,2X,18HCOST OF COMPONENTS)
3150 FORMAT (1H0,4X,10HEVAPORATOR,14X,F12.2,9H(DOLLARS))
3160 FORMAT (1H0,4X,9HCONDENSER,15X,F12.2,9H(DOLLARS))
3170 FORMAT (1H0,4X,11HGEN-TURBINE,13X,F12.2,9H(DOLLARS))
3180 FORMAT (1H0,4X,9HGENERATOR,15X,F12.2,9H(DOLLARS))
3190 FORMAT (1H0,4X,12HEVAP SW PUMP,12X,F12.2,9H(DOLLARS))
3200 FORMAT (1H0,4X,12HCOND SW PUMP,12X,F12.2,9H(DOLLARS))
3210 FORMAT (1H0,4X,13H3H3 CIRC PUMP,11X,F12.2,9H(DOLLARS))
3220 FORMAT (1H0,4X,16H3H3 RE-FLUX PUMP,8X,F12.2,9H(DOLLARS))
3230 FORMAT (1H0,28X,12H)
3240 FORMAT (1H0,10X,12HOPTIMUM-COST,6X,F12.2,9H(DOLLARS))
3250 FORMAT (1H0,2X,22HCOST PER NET KW OUTPUT,4X,F12.2,17H(DOLLARS)
1
)
END
C FUNCTION SUBROUTINES FOR SALT WATER AND AMMONIA
C SALT WATER DENSITY(LBM/FT3)
C
FUNCTION RHOSW (T)
RHOSW=63.90152+.017512*T-5.684E-04*T**2+6.336E-06*T**3-2.7949E-08*
T**4

```


C	FUNCTION VSNH3 (T)	J	2
	VSNH3=.55203968261-.003405489426*T+1.01587304E-05*T**2-1.5046298E-	J	3
	108*T**3	J	4
	RETURN	J	5
	END	J	6
C	SPECIFIC HEAT OF SAT AMMONIA LIQUID(BTU/LBM.F)	K	7-
C	FUNCTION CPNH3 (T)	K	1
	CPNH3=1.0829682542+.00041058198*T+1.7658742E-06*T**2+1.6203699E-08	K	2
	1*T**3	K	3
	RETURN	K	4
	END	K	5
C	THERMAL CONDUCTIVITY OF SAT AMMONIA LIQ(BTU/HR.FT.F)	K	6
C	FUNCTION TKNH3 (T)	L	7-
	TKNH3=.33517857143-.000720535715*T-2.2321429E-07*T**2	L	1
	RETURN	L	2
	END	L	3
C	ENTROPY OF SAT AMMONIA LIQUID(BTU/LBM.R)	L	4
C	FUNCTION SF (T)	L	5
	SF=.09771914+.002334056*T-1.66882E-06*T**2+2.1649E-09*T**3	L	6
	RETURN	M	1
	END	M	2
C	ENTROPY OF SAT AMMONIA VAPOR(BTU/LBM.R)	M	3
C	FUNCTION SG (T)	M	4
	SG=1.33473105-.001973293*T+4.0808E-06*T**2-7.5887E-09*T**3	M	5
	RETURN	M	6
	END	N	1
C	DENSITY OF SAT AMMONIA LIQ(LBM/FT3)	N	2
C	FUNCTION RFNH3 (T)	N	3
	RFNH3=41.415499-.0490092*T+.000039001*T**2-5.2019E-07*T**3	N	4
	RETURN	N	5
	END	N	6
C	DENSITY OF SAT AMMONIA VAPOR(LBM/FT3)	O	1
C	FUNCTION RGNH3 (P)	O	2
	RGNH3=.01242535+.0032785773*P-2.52513E-07*P**2+8.9285E-10*P**3	O	3
	RETURN	O	4
	END	O	5
C	TITANIUM TUBE WALL THICKNESS - PLAIN(INCH)	P	6-
C	FUNCTION TP (D)	P	1
	TP=.007966159+.040237327*D-.035418004*D**2+.015039976*D**3-.002418	P	2
	12547*D**4	P	3
		P	4
		P	5
		Q	6-
		Q	1
		Q	2
		Q	3
		Q	4
		Q	5


```

FUNCTION AEC (D)
AEC=2.157473-5.206014*D+7.336678*D**2-3.656495*D**3+.7204888*D**4
RETURN
END
COND ALUMINUM TUBE COST/FT - LINDE-PROMOTER($/FT)
FUNCTION ACC (D)
ACC=1.799865-4.543195*D+6.556578*D**2-3.305876*D**3+.6622916*D**4
RETURN
END

```

C
C

Y Y Y Y Z Z Z Z Z
3 4 5 6- 1 2 3 4 5 6-

LIST OF REFERENCES

1. Office of Technological Assessment, Renewable Ocean Energy Sources, Part 1 OTEC, p. 7, May 1978.
2. Claude, Georges, "Power from Tropical Sea," Mechanical Engineering, v. 52, No. 12, Dec. 1930.
3. Holman, J. P., Heat Transfer, 4th ed., p. 204-223, McGraw-Hill, 1976.
4. Tong, L. S., Boiling Heat Transfer and Two-Phase Flow, p. 76-79, Wiley, 1965.
5. Perry, J. H., and others, Chemical Engineers' Handbook, 4th ed., p. 18-82, 83, McGraw Hill, 1969.
6. Owens, W. L., "Correlation of Thin Film Evaporation Heat Transfer Coefficients for Horizontal Tubes," Proceedings of the Fifth Ocean Thermal Energy Conversion Conference, Vol 6 of 8, Miami Beach, Florida (February 20-22, 1978).
7. McAdams, W. H., Heat Transmission, 3rd ed., p. 325-343, McGraw-Hill, 1954.
8. Lorenz, J. J. and Yung, D., "Combined Boiling and Evaporation of Liquid Films on Horizontal Tubes," Proceedings of the Fifth Ocean Thermal Energy Conversion Conference, Vol 6 of 8, Miami Beach, Florida (February 20-22, 1978).
9. TRW Contract No. EG-77-C-03-1570, OTEC Power System Development Utilizing Advanced, High-Performance Heat Transfer Techniques, V. 2, p. I 1-36, 30 Jan 78.
10. Streeter, V. L. and Wylie, E. B., Fluid Mechanics, 7th ed., p. 235-239, McGraw-Hill, 1979.
11. Baumeister, T., and others, Marks' Standard Handbook for Mechanical Engineers, 8th ed., p. 3-57, 58, McGraw Hill, 1978.
12. Metrek Division of the Mitre Corporation Contract No. ET-78-C-01-2854, OTEC Power System Performance Model, by H. Abelson, P. 74-81, August 1978.

13. Neuman, G. and Pierson, W. J., Jr., Principles of Physical Oceanography, Prentice-Hall, 1966.
14. Sverdrup, H. V., Johnson, M. W., and Fleming, R. H., The Oceans Their Physics, Chemistry, and General Biology, p. 1053, Prentice-Hall, 1949.
15. Westinghouse Electric Co. Contract No. EG-77-C-03-1569, Ocean Thermal Energy Conversion Power System, Phase 1: Preliminary Design, p. 9-9, 4 Dec 1978.
16. Kostors, C. H. and Vincent, S. P., "Performance Optimization of an OTEC Turbine," Proceedings of the Sixth Ocean Thermal Energy Conversion Conference, Vol 1 of 2, Washington, D.C. (June 19-22, 1979).
17. Olsen, H. L., and others, "Preliminary Considerations for the Selection of a Working Medium for the Solar Sea Power Plant," Proceedings, Solar Sea Power Plant Conference and Workshop, June 27-28, 1973.
18. Vanderplaats, G. N., COPEs - A User's Manual prepared for a graduate course on "Automated Design Optimization" presented at the Naval Postgraduate School, Monterey, Calif., March-May 1977.
19. Vanderplaats, G. N., Numerical Optimization Techniques for Engineering Design, Class notes for a graduate course on "Automated Design Optimization" presented at the Naval Postgraduate School, Monterey, Calif., May 1978.
20. Vanderplaats, G. N., "The Computer for Design and Optimization," Computing in Applied Mechanics, AMD-Vol. 18, ASME Winter Annual Meeting, New York, Dec. 1976.
21. Vanderplaats, G. N., Method of Feasible Directions, Class notes for a graduate course on "Automated Design Optimization," presented at the Naval Postgraduate School, Monterey, Calif., July 1978.

INITIAL DISTRIBUTION LIST

	No. Copies
1. Defense Technical Information Center Cameron Station Alexandria, Virginia 22314	2
2. Library, Code 0142 Naval Postgraduate School Monterey, California 93940	2
3. Department Chairman, Code 69 Department of Mechanical Engineering Naval Postgraduate School Monterey, California 93940	1
4. Assoc. Professor R. H. Nunn, Code 69 Nn Department of Mechanical Engineering Naval Postgraduate School Monterey, California 93940	2
5. Asst. Professor G. H. Vanderplaats, Code 69 Me Department of Mechanical Engineering Naval Postgraduate School Monterey, California 93940	1
6. LCDR Raymond C. Schaubel 14673 Charter Oak Boulevard Salinas, California 93907	1
7. Dr. Harvey Abelson Argonne National Laboratory Washington Office Suite 185 400 N. Capitol Street, N.W. Washington, DC 20001	1
8. Mr. Gene Barsness OTEC Project Manager Westinghouse Electric Co. Lester Branch Box 9175 Philadelphia, PA 19113	1
9. Dr. James W. Connell Director, Thermal Sciences Energy Systems Division Alfa-Laval Thermal, Inc. South Deerfield, MA 01373	1

INITIAL DISTRIBUTION LIST (CONTINUED)

	No. Copies
10. Mr. Bruce E. Dawson Foster Wheeler Energy Corp. 110 South Orange Ave. Livingston, NJ 07039	1
11. Dr. Jeff Horowitz Dept. of Energy Chicago Operations Office Argonne National Laboratory 9700 South Cass Ave. Argonne, IL 60439	1
12. Mr. John Michel P.O. Box Y Bldg. 9204-1 Oak Ridge National Laboratory Oak Ridge, Tennessee 37830	1
13. Mr. Charles Rabidart Lockheed Missiles and Space Company 57-02 150 1 P.O. Box 504 Sunnyvale, CA 94088	1
14. Mr. Dan Rossard Westinghouse Electric Corp. Lester Branch Box 9175 Philadelphia, PA 19113	1
15. Mr. J. M. Shoji OTEC Project Engineer Rocketdyne, Dept. 545-113 6633 Canoga Avenue Canoga Park, CA 91304	1
16. Dr. J. E. Snyder OTEC Project Manager TRW Defense and Space Systems Group Mail Station 81/1538 One Space Park Redondo Beach, CA 90278	1
17. Dr. Jerry Taborek Heat Transfer Research, Inc. 1000 South Fremont Ave. Alhambra, CA 91802	1

INITIAL DISTRIBUTION LIST (CONTINUED)

	No. Copies
18. Mr. Lloyd Trimble	1
OTEC Power System Development	
Project Manager	
Lockheed Missiles and Space Company	
57-02 150 1	
P.O. Box 504	
Sunnyvale, CA 94088	

Thesis
S273 Schaubel
c.1 Optimization of a
low ΔT Rankine power
system.

191317

26 JUN 91

14221

Thesis
S273 Schaubel
c.1 Optimization of a
low ΔT Rankine power
system.

191317

Optimization of a low (ΔT) Rankine p



3 2768 002 00332 9

DUDLEY KNOX LIBRARY